Ore Geology Reviews 157 (2023) 105423

Contents lists available at ScienceDirect

Ore Geology Reviews

journal homepage: www.elsevier.com/locate/oregeorev

Review

Vanadium ore resources of the African continent: State of the Art

Maria Boni [a,b], Mohammed Bouabdellah [c], Wissale Boukirou [c], Francesco Putzolu [b], Nicola Mondillo [a,b,*]

[a] Dipartimento Scienze della Terra, dell'Ambiente e delle Risorse, Università di Napoli Federico II, 80126 Napoli, Italy
[b] The Natural History Museum, London SW7 5BD, UK
[c] Laboratoire des Gîtes Minéraux, Hydrogéologie and Environnement, Faculté des Sciences, Mohamed Premier University, Oujda 60000, Morocco

ARTICLE INFO

Keywords:
Vanadium
Africa
Metallogeny
Mineralogy
Resources
energy storage

ABSTRACT

As part of the critical metals group, vanadium is an essential commodity for the low- and zero-CO_2 energy generation, storage and transport. This contribution aims to carry out a review of the known vanadium ore sources and mineralizations located in Africa, which are highly diversified in their geological and mineralogical characteristics, and can be classified in:

1. Vanadiferous (titano)magnetite deposits;
2. Sandstone-hosted (U)-vanadium deposits;
3. Calcrete-hosted (U)-vanadium deposits;
4. Vanadate deposits;
5. Graphite-associated vanadium deposits;
6. Vanadium occurrences associated with laterite, bauxite, and phosphate ores.

The economically most significant vanadium sources in Africa are associated with titanomagnetite layers in mafic–ultramafic layered magmatic intrusions (e.g., the Bushveld Complex in South Africa and the Great Dyke in Zimbabwe). Vanadium has been historically mined also in vanadate deposits deriving from the supergene alteration of Pb-Zn-Cu sulfide ores in Namibia and Zambia. Several areas in these countries, where potentially re-processable old tailings and slags have been accumulated, still have economic potential. Vanadium mineralizations are associated with graphite bodies in the Mozambique Metamorphic Belt. Vanadium is also enriched in uranium ores occurring in the Upper Paleozoic-Mesozoic Karoo continental sediments: typical examples are found in Botswana, South Africa, and Zimbabwe. Significant uranium-vanadium concentrations (where carnotite prevails) occur in relatively recent (Tertiary-Quaternary) calcrete duricrusts in paleo-fluviatile beds, which are widespread throughout the African continent. These derive from the weathering of U-(V)-fertile source rocks, which under favorable paleoclimatic conditions resulted in the vanadium precipitation in the critical zone. Variable vanadium amounts have been also recorded in iron ore deposits, phosphorites, and laterites, even though the phosphate deposits seem to have the most favorable characteristics for potentially economic vanadium concentrations.

On the whole, South Africa holds the most significant vanadium ore resources globally. However, also many other African countries, where this metal could be profitably extracted as a by-product from other economic ores, will probably be at the forefront of vanadium production in the near future.

1. Introduction

Vanadium is currently considered a critical metal (CM) for the European Union (European Commission, 2023), Australia (Austrade, 2020) and the United States (USDOI, 2018; McNulty and Jowitt, 2021), either because the intensification in the number of vanadium-dependent technologies has produced a substantial rise in its demand in recent years (Roskill, 2021;Simandl and Paradis, 2022), and also because, at the same time, the world mine V production is limited to a few countries: China, Russia, Brazil and South Africa (Fig. 1) (U.S. Geological Survey,

* Corresponding author at: Dipartimento Scienze della Terra, dell'Ambiente e delle Risorse, Università di Napoli Federico II, 80126 Napoli, Italy.
E-mail addresses: boni@unina.it (M. Boni), mbouabdellah2002@yahoo.fr (M. Bouabdellah), wissale.boukirou@gmail.com (W. Boukirou), francesco.putzolu1@nhm.ac.uk (F. Putzolu), nicola.mondillo@unina.it (N. Mondillo).

https://doi.org/10.1016/j.oregeorev.2023.105423
Received 7 September 2022; Received in revised form 10 March 2023; Accepted 28 March 2023
Available online 31 March 2023

2023). In 2022, world vanadium resources have been estimated to exceed 63 million tons, whereas the reserves have been estimated to be around 26 million tons (Fig. 1)(U.S. Geological Survey, 2023). In the 2021–2022, the global V production was around 100 ktons/year (U.S. Geological Survey, 2023).

About 85% of metal vanadium is employed into iron-vanadium and vanadium-nitrogen alloys for steel production to improve its strength, toughness, ductility, and heat resistance (Petranikova et al., 2020). Due to its high-temperature strength, vanadium is used in the super alloy industry for crafting turbine blades, jet engines, and other moving parts exposed to overheating (Petranikova et al., 2020). In the chemical industry, vanadium compounds are used in oxidation catalysts to produce sulfuric acid and the cracking of petroleum products. Vanadium is also used as a glass and ceramic pigment, in permanent magnets, dryers, paints, and varnishes, processing of color films, small rechargeable batteries, and catalysts for the control of exhaust fumes in diesel engines. It is employed to suppress nitrous oxide production in power plants and can be used in refining uranium for nuclear purposes (Petranikova et al., 2020). Vanadium has also potential use in battery storage as alternatives to Li-ion batteries. These include Vanadium Redox Flow Batteries (VRFB) (Hund et al., 2020) that have potential for grid scale storage (Silin et al., 2020) and are high power, high capacity, efficient, rapid charging, safe, and low cost (Hope, 2022). An increase of an order of magnitude in the global demand for vanadium is expected to come in the next decade due to a progressive increase in the employment of vanadium in this industry (European Commission, 2023; Hund et al., 2020).

Although vanadium is found in trace amounts in most rocks, its economic concentrations predominantly occur in four main types of ore deposits, hosted either in mafic–ultramafic igneous systems or in sedimentary and (seldom) in metamorphic rocks: the classification of these deposits is reported in detail in paragraph n. 2 (Kelley et al., 2017). However, several other potential natural sources are still being discovered. For example, up to 1,500 ppm of vanadium have been measured in crude oil in several countries (Breit and Wanty, 1991).

Alternative V resources to natural ore deposits are the industrial and metallurgical wastes, like: tailings and slags from steel industries, or from ancient and modern mining of Zn and Cu ore deposits (Sracek et al., 2014; Lehmann et al., 2016; Ettler et al., 2020). In specific literature, these materials are generally called “secondary” vanadium resources (e.g. Petranikova et al., 2020; Gao et al., 2022). During the refining or burning of crude oil, coal, and tar sands, vanadium-bearing ash, slag, spent catalyst, or residues are produced, which can then be processed for vanadium recovery (e.g., Vanitec, 2022). For example, the amount of waste from burning crude oil in electrical power plants could include more than 10,000 tons/year of vanadium (e.g., in the case of Iraq, Hussein Al-Zuhairi, 2014). Vanadium can also be extracted from slurries/muds derived from uranium production (e.g., in Niger) (IAEA, 2020).

It is inferred that more than 97% of vanadium used in common devices is recyclable (e.g. Ciacci et al., 2015). However, in the alloys deriving from discarded products it is often included in small amounts (less than 1 wt%), making technological and economic recovery difficult (Graedel et al., 2011; Reck and Graedel, 2012).

The purpose of this paper is to provide a *State of the Art* snapshot of the most relevant vanadium-endowed mining regions and vanadium ore types across Africa which, for its peculiar geological features, can host the complete spectrum of vanadium ore deposit types. We will firstly provide a general geological setting of the African continent that could serve as a frame of the diverse vanadium mineralizations. We will then describe and underline the African vanadium mineralizations, including the historically significant ores of Namibia and South Africa, and the numerous occurrences in other countries, where vanadium minerals were only scantily explored or exploited with old artisanal methods, or even known only by mineral collectors. With this paper, we intend to reach not only economic geologists working in the field of battery metals, but also mining engineers and possible entrepreneurs who may need preliminary information on vanadium occurrences in the African continent. For this reason, we also report a good number of citations from company announcements (“grey literature”), which are generally not quoted in ordinary scientific papers.

2. Classification of vanadium ore deposits

According to Kelley et al. (2017), the main types of vanadium ore deposits, in order of economic importance, are:

1. Vanadiferous (titano)magnetite deposits;
2. Sandstone-hosted (U)-vanadium deposits;
3. Calcrete-hosted (U)-vanadium deposits;
4. Vanadate deposits;
5. Vanadium deposits associated with crude oil, coal, and shales;
6. Graphite-associated vanadium deposits;
7. Vanadium occurrences in laterite, bauxite, iron and phosphate ores.

A more complex classification of vanadium deposits was presented by Dill (2010). This codification also comprehends several minor types

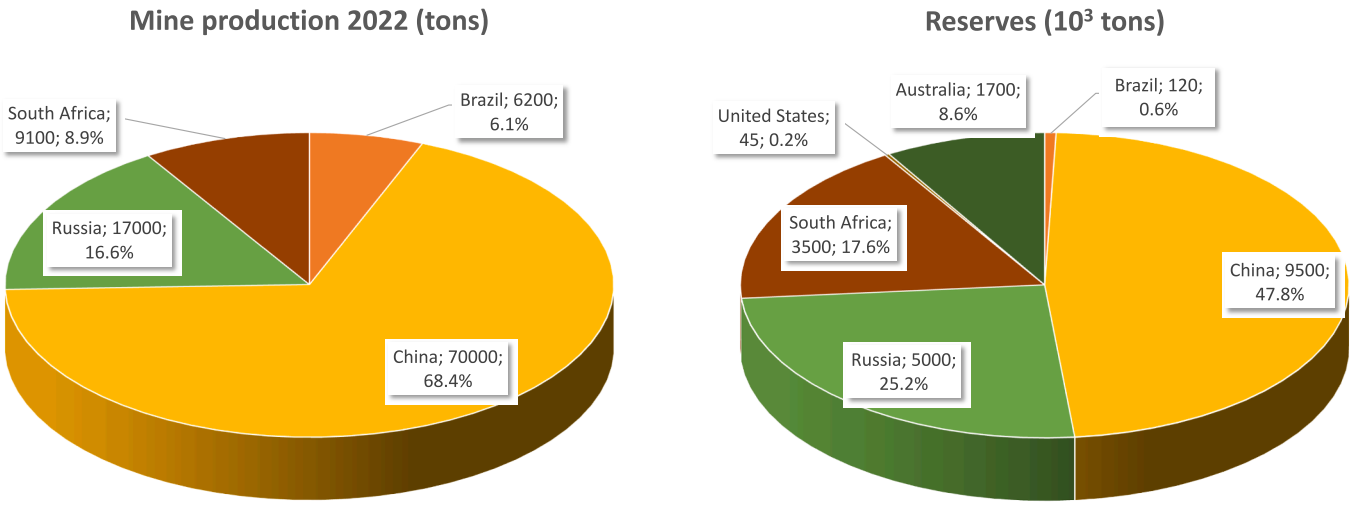

Fig. 1. World mine production and global reserves of vanadium subdivided by country (*For Australia, only Joint Ore Reserves Committee-compliant or equivalent reserves of 1,700 ktons are shown; U.S. Geological Survey, 2023).

of deposits, which occur in some parts of Africa. For the sake of simplicity, we have used the Kelley et al. (2017) classification. The exceptions to this general classification will be mentioned when encountered.

1. *Vanadiferous (titano)magnetite deposits ("VTD")* are the prime ore source of vanadium worldwide (Kelley et al., 2017). They are classified as igneous-hosted deposits originating from mafic-ultramafic intrusions, with the Bushveld Complex in South Africa representing the archetypal example (Cawthorn, 2005; Mosiane, 2006; Smith and Maier, 2021). Vanadium in VTD is hosted in (titano)magnetite, ilmenite, and rutile, resulting in a close V-Ti association. The resulting concentrations typically grade between 0.2 and 1% V_2O_5, and higher-grade deposits can attain over 2% V_2O_5. World-class vanadium (titano)magnetite deposits are, among others, located in the Sichuan province in China and Western Australia. Vanadiferous titanomagnetite sands or secondary vanadium oxides can also be economically valuable end-products of weathering of these magmatic deposits (Brought et al., 2019; Gilligan and Nikoloski, 2020; Perks and Mudd, 2021).

2. *Sandstone-hosted (U)-Vanadium deposits ("SSV"),* known as "sandstone-hosted uranium deposits", are subdivided into: (i) basal channel, (ii) tabular, (iii) roll front, (iv) associated with tectonic-lithologic features, (v) related to dykes/sills in Proterozoic sandstones (Simandl and Paradis, 2022). In these deposits the vanadium grade typically ranges between 0.1% and 1 % V. The main concentrations are present in the United States (roll front deposits), with the Colorado Plateau being the leading worldwide producer of this type of mineralization as a by-product of uranium mining (Breit, 2016; Kelley et al., 2017). Elsewhere, vanadium is generally not recovered from these deposits (Breit, 2016).

3. *Surficial deposits:* they are particular types of *Sedimentary U-(V) deposits* characterized by near-surface (usually less than 20 m deep) concentrations of U and V. The most significant and common style of surficial concentrations worldwide is represented by the calcrete-hosted uranium/vanadium ores (Carlisle, 1983; Van Gosen and Hall, 2017), with Namibia, the USA, and Australia containing the majority of the known deposits (IAEA, 2020). Calcrete deposits form in semi-arid to arid climatic regions (Hartleb, 1988) and contain primarily *carnotite*, an hydrated potassium uranyl vanadate [$K_2(UO_2)_2V_2O_8{\cdot}3H_2O$].

4. *Vanadate deposits:* these systems derive from lead-copper-zinc sulfide orebodies that have undergone supergene alteration. Vanadate deposits occur predominantly in arid climates, most notably in several regions of Africa, with the Otavi Mountainland in Namibia (Verwoerd, 1957; Boni et al., 2007) and Morocco (Bouabdellah and Sangster, 2016; Verhaert et al., 2017) being the best-known examples. The availability of lead during the ore-forming process is essential to precipitate vanadates. Conversely, the zinc and copper endowment of vanadate systems is not paramount and varies broadly depending on the metals footprint of the primary ore. In these deposits, V minerals are *vanadinite*, *descloizite*, and *mottramite*. The precipitation of the lead vanadate ores takes place in a near-surface environment with the V-mineralizing front that rarely expands deeper than the groundwater level.

5. *Vanadium associated with crude oil, coal, and shale deposits*: within crude oil, vanadium resides in the heavy fractions (Brough et al., 2019), with concentrations from 1,200 up to 5,000 ppm in asphaltene. Vanadium has been detected in crude oil in the Caribbean basin, in parts of the Middle East, and Russia, as well as in tar sands in western Canada and in coal in parts of China and the USA. In coal deposits, vanadium is mainly found in the organic-rich clayey layers, with values up to 420 ppm. In the shale-hosted (U)-vanadium mineralizations, referred to as "black-shale deposits", vanadium is concentrated in the organic fraction (i.e., kerogen). The genesis of these ores is not well understood, but their grade typically ranges between 0.2% and 2% V_2O_5 (Akinlua et al., 2016). Whereas the specific vanadium enrichment mechanisms are disputed, all require the reduction of dissolved V^{5+} (Breit and Wanty, 1991), which is the predominant redox state in the oceans (Collier, 1984). Vanadiferous black shales represent one of the largest vanadium resources in China (Li et al., 2010), with contents ranging between 0.13% and 1.2% V_2O_5 (Qi, 1999; Wu et al., 2021a,b).

6. *Graphite-associated vanadium deposits.* These deposits occur in metamorphic terranes of Eastern Africa, Madagascar, India, Korea, and the Baltic regions (Parnell, 2022). They have a characteristic metallic suite of V-Mo-U-C and may represent a product of metamorphosed black shale deposits. Initial vanadium enrichment of the sea floor sediments may have occurred in a euxinic marine environment similar to the present-day Black Sea. As in black-shale deposits, vanadium is captured by clays and settled on the organic-rich seafloor under anoxic conditions (Parnell, 2022). Oxidizing and low pH basinal fluids transported vanadium, molybdenum, and uranium to the reduced, organic-rich sites where they precipitated. The source of the metals may have been volcanic rocks in the sedimentary sequence and at least partly other black shales that had an initial seafloor metallic enrichment (AGP Mining Consultants Inc., 2011; Desautels et al., 2011). Vanadium initially bonds in the organic fraction and following burial diagenesis and metamorphism, is remobilized and fixed into phyllosilicates as *roscoelite* (Di Cecco et al., 2018; Parnell, 2022).

7. *Vanadium occurrences in laterite, bauxite, and phosphate ores:* vanadium can be associated with bauxites, laterites and supergene iron ores (Gamaletsos et al., 2017). The vanadium content depends on the origin and nature of the bauxite (lateritic or karstic) but commonly ranges from 0.05 to 0.25 wt% V_2O_5 (Patterson et al., 1986; Kelley et al., 2017). During the processing of bauxite ore, vanadium concentrates in residual sludge (*Red Mud*) and in secondary phases that contain as much as 10 to 18 wt% V_2O_5 (Zou et al., 2021). Phosphate deposits also contain vanadium, especially when associated with black shales (Piper, 1994). In phosphorite horizons, vanadium can be also present in U-bearing apatite (Abed et al., 2014). Vanadium extraction from phosphorites is not always economically acknowledged, but when considered profitable, it should follow the initial leaching process (Brough et al., 2019).

3. Geological setting of the African continent

The African continent consists of three major cratons (i.e., the West African, Greater Congo, and Kalahari Cratons), which grew through the Paleoproterozoic and Mesoproterozoic orogenic cycles and were stabilized in late Neoproterozoic (Frost-Killian et al., 2016). The collision of these cratons during the Pan-African and Brasiliano orogenies (550 ± 100 Ma) resulted in the formation of several mobile belts, and the assemblage of the Gondwana supercontinent (Fig. 2) (Goscombe et al., 2004; Johnson et al., 2006; Abbate et al., 2015; Frost-Killian et al., 2016; Ntiharirizwa et al., 2018). In Namibia and Botswana, the Damara orogen resulted from the collision of the Sao Francisco-Congo and Kalahari cratons (Gray et al., 2006; Miller, 2008). In the East Africa, the Mozambique Mobile Belt extends from Ethiopia, Kenya, and Somalia via Tanzania to the north and Malawi and Mozambique to the south (Fig. 2) (Ray, 1974). The northern part of the Mozambique Belt consists predominantly of high-grade metamorphic terranes dated at 1,100 and 970 Ma, with some older components. They constitute a mega-nappe superimposed over the ca. 1,140–1,120 Ma Nampula Block during the Pan-African continental collision (Grantham et al., 2008; Frost Killian et al., 2016). The Neoproterozoic lithologies of the Mozambique Belt occupy the central parts of Kenya, while the Madagascar island consists of two geological domains: the Precambrian crystalline basement and the overlying Phanerozoic unmetamorphosed sedimentary successions. The central and eastern two-thirds of the island are mainly composed of Archean to Neoproterozoic basement rocks, made up of metamorphic schists and gneiss intruded by granite and mafic igneous rocks (e.g., Roig et al., 2012). In Tanzania the Mozambique Belt surrounds the Craton consisting of Archean granite and greenstone rock assemblages (Kabete et al., 2012).

The West African Craton (WAC) covers an area of more than 1,500 km^2, stretching from Senegal, Guinea, Sierra Leone, Mali, Ghana, and Niger, between the Reguibat and the Man Shields. In the western part,

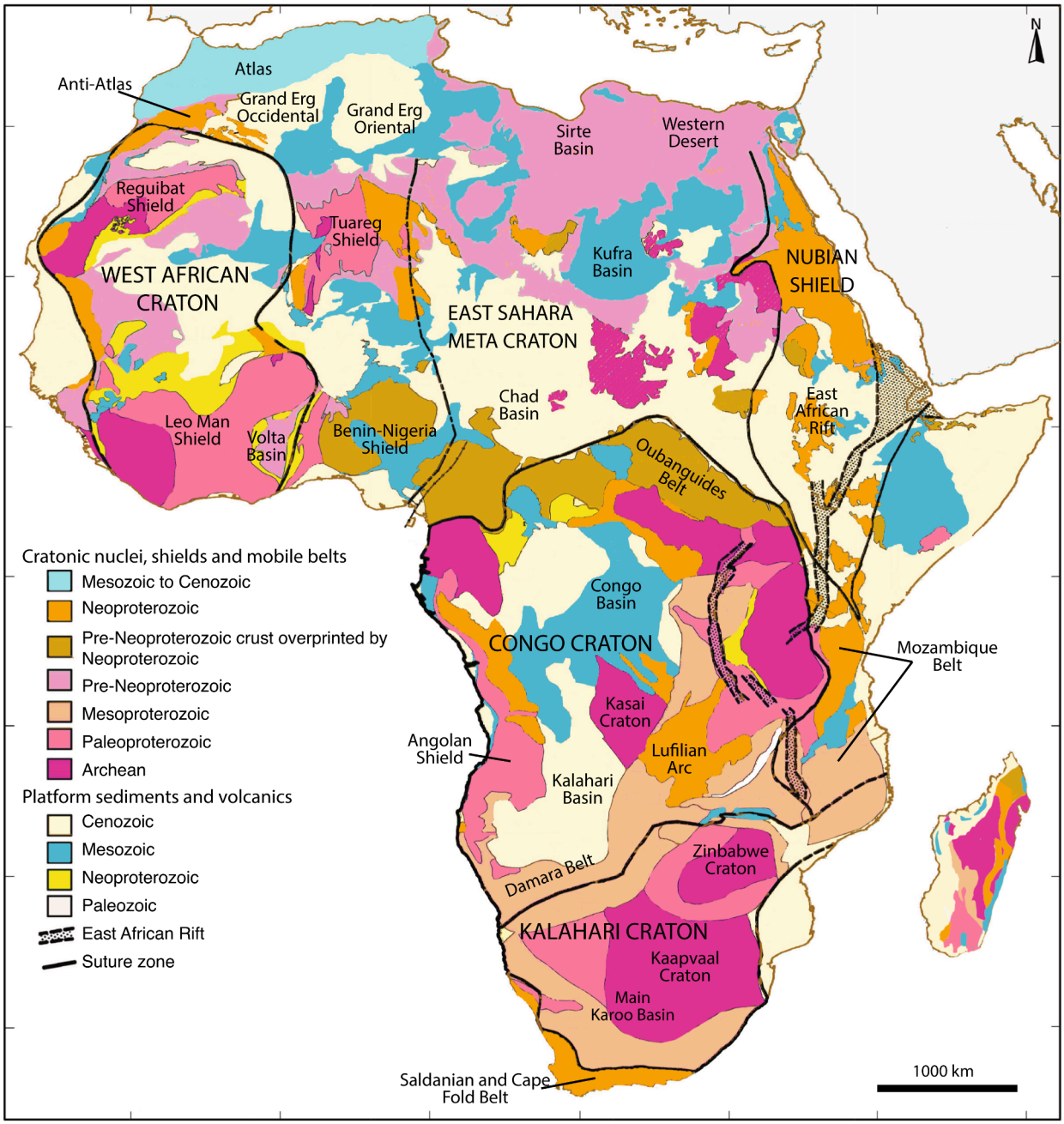

Fig. 2. Geological sketch map of the Africa continent (modified from Frost-Killian et al., 2016).

the Man Shield comprises Archean rocks metamorphosed during the Liberian Orogeny (2.5–3.0 Ga), whereas the easternmost side was affected by tectono-thermal reworking during the Eburnean (i.e., Birimian) orogeny in the Paleoproterozoic (1.9–2.3 Ga) (Dorbor, 2010). The craton margins are defined by Neoproterozoic Pan-African belts (ca. 550 Ma) (Fig. 2) (Gunn et al., 2018). The Archean part of the WAC in the South is a granite-greenstone terrane comprising older granitic gneisses and migmatites. In Burkina Faso, three major Birimian greenstone belts occur in the south and the west of the country, and a fourth in the central and northeastern regions (Dorbor, 2010).

Rocks of the alleged Neoarchean Kasai Craton outcrop in the northeast of Angola. In the Democratic Republic of Congo (DRC) the basement consists of Archean pre-Mayombean and Ruzizian gneisses and migmatites, and Middle Proterozoic metamorphosed sedimentary sequences (Kadima et al., 2011). Possible equivalents of the Franceville Series of Gabon (1,700 Ma) occur unconformably on the basement over large areas in the north of the Congo Basin and in parts of the area north of the Katanga Copperbelt (Kadima et al., 2011).

The major tectono-stratigraphic domains recognized in Northern Africa are: (1) the Precambrian province that includes the West African Craton and the intervening Tuareg Shield and "Saharan Metacraton"; (2) the Variscan (Paleozoic) Fold Belt; and (3) the Atlas-Alpine (Mesozoic-Cenozoic) system (Bouabdellah and Slack, 2016). The oldest rocks in Northern Africa have Archean to Paleoproterozoic age (~3.5–2.5 Ga) and occur in the Reguibat and the Tuareg shields along with the Saharan Metacraton (Fig. 2). They consist of medium- to high-grade gneiss, migmatite, and granulite, together with low-grade volcano-sedimentary rocks, all of which are intruded by ca. 750 to 550 Ma Neoproterozoic granitoids. The Phanerozoic evolution (2.5–0.57 Ga) reflects in Northern Africa both the assembly of Pangea and the polyphasic break-up of the Gondwana supercontinent. The belt development around the West African Craton by the end of Early Cambrian and during the Variscan

Orogeny resulted in the formation of the Maghrebian and Mauritanides Belts (Guiraud et al., 2005). Overall, the stratigraphy of the Paleozoic consists of a succession of greater than 4,000 m folded and metamorphosed (greenschist-facies) Cambrian-Ordovician to Carboniferous marine to continental sediments, locally intruded by late Variscan calc-alkaline granitoids. The Variscan orogeny (from 330 to 290 Ma) reactivated the older Pan-African structures and constituted the fundamental tectonic control for the late Variscan tectonic inversion and Alpine deformations in the northern part of the African continent.

The Mesozoic and Cenozoic geological evolution in Northern Africa involved two major events: (1) the opening of the North Atlantic and Neotethys oceans in the early Mesozoic, and (2) the continental collision between the African-Arabian and Eurasian plates in the middle Cenozoic. These events resulted in the development of the Alpine Maghrebian Belts (i.e., the Rif-Tell fold-and-thrust belt in the north, the Atlas, and the Anti-Atlas Mountains in the south) along the northern African-Arabian margin (Michard, 1976; Gomez et al., 2000). During the Cretaceous and most of the Tertiary, several basins developed in different regions of Northern Africa. These basins reflect several stages of opening of the Atlantic Ocean, coupled with the evolution of northern and southern Peri-Tethys platform areas on both sides of the African/Arabian-Eurasian convergent plate boundary (Meulenkamp and Sissingh, 2003; Bouaziz et al., 2002).

In southern, southwestern and southeastern Africa a series of basins formed during the break-up of Gondwana (Fig. 2) (Johnson et al., 2006). In South Africa, the Main Karoo Basin is the largest Phanerozoic basin, ranging in age from late Carboniferous to early Jurassic (Fig. 2). In Namibia, Angola, Botswana and southern DRC Paleozoic to Cenozoic rocks of the Karoo and Kalahari Supergroups cover the Proterozoic rocks (Milési et al., 1992; Kadima et al., 2011; Schlüter, 2016). During Cretaceous the tropical climate triggered deep weathering and rapid erosion, and at the end of this period, southern Africa, Namibia, and northern Botswana were transected by a major erosional surface known as the "African surface" (related to the African erosion cycles) (Partridge and Maud, 1987). Thick successions of detrital sediments of the Kalahari Supergroup are also widespread in the above regions, and calcrete soils developed when climate switched from a tropical to arid regime in the Miocene (Johnson et al., 2006).

In Kenya, Ethiopia, Somalia, Tanzania, Malawi, Mozambique and Madagascar, sedimentary sequences ranging in age from Mesozoic to Recent correlate with the continental Karoo sequence of southern Africa (Ray, 1974; Roig et al., 2012).

A large variety of mafic intrusions were emplaced through the cratons and in the surrounding belts, and into the sedimentary basins from Archean to Holocene. These intrusions form pipes, volcanic complexes, dykes, sills, laccoliths, lopoliths, and large layered intrusive bodies and host some of the most significant mineral deposits of the continent (Frost-Killian et al., 2016). Considering the purposes of this paper, it is relevant here to mention the Bushveld Complex, which intruded the Transvaal Supergroup sedimentary succession in the north-central portion of the Kaapvaal Craton (South Africa) at about 2.05 Ga (e.g., Eales and Cawthorn, 1996), and the 2.54 Ga old Great Dyke of Zimbabwe, a 550 km long layered ultramafic to mafic igneous complex consisting of four amalgamated funnel-like intrusions (e.g., Wilson, 1996). More recent dolerite sills and dyke swarms intruded the Karoo sedimentary and volcanic rocks (McCourt, 2016). The effusive basaltic volcanic event of the Etendeka Group (Johnson et al., 2006) marks the break-up of Gondwana and the formation of the South Atlantic Ocean in the Early Cretaceous. The development of the East African Rift System caused the deposition of several types of volcanic products in the tectonic rift valley (Akech et al., 2013). Miocene magmatic rocks occur in the northernmost part of Tunisia (e.g., Bouaziz et al., 2002).

4. Vanadium deposits and occurrences in southern and southwestern Africa

4.1. Botswana

The Kihabe and Nxuu Zn-Pb-V > (Cu-Ag-Ge) prospects occur at the boundary between Namibia and Botswana (Aha Hills, Ngamiland District) in a deformed Proterozoic fold belt, corresponding to the NE extension of the Namibian Damara Orogen, called the Ghanzi–Chobe zone (Figs. 3 and 4) (Loxton, 1981;Carney et al., 1994; Key and Ayers, 2000). The Kihabe prospect contains Zn-Pb resources of 14.4 million tons at 2.84% zinc equivalent, Ag resources of 3.3 million ounces, and V-Ge amounts still not evaluated at a resource level (Table 1) (Mondillo et al., 2020). The ores are represented by mixed sulfide–nonsulfide mineralizations. Sulfide minerals consist mainly of sphalerite, galena, and pyrite in a metamorphic quartzwacke. Among the nonsulfide assemblage, two styles of mineralizations occur: i. early hydrothermal willemite and fraipontite; ii. late supergene smithsonite, cerussite, hemimorphite, Pb-phosphates, arsenates, Zn-smectite and vanadates (Mondillo et al., 2020; Putzolu et al., 2023). The Kihabe orebody has an elongated shape, with an average width of 27 m and a strike length of 2.4 km (Mapeo, 2007). The sedimentary sequence from the bottom to the top consists of: i. deformed barren dolostone; ii. deformed quartzwacke (Aha Hills Formation), which hosts the mineralizations; iii. recent sediments, mainly consisting of calcrete, located at the bottom of the Kalahari Group, with a thickness ranging between 5 and 15 m (Key and Ayers, 2000; Mondillo et al., 2020). The Nxuu prospect consists mainly of oxidized mineral phases, with only traces of remnant sulfides. In both prospects, variable amounts of vanadium and traces of Ag and Ge have also been detected (Mount Burgess Mining N.L., 2020). At Kihabe, vanadium is mainly hosted in descloizite, which occurs as small crystal aggregates and crusts around quartz clasts in calcrete. In the Nxuu prospect, vanadium is enriched at the bottom of the Kalahari sediments and in small veins cutting the underlying quartzite (Putzolu et al., 2023). The most abundant V-bearing mineral at Nxuu is descloizite, which in the Kalahari sediments displays textures suggesting a supergene origin. In the quartzite, vanadium is associated with hydrothermal carbonates such as Zn-dolomite and Pb-calcite. This kind of occurrence has also been observed in the Berg Aukas mine in the Otavi Mountainland (Namibia) (Boni et al., 2007). It suggests that the vanadates are genetically related to the calcrete formation, and thus to the climatic shift toward more arid conditions.

Several sandstone-hosted roll-front/calcrete U-(V) deposits have been investigated in Botswana, among which the Letlhakane project in the Karoo sediments in the northeast of the country is the most significant. Supergene remobilization and reprecipitation of uranium have also resulted in the formation of calcrete-hosted *carnotite*, occurring as fine, yellow coatings on fracture surfaces and bedding planes (Kinnaird and Nex, 2016). A deposit containing a lead–uranium-vanadium hydrate has been found at Mokobaesi in the Serule area of eastern Botswana in nodular calcrete formed within a palaeodrainage channel (IAEA, 2020).

4.2. Namibia

Two vanadium ore deposit types have been described so far in Namibia (Fig. 3; Table 1). The first and most significant ores are the vanadate concentrations spread across the Otavi Mountainland (OML) (Fig. 5). The second type consists of the calcrete U-(V) deposits in the Erongo region.

The Zn-Cu-Pb vanadate ores in the OML represent a peculiar, low-temperature, weathering-related, nonsulfide ore type. These were considered the largest vanadium deposits in the world, with resources estimated at several million tons of ore. The content of the already exploited deposits amounts to more than 50,000 tons of V_2O_5 (Wartha and Schreuder, 1992). The vanadium ores occur in collapse breccias and solution cavities in karstic networks associated with the post-Gondwana

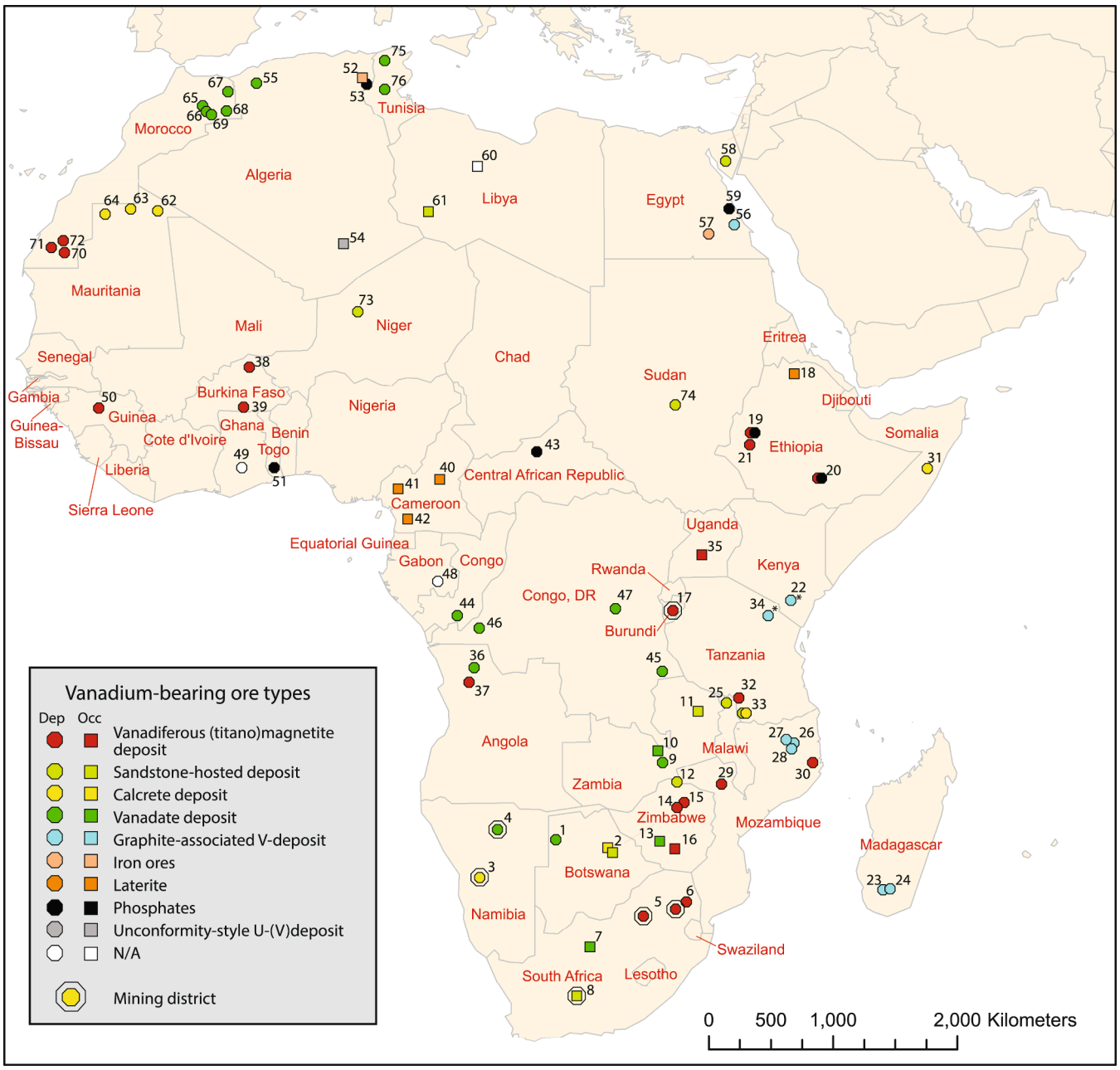

Fig. 3. Location of main vanadium occurrences and deposits, subdivided by ore-types, in the African countries. Numbers and References are reported in Table 1.

land surfaces (Figs. 6 and 7A,B). Economic concentrations are hosted in carbonate rocks of the Neoproterozoic Otavi Group, which also contain sulfide and nonsulfide orebodies. Descloizite occurs in the areas surrounding Zn-rich orebodies (Berg Aukas type) (Fig. 7C,D) (Pirajno and Joubert, 1993). Vanadinite, although present, is less common (Fig. 7E) (Boni et al., 2007). Mottramite and Cu-descloizite are particularly abundant around primary Cu sulfide deposits (Tsumeb type; Fig. 7F). Carbon and oxygen stable isotope data of coeval carbonates indicate that most vanadate deposits were formed at temperatures of ~ 40° to 50 °C by meteoric waters interacting with Neoproterozoic shales, carbonates, and related primary sulfide ores (Boni et al., 2007). The source of vanadium is mainly in the siliciclastic country rocks of the Nosib Group and in the mafic rocks of the Archean and Paleoproterozoic basement. The base metals were derived from primary sulfide deposits undergoing oxidation (Van der Westhuizen et al., 1988).

Vanadium-rich tailings around the Berg Aukas old mine in northeastern Namibia, have a volume of 343,500 m^3 (Mapani et al., 2010; Sracek et al., 2014). The tailings could be a good source of secondary vanadium and can be exploited as such; in fact, several junior companies (e.g., Sabre Resources Ltd., Golden Deeps Ltd.) actively explore possible vanadate resources in and around the old mining areas of Abenab, Berg Aukas, and Baltika. High concentrations of vanadium (average V grades above 1.20% V_2O_5 up to 3.7% V_2O_5 at the Nosib Prospect) have been detected and are currently being processed from tailings and dumps of the historic mining operations.

The Erongo U-(V) mineralizations in Central Namibia are enriched in carnotite formed under semi-arid to arid climate (Hambleton-Jones, 1976; Hartleb, 1988) (Figs. 8 and 9). The typical Langer Heinrich (Becker and Kärner, 2009) and Klein Trekkopje (Bowell et al., 2008) deposits are located within the Namib Desert (Bowell and Davies, 2017). Both deposits are hosted by calcretes developed within Tertiary paleochannels (Figs. 8 and 9) (Trittschack, 2008). The weathered

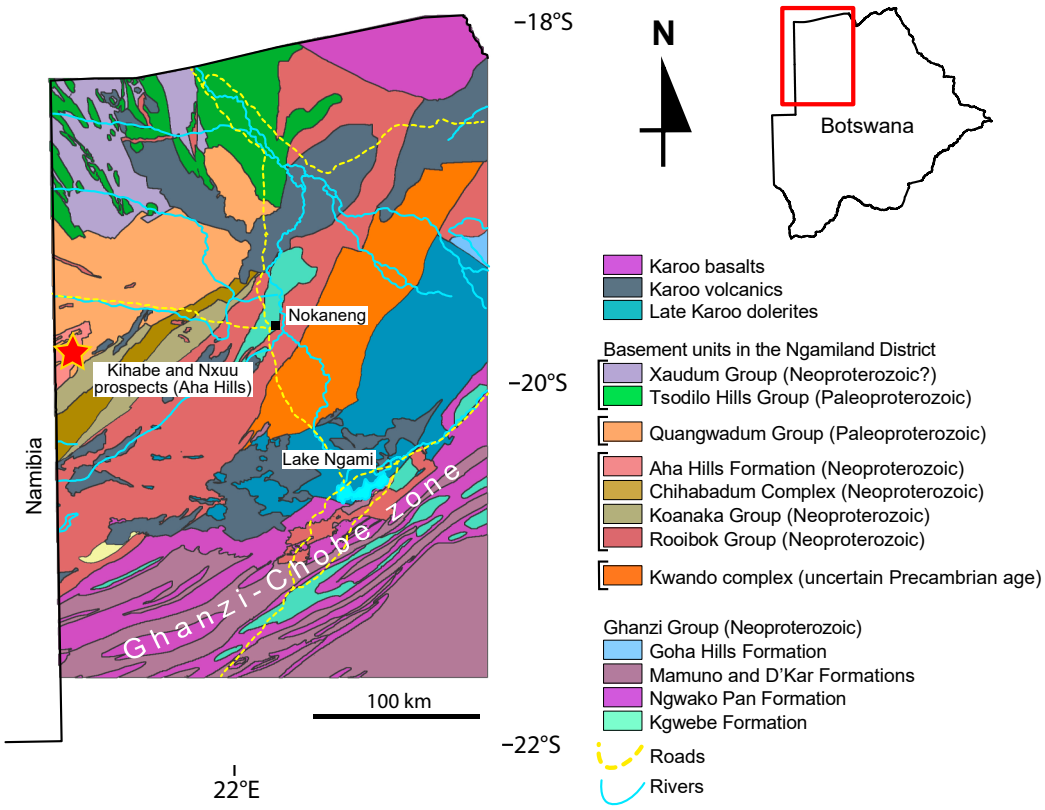

Fig. 4. Geological map of northern Botswana, with the location of the Kihabe and Nxuu projects (reproduced from Mondillo et al., 2020). The Kalahari sedimentary cover is not shown.

Bloedkoppie granite (containing 5 to 15 ppm U) is considered the source of U for the Langer Heinrich deposit, while the Tinkas schists (containing 120 to 160 ppm V), was the source of V (Lilende, 2012). Over 9,000 tons of V_2O_5 were also assessed during 2015 by Areva at Klein Trekkopje, as a by-product of uranium exploitation (Kinnaird and Nex, 2016). The source of vanadium was from the Kuiseb schists, which contain about 100 to 160 ppm V (Youlton, 2007).

4.3. South Africa

Vanadiferous (titano)magnetite (VTM) deposits in South Africa are the principal vanadium source of the African continent and one of the most significant in the world (Kelley et al., 2017). The VTM deposits consist of magmatic accumulations of (titano)magnetite and ilmenite, which could host more than 1.5 wt% V_2O_5 (Reynolds, 1985), as is the case of the Paleoproterozoic Bushveld Complex (Figs. 2, 3 and 10). This igneous complex (2.06 Ga) extends along the North-West Limpopo and Mpumalanga Provinces, and it is well-known for hosting the most significant chromite deposits and related platinum group metals (PGMs) of the world (Cawthorn et al., 2002; Cawthorn, 2005; Naldrett, 2010; Zientek, 2012). The Bushveld complex displays discrete alternating layers (Tegner et al., 2006) with cumulative thicknesses of about 9 km that are concordant with the 0.1 to 10 m-thick igneous layering (Figs. 10 and 11). The oxide layers can be traced for hundreds of kilometers along strike. The mafic to ultramafic host rocks occur as stratiform tabular bodies, such as sills and laccoliths. Vanadium-bearing (titano)magnetite- and apatite-bearing layers occur at the top of the magmatic sequence (Fig. 11) (Reynolds, 1985; Cawthorn and Molyneux, 1986). Exposure to weathering of magnetite resulted in the formation of vanado-maghemite [$(FeTi)_2O_3$] and hematite (Matrix Reference Materials, 2021). Major mining operations occur for example at Vametco and Brits (Bushveld Vanadium), Mapochs in Mpumalamga (Limpopo Province; Highveld Steel and Vanadium Corporation), Rhovan in the southwestern limb of the Bushveld Complex, and Steelpoortdrift, which is situated about 200 km from Johannesburg. The Vametco deposit has a 184.2 Mt JORC-compliant resource, including 46.4 Mt in reserves, with averaging 2.0% V_2O_5 in magnetite (MSA Group Pty Ltd, 2022; http://www.bushveldminerals.com). The Brits deposit reports Inferred and Indicated Mineral Resource distributed across the three seams (the Lower, Intermediate, and Upper Seams) of 66.8 Mt at an average grade of 1.6% V_2O_5 in magnetite (Witley et al., 2019).

Another V-ore type in South Africa includes the Phalaborwa carbonatite complex in the Limpopo Province. The complex formed through an alkaline intrusive cycle and consists of pyroxenite, syenite, and ultramafic pegmatoids, followed by phoskorite and banded carbonatite plugs. The Paleoproterozoic age of the main carbonatite bodies (2.06 Ga) is similar to the age determined for the Bushveld Complex. The magnetite by-products, contained mainly in phoskorite and banded carbonatite, can host more than 2,000 ppm V (Milani et al., 2017).

Since 1970, many uranium occurrences of variable grades have been discovered in the southwestern parts of the Karoo Supergroup. The uranium ore is disseminated, sandstone-hosted and occurs in peneconcordant, tabular orebodies. Most common uranium minerals consist of uraninite, coffinite, and uranium–carbon complexes. Among subordinate secondary minerals, carnotite has been detected, which formed from recent oxidation and weathering (IAEA, 2020). However, it is worth mentioning that in the southern African Karoo U systems, the V potential is generally not considered economic.

Fluvial and lacustrine sediments with variable amounts of carnotite unconformably overlie the Senonian to Miocene African surface in many parts of South Africa, especially in the arid and semi-arid areas of the Northern Cape Province. Both U and V were sourced from granite

Table 1
Main vanadium occurrences and deposits in Africa.

Region	Country	Region/District/ Deposit	Type	Main host minerals and features	Main co-elements	Historical production and local concentrations	Vanadium resources	Reference	Position in Fig. 3
Southern and Southwestern Africa	Botswana	Kihabe and Nxuu (Aha Hills, Ngamiland District)	Vanadate deposit	Descloizite, Vanadinite	Zn, Pb, Ge, Ga	N/A	Not evaluated	Mondillo et al., 2020	1
	Botswana	Letlhakane project (Francistown, Northeastern district)	Sandstone-hosted deposit	Carnotite in roll-front U ores and V in calcretes	U	N/A	Not evaluated	Acap Energy, 2015; Kinnaird & Nex, 2016	2
	Namibia	Larger Heinrich, Klein Trekkopje and others (Erongo Region)	Calcrete deposit	Carnotite	U		Langer Heinrich: 9,000 tons V_2O_5; Klein Trekkopje: 18,000 tons vanadium	Hartleb, 1988; Lilende, 2012; Kinnaird & Nex, 2016	3
	Namibia	Otavi Mountainland District (e.g., Abenab, Berg Aukas, Baltika, Okorundu deposits)	Vanadate deposit	Descloizite, Vanadinite, Mottramite	Zn, Pb, Cu, Ge	1919–1978 50,000 tons V_2O_5	2.35 Mt @ 2.1–1.03% V_2O_5 (Abenab & Berg Aukas). Abenab: Inferred Mineral Resource 2.80 Mt @ 0.66% V_2O_5	Verwoerd, 1957; Van der Westhuizen et al., 1988; Warta & Schroeder, 1992; Boni et al., 2007; Golden Deeps, 2022	4
	South Africa	Bushveld Complex District (mainly Limpopo and Mpumalanga Provinces); Mapochs, Brits, Steelpoortdrif mines etc.	Vanadiferous (titano)magnetite deposit	Magnetite, Coulsonite	Fe, Ti, P (Cr-PGE)	2021 South Africa Vanadium production: 9,100 Mt	Estimated reserves 3,500 thousand tons	Reynolds, 1985; Frost-Killian et al., 2016; Kelley et al., 2017; U.S. Geological Survey, 2022	5
	South Africa	Phalaborwa Complex (Limpopo Province)	Vanadiferous (titano)magnetite deposit	Magnetite in carbonatite	Cu, Ti, P, REE	N/A	Not evaluated	Milani et al., 2017	6
	South Africa	Pering deposit	Vanadate deposit	Descloizite and vanadinite in base metal ores in Transvaal dolomites	Zn, Pb	N/A	Not evaluated	Cairncross & Dixon, 1995	7
	South Africa	Karoo Uranium Province (between Laingsburg, Cradock and Bloemfontein)	Sandstone-hosted deposit	Carnotite in roll-front U ores	U	N/A	Not evaluated	IAEA, 2020	8
	Zambia	Kabwe mine and surroundings (Central Province)	Vanadate deposit	Descloizite, Mottramite, Vanadinite	Pb, Zn, Ge, Ba	Until 1994: 7,820 tons up to 2.40% V_2O_5. From 2019 exploitation of waste material containing 1.26% V_2O_5.	Not evaluated	Taylor, 1955; Cairney & Kerr, 1998; Kamona & Friedrich, 2007	9
	Zambia	Copperbelt in the Mukambala and Kabamba areas (Mkushi and Masaiti Districts, Central Province)	Vanadate deposit	Vanadium associated with sulfides and manganese	Mn, Cu, Zn	N/A	Not evaluated	Maxtech Mining Zambia, 2018	10
	Zambia	Mutanga (North East Zambia)	Sandstone-hosted deposit	Not detected, but vanadium traces in Karoo sediments	U	N/A	Not evaluated	IAEA, 2020; Yeo, 2011	11
	Zimbabwe	Kanyemba (Guruve District, Mashonaland Central)	Sandstone-hosted deposit	Not detected (Carnotite?) in the Karoo sediments	U	N/A	12.8% V_2O_5 in U ore	Komuro et al., 1994	12
	Zimbabwe	Bulawayo area	Vanadate deposit	Vanadate minerals	not detected	N/A	Not evaluated	Amm, 1940; Fischer, 1975	13

(*continued on next page*)

Table 1 (*continued*)

Region	Country	Region/District/ Deposit	Type	Main host minerals and features	Main co-elements	Historical production and local concentrations	Vanadium resources	Reference	Position in Fig. 3
	Zimbabwe	Darwendale Platinum Project	Vanadiferous (titano)magnetite deposit	Magnetite	Fe, Ti, Cr, Pt	N/A	Not evaluated	JSC Afromet	14
	Zimbabwe	Chuatsa Vanadium Project (Mt Darwin)	Vanadiferous (titano)magnetite deposit	Magnetite	Cu, Co, Ti, Fe	Historical data (1960) 0.8–1 % V_2O_5	Not evaluated	Six Sigma Metals, 2018	15
	Zimbabwe	Mberengwa area	Vanadiferous (titano)magnetite deposit	Magnetite	Cu, Co, Ti, Fe	Historical data (1960) 0.8–1 % V_2O_5	Not evaluated	Northern Shaft, 2020	16
Eastern Africa	Burundi	Mukanda (Gitega Province)	Vanadiferous (titano)magnetite deposit	Ti-Magnetite	Fe, Ti	N/A	Mukanda vanadium: total of 6,500,000 tons of vanadium Proven Reserves at 0.63 % V (cut-off 0.2 % V), 7,300,000 tons of Probable and 5,000,000 tons of Possible Reserves.	Smejkal, 1985; Nimpagaritse, 1986; Burundi Ministry of Energy and Mines, 1991; Deblond, 1993; Deblond & Tack, 1999; Yager, 2009	17
	Ethiopia	Shire (Tigray)	Laterite	Fe-oxy-hydroxides) in ferricrete	Fe	1,300 ppm	Not evaluated	Konka et al., 2013	18
	Ethiopia	Bikilal	Vanadiferous (titano)magnetite deposit	Ti-Magnetite	Fe, Ti	N/A	Not evaluated	Gautneb et al., 2001; Ghebre, 2010	19
	Ethiopia	Melka Arba	Vanadiferous (titano)magnetite deposit	Ti-Magnetite	Fe, Ti	N/A	Not evaluated	Gautneb et al., 2001	20
	Ethiopia	Gimbi-Dalati	Vanadiferous (titano)magnetite deposit	Ti-Magnetite	Fe	N/A	Not evaluated	Tadesse et al., 2003	21
	Kenya	Lualenyi Mine; Kide Hill (Taita Hills district); Mwatata province	Graphite-associated vanadium deposit	Vanadium grossular "*Tsavorite*"	Vanadian garnet gems	N/A	Not evaluated	Pohl et al., 1979; Suwa et al., 1996; Giuliani et al., 2018	22
	Madagascar	Green Giant cluster (e.g., Jaky, Manga, and Mainty)	Graphite-associated vanadium deposit	*Roscoelite* (up to 8.45% V_2O_3), rutile, schreyerite, oxyvanite, karelianite, V-bearing sulfides	graphite	N/A	Total Indicated resource: 49.5 Mt @ 0.693% V_2O_5, containing 756.3 Mlb of vanadium pentoxide. Total Inferred resource: 9.7 Mt @ 0.632% V_2O_5, containing 134.5 Mlb vanadium pentoxide	Barrie, 2009; Desautels et al., 2011; 2012; Di Cecco & Tait, 2018; Parnell, 2022	23
	Madagascar	Molo (Tulear Region)	Graphite-associated vanadium deposit	*Roscoelite*	graphite	N/A	Not evaluated	AGP Mining Consultants Inc., 2011; Scherba et al., 2018	24
	Malawi	Kayelekera Uranium deposit (Northern Malawi)	Sandstone-hosted deposit	Not detected (Carnotite?) in the Karoo sediments	U	N/A	Not evaluated	Bowden and Shaw, 2007; IAEA, 2020; Becker et al., 2014	25
	Mozambique	Montepuez and Balama Graphite Projects (Cabo Delgado)	Graphite-associated vanadium deposit	*Roscoelite*	graphite	N/A	Balama: 1.422 Bt graphite at 0.2 % V_2O_5;	Syrah Resources, 2019; Battery Minerals, 2019	26
	Mozambique	Caula Project (Cabo Delgado)	Graphite-associated vanadium deposit	*Roscoelite*	graphite	N/A	JORC (Measured) vanadium-graphite resource: 22 Mt @ 0.37% V_2O_5 (0.2% cut-off) and 13.4% TGC (8% cut-off) for 81,600 tons of vanadium	New Energy Minerals, 2018; Marketscreener.com., 2018	27

(*continued on next page*)

Table 1 (*continued*)

Region	Country	Region/District/ Deposit	Type	Main host minerals and features	Main co-elements	Historical production and local concentrations	Vanadium resources	Reference	Position in Fig. 3
							pentoxide (180 million pounds).		
	Mozambique	Nicanda Hill Project (contained in Balama project)	Graphite-associated vanadium deposit	*Roscoelite* and others	graphite	N/A	JORC Inferred and Indicated Mineral Resource: 1.44Bt @ 11.1% TGC and 0.29% V_2O_5 for 160.3 million tons of contained graphite and 4.2 million tons of contained vanadium.	Triton Minerals, 2020	28
	Mozambique	Tete Mafic Complex (NW Mozambique)	Vanadiferous (titano)magnetite deposit	Magnetite	Fe, Ti	N/A	At Chitongue Grande there are: 47.7 Mt JORC inferred resource, head grade of 25.3% Fe, 0.18% V_2O_5 and 9.69% TiO_2	Barr & Brown, 1987; Baobab, 2010; Callaghan, 2011; Frost-Killian et al., 2016	29
	Mozambique	Memba Project (Nampula Province)	Vanadiferous (titano)magnetite deposit	Magnetite	Fe, Ti	N/A	Not evaluated		30
	Somalia	Uranium deposits (Mudugh Province, Dusa Mareb-El Bur region)	Calcrete deposit	Carnotite	U	N/A	Not evaluated	Briot, 1984	31
	Tanzania	Liganga, Uluguru Mountains, Mbabala, Karema, Manyoro Gondite, Itewe (Ludewa District, Njombe Region)	Vanadiferous (titano)magnetite deposit	Magnetite	Fe, Ti	N/A	Not evaluated	Geological Survey of Tanzania, 2015	32
	Tanzania	Mkuju River, Mbamba Bay projects (southern Tanzania)	Sandstone-hosted deposit	Carnotite in sandstones and calcrete in Karoo sediments	U	N/A	Not evaluated	IAEA, 2020; Schlüter, 2008	33
	Tanzania	Lemshuku (Mererani area)	Graphite-associated vanadium deposit	Vanadium grossular *Tsavorite*	Vanadian garnet gems	N/A	Not evaluated	Feneyrol et al., 2012, 2017	34
	Uganda	Nangalwe, Sikusi, Surumbusu (Bukusu Mbale District)	Vanadiferous (titano)magnetite deposit	Magnetite in carbonatite	Fe, Ti	N/A	Not evaluated	Welch, 1958	35
Western Africa	Angola	Lueca mine (northern Damba region)	Vanadate deposit	Mottramite > Descloizite, Vanadinite	Cu, Zn, Pb	N/A	Not evaluated	Millman, 1960; Pauly, 1962; Fischer, 1975	36
	Angola	Kassala-Kitungo deposit (Kwanza Norte Province)	Vanadiferous (titano)magnetite deposit	Magnetite	Fe	N/A	Not evaluated	–	37
	Burkina Faso	Tin Edia (Oudalan province)	Vanadiferous (titano)magnetite deposit	Ti-Magnetite	Fe, Ti	N/A	Reserves: 60 Mt magnetite with a 1 % V_2O_5 and 8–14% TiO_2 average.	Soussou, 1974; Neybergh et al., 1980; Markwitz et al., 2015	38
	Burkina Faso	Nahouri Project (southeast of Tiebele)	Vanadiferous (titano)magnetite deposit	Ti-Magnetite	Fe, Ti	N/A	Exploration target: between 22.5 Mt and 171 Mt (Magnetite); 0.2–05%	Vital Metals (2018)	39
	Cameroon	Ngaoundal (Adamaoua Region)	Laterite	Fe-hydr(oxides) in bauxites deriving from basalts	Fe, Ti, Al	0.37–1.18% V_2O_5 Ngaoundal	Not evaluated	Hiéronymus, 1985; Ndema Mbongué, 2020	40
	Cameroon	Fongo-Tongo bauxites (West Cameroon)	Laterite	Fe-hydr(oxides) in bauxites deriving from basalts	Fe, Ti, Al	60–438 ppm in bauxite	Not evaluated	Hiéronymus, 1985; Ndema Mbongué, 2020	41

(*continued on next page*)

Table 1 (*continued*)

Region	Country	Region/District/ Deposit	Type	Main host minerals and features	Main co-elements	Historical production and local concentrations	Vanadium resources	Reference	Position in Fig. 3
	Cameroon	Nkomakak area (South Cameroon)	Laterite	Fe-hydr(oxides) in bauxites deriving from basalts	Fe, Ti, Al	1.19% V_2O_5 Nkomakak	Not evaluated	Hiéronymus, 1985; Ndema Mbongué, 2020	42
	Central African Republic	Bakoumi District	Phosphates	Fluoroapatite in continental phosphatic sediments	P, U	N/A	Not evaluated	IAEA, 2020	43
	Congo Brazzaville	M'Passa deposit (Niari syncline)	Vanadate deposit	Vanadates of supergene origin	Cu, Pb, Zn	N/A	Not evaluated	Buffet et al., 1987	44
	DRC Congo	Mutoshi mine (Katanga)	Vanadate deposit	Vanadium traces in supergene enrichment zone above Copperbelt sulfides	Cu, Co, Zn	N/A	Not evaluated	Cox et al., 2003; IAEA, 2020	45
	DRC Congo	Bamba Kilenda (Bas-Congo Province)	Vanadate deposit	Vanadates and oxides in supergene enrichment zone	Cu, Pb, Zn	N/A	Not evaluated	Lesaffer, 2014	46
	DRC Congo	Kusu deposit (Congo Central)	Vanadate deposit	Vanadates (*kusuite*) and oxides in supergene enrichment zone	Cu, Pb, Zn	N/A	Not evaluated	Deliens & Piret (1977	47
	Gabon	Oklo & Mounana Uranium-(V) deposits (Franceville basin SE Gabon)	N/A	Urano-vanadiferous mineralization: *francevillite* and black oxides in sandstone and black shales	U	N/A	Not evaluated	Bros et al., 1992; Gauthier-Lafaye, 1986; Horie et al., 2005; IAEA, 2020; Ossa Ossa et al., 2020	48
	Ghana	Nsuta Mine (Ashanti Belt)	N/A	Vanadium-bearing jacobsite in weathered hydrothermal Mn deposits (rhodocrosite and alabandite)	Mn	N/A	Not evaluated	Mücke et al., 1999	49
	Guinea	Merela Project	Vanadiferous (titano)magnetite deposit	V-bearing magnetite & Ti-bearing ilmenite	Fe-Ti-Ni-Co-Sc	N/A	141 Mt pyroxenite @10% TiO_2, 0.1% V_2O_5	Douglas-Hamilton, 2023; Optiva Resources Ltd., 2023	50
	Togo	Hahotoé-Kpogamé phosphorites (south Togo)	Phosphates	Vanadium traces in sedimentary phosphorites	P	N/A	Not evaluated	Tanouayi et al., 2016	51
Northern Africa	Algeria	Djebel Had (Tebessa province)	Iron ores	Goethite (512–560 ppm V)	Fe	N/A	Not evaluated	Schwertmann & Pfab, 1997; Diab et al., 2020	52
	Algeria	Djebel Onk mines (Bir El Atar area, Tébessa province)	Phosphates	Vanadium traces in sedimentary phosphorites	P	N/A	Not evaluated	Bezzi et al., 2012	53
	Algeria	Tahaggart deposit (Hoggar-Sud)	Unconformity-style Uranium deposits	Carnotite	U	N/A	Not evaluated	Kinnaird & Nex, 2016; Badahmaoui et al., 2020	54
	Algeria	Saida area (Oran)	Vanadate deposit	Descloizite, Endlichite, Vanadinite	Zn, Pb	N/A	Not evaluated	Lacroix, 1908	55
	Egypt	Mersa Alam (South Eastern Desert)	Graphite-associated vanadium deposit	V associated with graphite	graphite	N/A	Not evaluated	Bishady, 2017; Parnell, 2022	56
	Egypt	Aswan (South Egypt)	Iron ores	V in high-phosphorus iron ore	Fe, P	484 ppm in iron ore	Not evaluated	Baioumy et al., 2017	57
	Egypt	Bir Nasib & Wadi Nasieb deposits (West Central Sinai)	Sandstone-hosted deposit	Carnotite in iron-copper-manganese mineralization in siltstone	U, Fe, Cu, Mn	N/A	Not evaluated	IAEA, 2020	58

(*continued on next page*)

Table 1 (*continued*)

Region	Country	Region/District/ Deposit	Type	Main host minerals and features	Main co-elements	Historical production and local concentrations	Vanadium resources	Reference	Position in Fig. 3
	Egypt	Red Sea area	Phosphates	Vanadium traces in sedimentary phosphorites	P	1,056 and 2,800 ppm V in phosphorite	Not evaluated	Baioumy & Ismael, 2010; Baioumy, 2021	59
	Libya	Hun Graben (South Eastern Lybia)	N/A	V in goethite nodules in evaporites	Not detected	3,380 ppm V in nodules	Not evaluated	Lashhab & West, 1992	60
	Libya	Murzuk Basin (South Western Lybia)	Sandstone-hosted deposit	Carnotite, Tyuyamunite in roll-front U ores	U		Not evaluated	IAEA, 2020	61
	Mauritania	Tiris deposit (Sahara Desert North Eastern Mauritania)	Calcrete deposit	Carnotite	U	N/A	18.4 million pounds V	Kinnaird & Nex, 2016; Aura Energy Ltd., 2022	62
	Mauritania	Ain Ben Tili	Calcrete deposit	Carnotite	U	N/A	Not evaluated	Taylor et al., 2012; Kinnaird & Nex, 2016	63
	Mauritania	Bir Moghrein	Calcrete deposit	Carnotite	U	N/A	Not evaluated	Taylor et al., 2012; Kinnaird & Nex, 2016	64
	Morocco	Zeida deposit (Upper Moulouya District)	Vanadate deposit	Vanadinite, Descloizite, Mottramite	Pb, Ba, U, Cu	N/A	Not evaluated	Bouabdellah & Slack, 2016; Bouabdellah et al., 2021	65
	Morocco	Mibladen deposit (Upper Moulouya District)	Vanadate deposit	Vanadinite, Mottramite, Descloizite	Pb, Ba, Cu, Zn	N/A	Not evaluated	Bouabdellah et al., 2021	66
	Morocco	Touissit-Bou Beker (Jerada Province)	Vanadate deposit	Vanadinite, Mottramite	Pb, Zn, Cu, Ag	N/A	Not evaluated	Bouabdellah et al., 2021	67
	Morocco	Jbel Haouanit (Eastern High Atlas)	Vanadate deposit	Mottramite	Zn, Pb, Cu	N/A	Not evaluated	Verhaert et al., 2017	68
	Morocco	Toulal (Fès-Meknès Region)	Vanadate deposit	Desclozite	Zn, Pb	N/A	Not evaluated	Choulet et al., 2014	69
	Morocco	Gleibat Lafhouda (Moroccan Sahara)	Vanadiferous (titano)magnetite deposit	Magnetite in carbonatite	Fe, REE, Nb, U, Ti	N/A	Not evaluated	Bouabdellah et al., 2012; Boukirou et al., 2022	70
	Morocco	Twihinate (Moroccan Sahara)	Vanadiferous (titano)magnetite deposit	Magnetite in carbonatite	Fe, REE, U, Ti, Th	N/A	Not evaluated	Bouabdellah et al., in press	71
	Morocco	Awark, Aghracha, Awhifrite prospects (Moroccan Sahara)	Vanadiferous titanomagnetite/ magnetite and Calcrete deposit	Magnetite in carbonatite; carnotite-bearing calcrete	Fe, U	50 to up to 1,495 ppm	Not evaluated	www.ONHYM.com	72
	Niger	Imouraren (Agadez Region)	Sandstone-hosted deposit	Molybdenum-vanadium oxides; montroseite	U, Zr, Mo, Zn	N/A	Not evaluated	IAEA, 2020; Mamadou et al., 2022; Pagel et al., 2005	73
	Sudan	Kurun and Uro areas (Nuba Mountains); Hufrat EL Nahas (Darfur)	Sandstone-hosted deposit	Not detected	U	N/A	Not evaluated	Adam et al., 2014; Osman Sedig, 2018	74
	Tunisia	Djebba mine (Beja Governate, NW Tunisia)	Vanadate deposit	Descloizite, Vanadinite	Pb, Zn, Ba > Cu, As, P	N/A	Not evaluated	Solignac, 1935; Sainfeld, 1952; Mahjoub, 1973; Garnit et al., in press	75
	Tunisia	Jebel El Agab (Central Tunisia)	Vanadate deposit	Descloizite, Vanadinite	Pb, Zn, Ba > Cu, As, P	N/A	Not evaluated	Solignac, 1935; Sainfeld, 1952; Mahjoub, 1973; Garnit et al., 2022	76

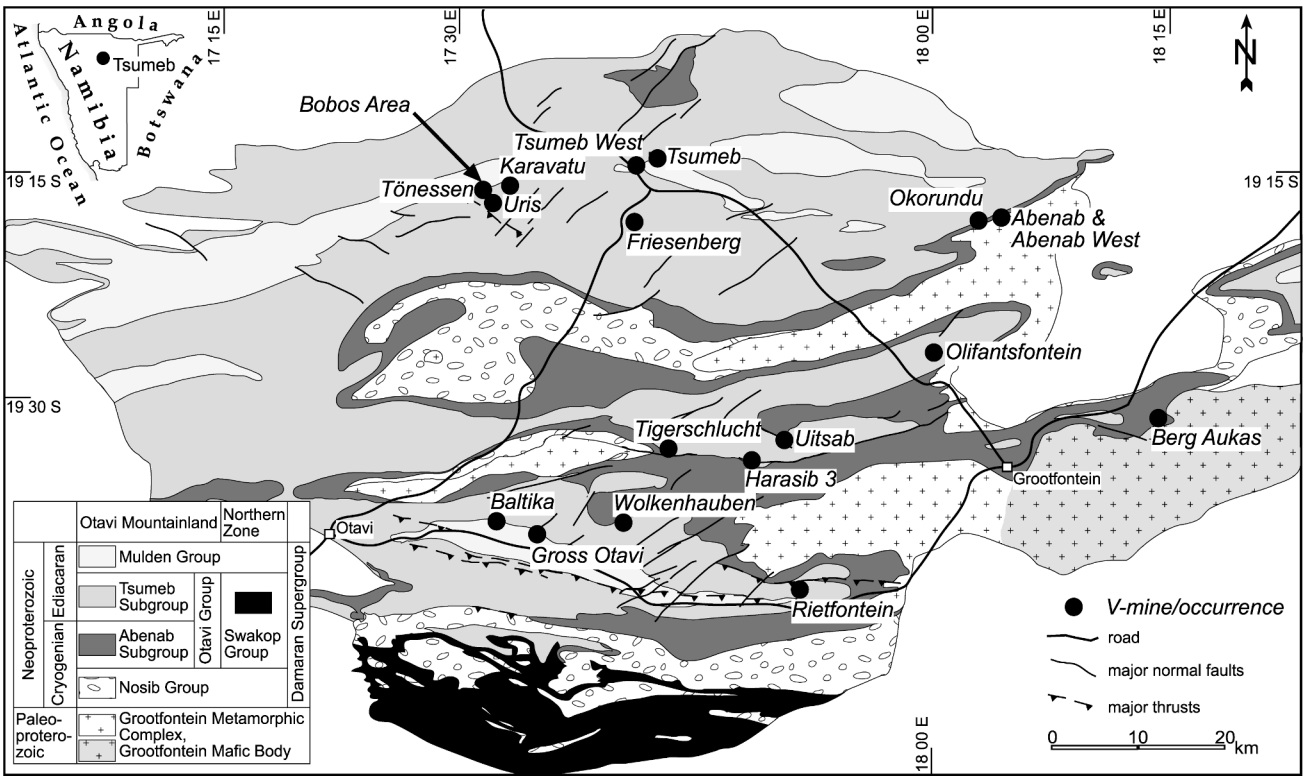

Fig. 5. Namibia. Geological map of the Otavi Mountainland (reproduced from Boni et al., 2007).

gneisses of the Namaqualand Metamorphic Complex (IAEA, 2020).

Small amounts of vanadates (descloizite and mottramite) were detected in several base metal mines hosted in the Transvaal dolomites (Cairncross and Dixon, 1995). However, even in the past, the amounts of these vanadates never reached the economic levels recorded by the Namibian ores.

4.4. Zambia

Vanadium-bearing mineralizations in Zambia have been traditionally described in the Kabwe mining district, located about 110 km north of Lusaka (Kampunzu et al., 2009), where several ore concentrations of different sizes have been discovered and partly exploited (Fig. 3; Table 1). The Kabwe Zn-Pb deposit (formerly known as "Broken Hill") consists of mixed sulfide-nonsulfide orebodies distributed over an area of ca. 25 km^2 (Kamona and Friedrich, 2007). During its lifespan, until mine closure in 1994 (Kamona and Friedrich, 2007), Kabwe was the most significant Zn-Pb mine in Zambia, with a production of 1.8 million tons of Zn, 0.8 million tons Pb, 79 tons Ag, 7,820 tons V_2O_5, 235 tons Cd and 64 tons Cu.

The country rocks in the Kabwe region include Neoproterozoic metasediments, which unconformably cover a Paleo- to Mesoproterozoic basement consisting of granite gneiss with minor amphibolite, schist, quartzite, and pegmatite (Cairney and Kerr, 1998; Kamona and Friedrich, 2007; Kampunzu et al., 2009).The mineralization is structurally controlled and includes two ore types: a sulfide core, commonly made up of massive sulfides, surrounded by an outermost zone of Zn-silicate ore (i.e, willemite). Vanadium minerals include vanadinite, descloizite, and mottramite (Kamona and Friedrich, 2007). The vanadium content in sulfide ore is less than 0.01 % V_2O_5, whereas in the outer shell and in the oxide zone is 1.87 to 2.43 % V_2O_5 (Taylor, 1955). In the Kabwe mining district, the large amounts of disposed slags and tailings are expected to have more than 356 kt of Zn, 351 kt of Pb, and 1.26% equivalent V_2O_5) (Ettler et al., 2020).

High-grade manganese mineralizations, which also contain V, occur in the Mukambala area within the Mkushi district of the Central Province, and in the Kabamba area within the Masaiti and Mkushi districts of the Copperbelt and Central Provinces (Maxtech Mining Zambia, 2018).

A sandstone-hosted uranium deposit with traces of vanadium occurs at Mutanga in northeast Zambia (IAEA, 2020; Yeo, 2011).

4.5. Zimbabwe

The vanadium resources in Zimbabwe are mainly related to mafic-magmatic intrusions, among which the 2.7 Ga Great Dyke is the most significant example (Fig. 3; Table 1) (Wilson, 1986). In the historically proven vanadium-titanium deposit in the Mberengwa area, drilled cores report average of 0.56% V_2O_5 and 5.5% TiO_2 in association with magnetite seams having a thickness up to 10 m (Northern Shaft, 2020). This area is situated within the northern zone of the Limpopo Metamorphic Belt, where granulite-gneisses are widespread. In the Darwendale platinum project, also located in the Great Dyke area, attractive vanadium concentrations have been recently detected (JSC Afromet and Zimbabwe's Landela Mining Venture).

High-grade vanadium mineralizations have also been reported at Chuatsa, approximately 20 km north of the town of Mount Darwin, (Six Sigma Metals, 2018). The V_2O_5 content over a 2.5 km long zone of layered intrusive rocks is high-grade, along with elevated Cu, Co, Ti, and Fe levels detected in soil and rock samples. The mineralizations occur in three folded, steeply-dipping, arcuate portions of a layered gabbroic sill that is part of the Nyamhanda Complex of the Rushinga Group (Six Sigma Metals, 2018). Major commodities include Ti in ilmenite, V in magnetite, and Cu in chalcopyrite and bornite. The exploration of the Chuatsa project was carried out by Anglo American Prospecting between 1962 and 1964. The analyzed samples from the 1960s Chuatsa exploration produced 7.8% TiO_2, 0.38% Cu, and 0.8% V_2O_5 from trenching and borehole sampling.

Small U-(V) mineralizations are located at Kanyemba in the Guruve district, Mashonaland Central, near the boundary with Mozambique and Zambia. The deposit is a tabular ore concentration consisting of several

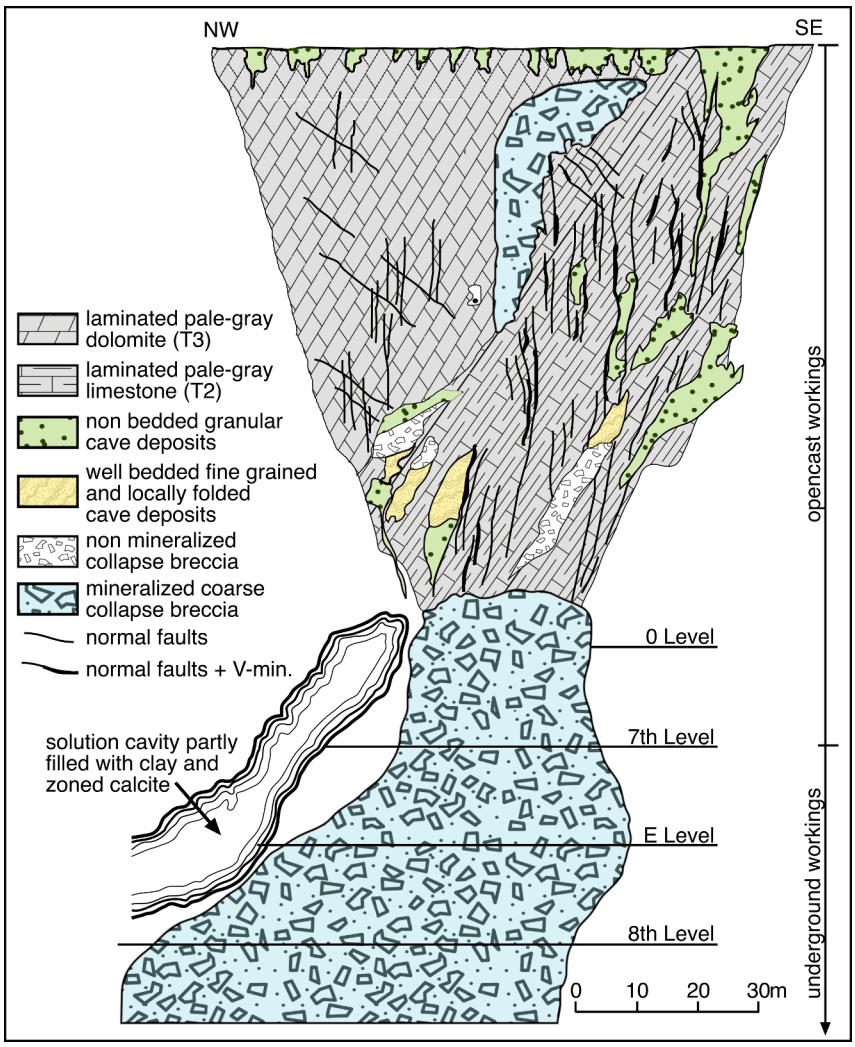

Fig. 6. Namibia. Schematic section through the Abenab pipe main orebody (modified from Schwellnus, 1945).

lens-shaped bodies, 0.20–3 m thick, 20–100 m wide, and up to 600 m long. The ores occur in the fluvial-derived sandstones of the Upper Pebbly Arkose Formation, which belong to the Upper Karoo System (Upper Triassic) (Komuro et al., 1994). The identified resources of the Kanyemba deposit are 1,800 tons (in situ) at an average grade of 0.6% U, combined with 12.8% V_2O_5.

Small concentrations of vanadate minerals of no current economic importance have been detected and exploited in the Bulawayo area (Amm, 1940; Fischer, 1975).

5. Vanadium deposits and occurrences in Eastern Africa

5.1. Burundi

The Kabanga-Musongati 350 km long alignment, with an emplacement age of 1,275 ± 11 Ma (U-Pb on zircons), stretches across Burundi to Uganda (Deblond and Tack, 1999). In Burundi it comprehends nine main stratigraphic units with Fe-Ti-V oxide deposits comparable to those identified in other African layered magmatic intrusions (i.e., Great Dyke and the Bushveld Complex) (Fig. 3). The main Fe-Ti-V oxide deposit is the Mukanda V-orebody (Fig. 3), located in the northern part of the Mukanda-Buhoro mafic intrusion (Fig. 12; Table 1) (Paredis et al., 2017). Minor mineralized bodies have been discovered in other areas: the Makebuko (Rwesera), Rutegama, Itaba, Funyangeso, Kabago, and Ruvumu Fe-Ti-V mineral showings in the Mukanda-Buhoro Massif, the Kivoga vanadiferous Ti-hematite deposit in the Musongati Massif, the vanadiferous Ti-magnetite deposit in the Rutovu Massif, and several Fe deposits in the Nyange-Songa Massifs (Deblond and Tack, 1999). The Fe-Ti-V oxides are associated with anorthositic cumulates and occur at the boundaries between the intrusion and the country rocks. The Mukanda V-bearing deposit is a stratiform orthomagmatic body (Smejkal, 1985; Nimpagaritse, 1986), concordant with the magmatic layering in the anorthositic cumulates of the Mukanda Anorthositic-Noritic Unit of the gabbronoritic subzone (mafic zone) (Deblond, 1994). The ore consists of massive to submassive (less than 40 vol% of the rock) (titano)magnetite and ilmenite in an anorthositic groundmass. The lens has a thickness variable between 5 and 15 m, and a length of 1,300 m along an east–west strike (Deblond and Tack, 1999). In 2006 the vanadium resources of the Mukanda prospected mine amounted to 9.7 million tons that graded 0.63% vanadium (Burundi Ministry of Energy and Mines, 1991, p. 25; International Gold Exploration AB, 2007, p. 15; Yager, 2009). Currently, Mukanda vanadium mineral resources cover an area of approximately 144 km^2, with a total of 6,500,000 tons of Proven Reserves at 0.63 % V (cut-off 0.2 % V), 7,300,000 tons of Probable, and 5,000,000 tons of Possible V Reserves.

5.2. Ethiopia

In Ethiopia, three different types of iron deposits are perspective for vanadium. They include magmatic iron (Fe-Ti type) of Precambrian age

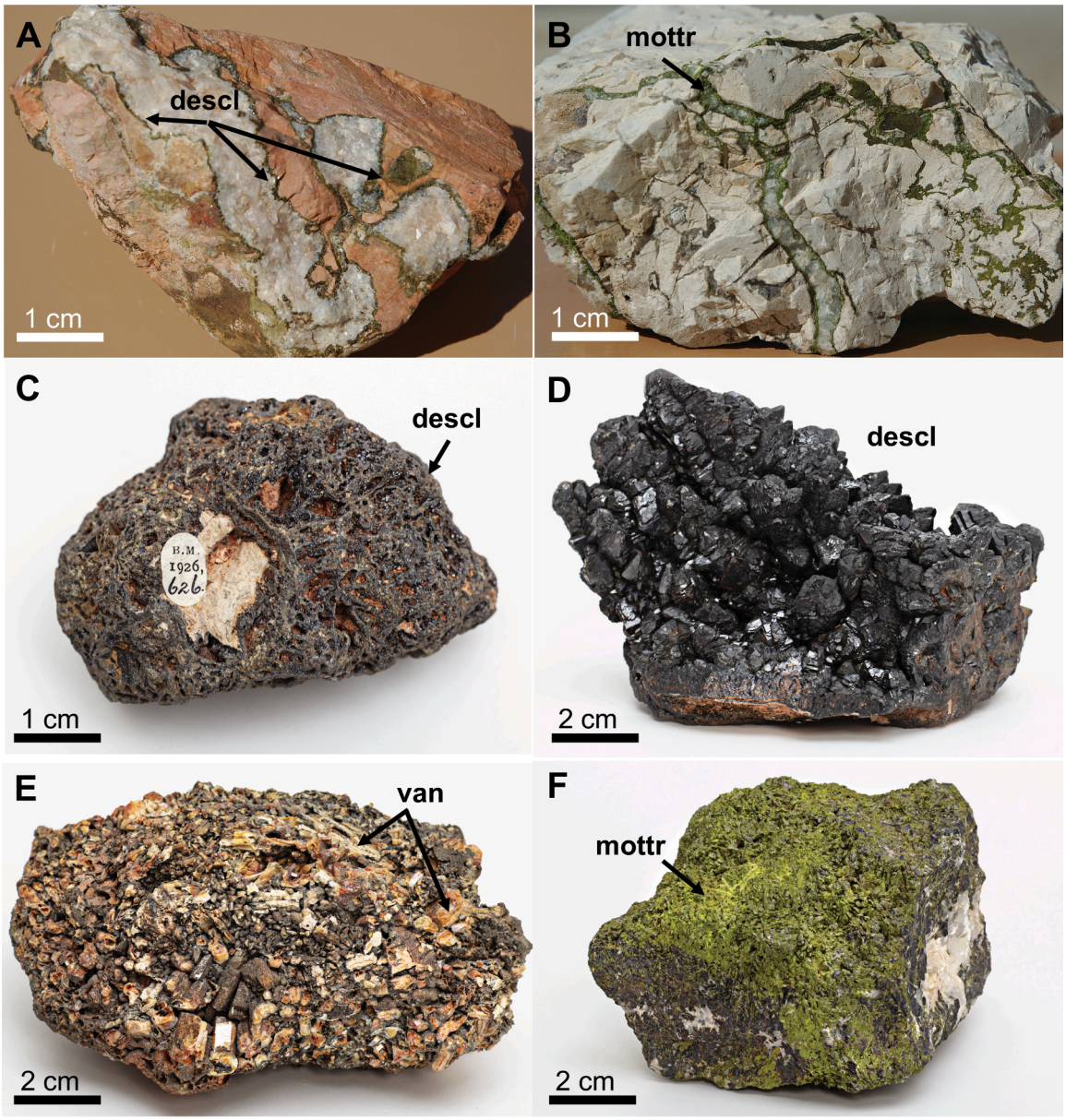

Fig. 7. Vanadium mineralization in the Otavi Mountainland (Namibia). A) Descloizite from karst-filling in the Berg Aukas mine. B) Mottramite veinlets in the Gross Otavi prospect. C) Descloizite specimen from the Otavi Mountainland (NHM Mineralogy collection, specimen # BM.1926,626). D) Descloizite specimen from the Otavi Mountainland (Harris's farm, 50 km SE of Tsumeb) (NHM Mineralogy collection, specimen # BM.1937,272). E) Vanadinite specimen from the Uitsab mine (NHM Mineralogy collection, specimen # BM.1929,1873). F) Mottramite specimen from the Uris prospect (NHM Mineralogy collection, specimen # BM.1931,22).

from the Bikilal and Melka Arba areas, associated with Precambrian gabbroic, apatite-rich intrusions (Gautneb et al., 2001; Ghebre, 2010), banded iron formation (BIF type) of Precambrian age, and lateritic (also gossan-related) iron deposits (residual type). In the Bikilal and Melka Arba titaniferous iron ores, the dominant minerals are magnetite (40%) and ilmenite (29%) associated with phosphates and silicates (about 30%). The Melka Arba (titano)magnetites have variable vanadium contents. In the Gimbi-Dalati area, Ti, Fe, and V have been detected in anorthosite-hosted ilmenite and hematite concentrations and in alluvial–eluvial placers from the recent sediments of the Sacco River (Tadesse et al., 2003).

Proterozoic metamorphic rocks from the northern segment of the Mozambique Belt host variably economic graphite bodies (Fentaw et al., 2000). As in Madagascar and Mozambique, these systems could contain valuable vanadium credits (Asia Pacific Gold Mining Investment Ltd. 2013; Parnell, 2022).

Vanadium shows significant concentrations in the ferricrete of the Shire area with more than 1,300 ppm V in ferricrete compared to ca. 300 ppm in source sandstone (Konka et al., 2013; Ezana Mining Development P.L.C.) (Fig. 3; Table 1).

5.3. Kenya

In the basement terranes of the Mozambique Belt in Kenya (Grantham et al., 2003), the gneiss contains scapolite, vanadian zoisite, vanadian diopside, vanadian sphene, and vanadian magnetite, in addition to porphyroblasts of green vanadium grossular (Pohl et al., 1979; Suwa et al., 1996) (Fig. 3; Table 1). Other V-bearing minerals (muscovite, zoisite,sphene, and rutile) also occur in the host marble. *Schreyerite* ($V_2Ti_3O_9$) is a rare vanadium and titanium oxide (Medenbach and Schmetzer, 1978), found in the Lasamba Hill, Kwale district in the Coast Province of Kenya. It is polymorphous with *kyzylkumite*

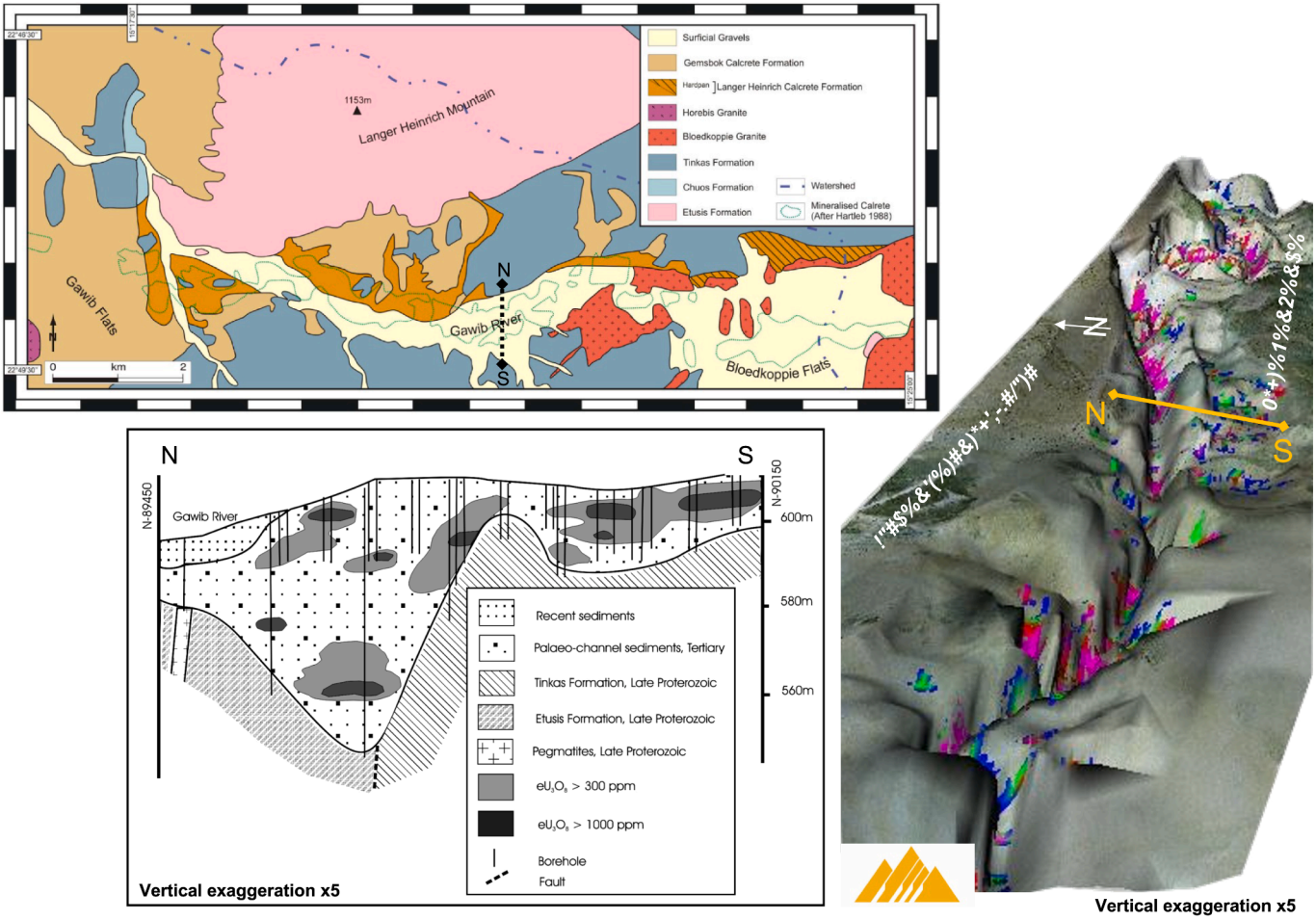

Fig. 8. Namibia. (up left) Map showing the distribution of Proterozoic Damara bedrock as well as Cenozoic cover sediments within the Langer Heinrich area. The Gawib River is a present-day drainage system, which mirrors the course of the underlying Langer Heinrich paleo-channel to a large extent (reproduced from Becker and Kärner, 2009). Schematic 3D model and N-S section of the Langer Henrich U-(V) deposit (the section trace is indicated in both the map and the 3D model - reproduced from Langer Henrich Uranium project).

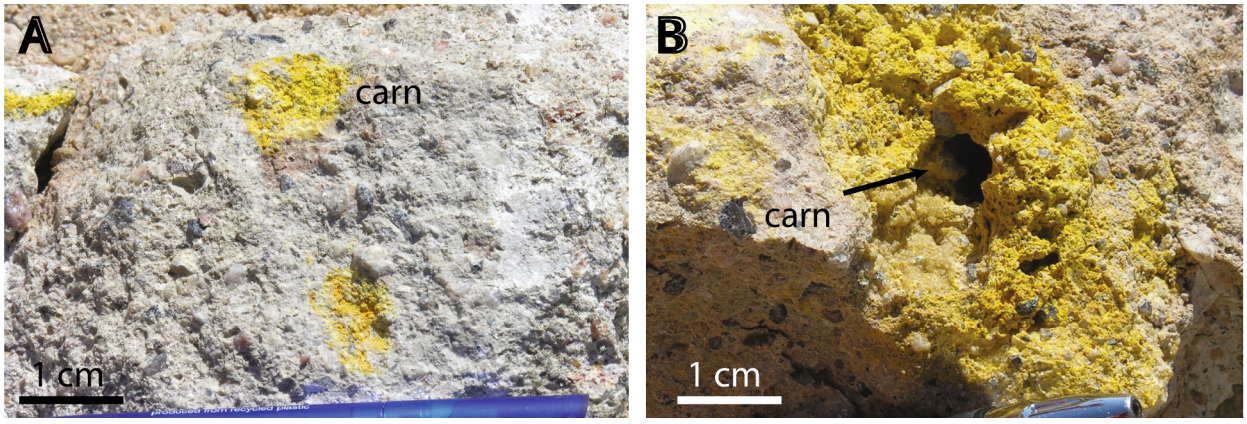

Fig. 9. Namibia. Carnotite from the Langer Henrich U-(V)deposit.

$[V^{3+}Ti_2O_5(OH)]$. Schreyerite has no economic significance so far as a vanadium resource. Conversely, the green vanadium grossular, that is called *tsavorite*, associated with high-grade metamorphic rocks in the Mwatata province, has a *gem*-quality and is exploited as such.

5.4. Madagascar

The Green Giant and Molo deposits in the Tulear Region are the most important vanadium-graphite concentrations in Madagascar (De Bruin, 2017; Next Source Materials 2017; Scherba et al., 2018) (Fig. 3; Table 1). The Bekily Block, within which the Green Giant project lies, is situated in southwest Madagascar and is considered to be of Proterozoic age. The

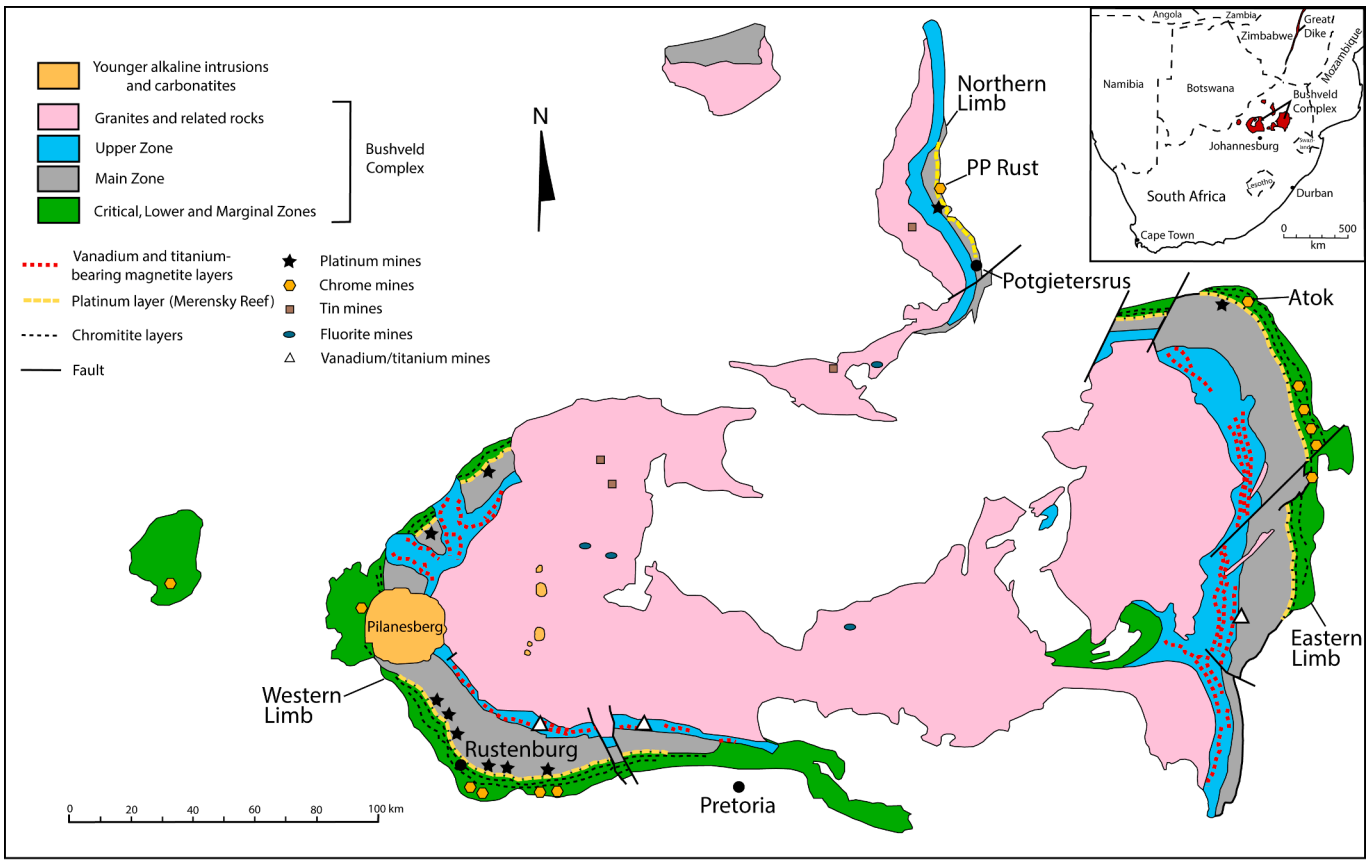

Fig. 10. South Africa. Geological sketch map of the Bushveld complex (modified from Taylor et al., 2009).

Block is dominated by high-grade metamorphic rocks with frequent graphitic sequences (Nicollet, 1990; Martelat et al., 2000; Collins, 2006) and numerous syntectonic mafic and felsic intrusions. The Green Giant Project, located 145 km southeast of the city of Toliara, is situated within the NNE striking Ampanihy shear zone and covers an area of 225 km^2 in two separate blocks (Fig. 13). The Green Giant project hosts three deposit types: (1) Algoma-type iron formation, (2) volcanogenic massive sulfides deposits (VMS), and (3) metamorphosed black shale/roll-front vanadium deposits. The latter type, with its metallic suite of V-Mo-U-C, is a typical product of metamorphism of black shale deposits (Barrie, 2009; Desautels et al., 2011; 2012; Parnell, 2022). Green Giant type (3), described as the largest known vanadium deposit in the world, consists of a series of graphite-bearing bodies (Jaky, Manga, and Mainty) that are 15 km away from the Molo Graphite Project (AGP Mining Consultants Inc., 2011; Next Source Materials, 2017; Scherba et al., 2018). The lithostratigraphy of the Green Giant property mainly consists of quartz-feldspathic gneisses (Lardeaux et al., 1999; Scherba et al., 2018), with bands of hornblende, biotite gneiss, marble, granitoid, and amphibolite. The rocks with the highest vanadium content are sillimanite- and graphite-bearing quartz-feldspathic gneiss with minor phlogopite, graphite, pyrite, muscovite, apatite, titanite, chalcopyrite, hematite, and calcite.

The vanadium host minerals are the vanadium mica *roscoelite* ($KV^{5+}_{0.8}Al_{0.6}Mg_{0.4}AlSi_3O_{10}(OH)_2$, containing up to 8.45% V_2O_3), rutile, schreyerite, oxyvanite, karelianite, and three unidentified vanadium-bearing sulfides (Di Cecco and Tait, 2018). Gangue minerals include quartz, K-feldspar, and graphite. The mineralizations occur both at depth in the unweathered rock and in the upper oxidized horizon. In the supergene zone oxide minerals are the main vanadium sinks, with low vanadium levels detected also in clays and micas.

The estimates in the deposits of the Green Giant property, show Indicated Resource of 49.5 million tons at 0.693% V_2O_5, containing 756.3 Mlb of V_2O_5, and a total Inferred Resource of 9.7 million tons at a grade of 0.632% V_2O_5, containing 134.5 Mlb of V_2O_5 (AGP Mining Consultants Inc., 2011).

In Madagascar also several mines of the semi-precious green vanadium grossular tsavorite are currently active (Adamo et al., 2012). A typical occurrence of a Fe- and V-rich tsavorite is located in the remote locality of Itrafo, in the Andrembesoa area, Central Madagascar (Adamo et al., 2012), but other exploited concentrations have been recorded at Gogogogo in the Southwest of the country (Mercier et al., 1997).

5.5. *Malawi*

In Malawi, sandstone-hosted uranium mineralizations occur in the Karoo sediments (IAEA, 2020), such as the giant Kayelekera deposit (Bowden and Shaw, 2007; Becker et al., 2014). Minor amounts of vanadium may be associated with this kind of ores and their surficial weathering products, even if a study from Dill (2007) could not identify this element in the above deposit.

5.6. *Mozambique*

The Montepuez Graphite Project is located within the Xixano Complex, along the tectonic contacts between the Nairoto, Xixano, and Montepuez Complexes (Fig. 3; Table 1). The Xixano Complex consists of a variety of *meta*-supracrustal rocks including mafic igneous rocks and granulites that form the core of a regional synform (Boyd et al., 2010). Graphite-bearing mica schist and gneiss with variable amounts of vanadium occur in this Complex. As V_2O_5 would be a common by-product of the graphite production, the inferred V_2O_5 mineral resource is reported to be above 4.3% total graphite content cut-off grade (Battery Minerals, 2019).

Another occurrence of similar type is the Caula graphite-vanadium

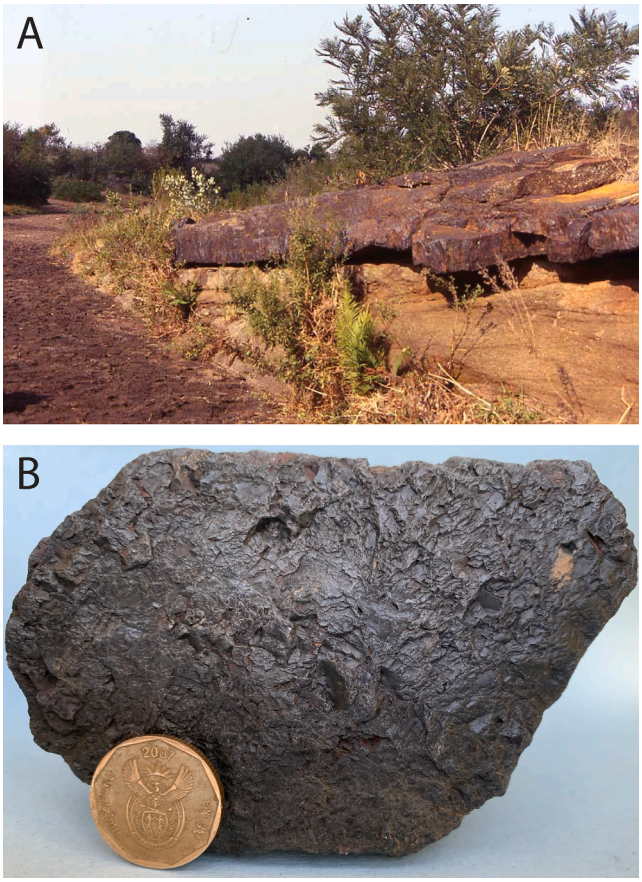

Fig. 11. South Africa, Bushveld complex. A) Magnetite layer at the Magnet Heights, Limpopo Province. B) Vanadiniferous magnetite specimen from the Bushveld complex.

mine, located in the Cabo Delgado Province, in the Northern part of the country (Marketscreener.com, 2018). As in Montepuez, the Caula graphite mineralizations are hosted in quartzitic schists of the Xixano Complex. The project area is situated in the Mozambique Belt and contains metamorphosed *meta*-sediments and *meta*-volcanics (amphibolite to granulite facies), including graphitic schists, gneisses, and pegmatoidal zones. Caula has a JORC (Measured) vanadium-graphite resource of 22 million tons at 0.37% V_2O_5 (0.2% cut-off) and 13.4% total graphite content (8% cut-off) for 81,600 tons of V_2O_5 (180 million pounds) and 2.93 million tons of contained graphite (New Energy Minerals, 2018). Vanadium is hosted mainly in roscoelite.

The Balama graphite deposit is also highly anomalous in vanadium (hosted in roscoelite) (https://www.syrahresources.com.au), being characterized by estimated resources of 1.422 billion tons, at 12% TGC and at 0.2 % V_2O_5 (Syrah Resources, 2019).

In the Cabo Delgado area, the vanadium-graphite Nicanda Hill ores (Dickinson, 2014; Triton Minerals, 2020) are characterized by JORC Inferred and Indicated Mineral Resource of 1.44 billion tons at 11.1% total graphite content and 0.29% V_2O_5 for 160.3 million tons of contained graphite and 4.2 million tons of contained vanadium (2015 estimate).

In addition to the above-mentioned deposits and prospects in graphitic schists, the Tete metagabbro–anorthosite intrusion (Barr and Brown, 1987) contains significant bodies of vanadium-bearing titanomagnetite totaling up to 0.66 % V_2O_5 (Frost-Killian et al., 2016). These orebodies consist of predominantly magnetite-ilmenite intergrowths (Callaghan, 2011). Exploration licenses held by Baobab Resources cover the Singore and Massamba vanadiferous (titano)magnetite deposits of the Tete Mafic Complex (Baobab, 2010; Baobab-Steel.com, 2022). The Massamba Group zone is 8 km long and comprises five prospects (Chitongue Grande, Pequeno, Caangua, Chimbala and South Zone). The Chitongue Grande prospect, has a 47.7 million tons JORC inferred resource with a head grade of 25.3% Fe, 0.18% V_2O_5, and 9.69% TiO_2, with a possible resource established by independent interpretation of 400–750 million tons to 250 m depth (announced to AIM on 24 September 2009). An estimate of the average concentrate grade is 63.7% Fe, 0.068% V_2O_5, and 4.86% TiO_2.

The Atchiza suite, a mafic to ultramafic intrusion close to the Cabora Dam, which contains small amounts of vanadium, is considered to be the continuation of the Great Dyke of Zimbabwe (Ibraimo and Larsen, 2015).

An additional project has been discovered at Memba in the Nampula Province, where the main host rocks are Proterozoic gneisses.

5.7. Somalia

Surficial uranium-(vanadium) deposits in Somalia belong to the valley-fill calcrete type (Fig. 3; Table 1) (Briot, 1984). They occur in the arid Mudugh Province of the Dusa Mareb-El Bur region along a 240 km-long belt, oriented parallel to the north–south regional tectonic framework. Uranium mineralizations in the form of *carnotite* occur in the uppermost Mercia Series.

5.8. Tanzania

In the Tanzanian part of the Mozambique Belt (Feneyrol et al., 2017), a Neoproterozoic high-grade metasedimentary suite (the "Kurase Group") hosts the gemstone grossular tsavorite (Fig. 3; Table 1). Tsavorite is exploited at Lemshuku, and Namalulu, 80 km south of Merelani. Moreover, tanzanite, a blue vanadium-bearing variety of zoisite (Fig. 14), has been recognized in the Merelani area (Harris et al., 2014). The Merelani graphite-tanzanite deposit is situated in northeast Tanzania, approximately 65 km southeast of the town of Arusha (Malisa and Muhongo, 1990), where the precious and semi-precious stones are mined in licensed as well as in artisanal operations.

Iron ore-bearing bodies are located in the Ludewa District of the Njombe Region. They occur mainly in the Liganga area (Geological Survey of Tanzania, 2015), the Uluguru Mountains, Mbabala near Lake Tanganyika, Karema, Manyoro Gondite, Itewe, and Kisaki in Morogoro District. The Liganga iron mine is associated with anorthosites and holds the largest resources with proven reserves of 1.26 billion tons grading 35% iron metal. Apart from iron potential, Liganga has high values of titanium and vanadium (not evaluated). The titaniferous ore is rich in V_2O_5 and TiO_2. The ore deposits at Liganga/Maganga Hills have received economic interest for many years. Past investigations of the deposits have indicated that these hills are rich in FeO_t (51–63%), V_2O_5 (0.5–1.7%), and TiO_2 (13%).

The Karoo Basin across southern Tanzania, contains several thousand meters of terrigenous sediments that were accumulated during Late Palaeozoic–Early Mesozoic (Kabete et al., 2012). Uranium-(vanadium) mineralizations occur in the sediments (Schlüter, 2008) (e.g., the Mkuju River, Mbamba Bay, and southern Tanzania projects). Most ore occurrences are in palaeochannels, associated with calcrete- and sandstone-hosted targets within the Bahi catchment (Bahi North and Handa projects) (IAEA, 2020).

5.9. Uganda

In the highly weathered Bukusu alkaline complex of southeastern Uganda, vanadium is contained within magnetite ore (Nangalwe area, Fischer, 1975). The most important deposit is located within a 6 to 8 km-diameter roughly circular intrusion of syenites, ijolites, and pyroxenites, around a central carbonatite core. Concentrations of 0.35% V_2O_5 have been detected in the low-titanium magnetite deposit of Nalgalwe Hill (Welch, 1958).

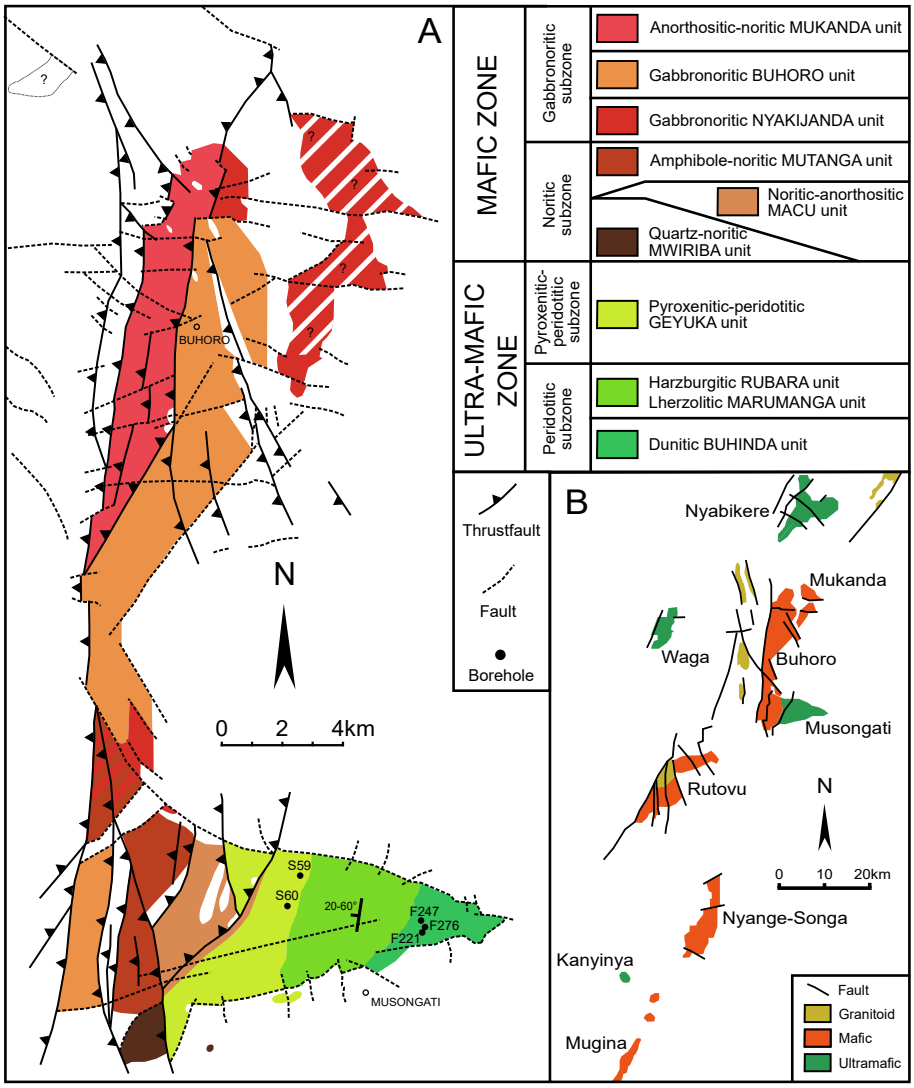

Fig. 12. Burundi. A) Simplified geological map of the Mukanda-Buhoro-Musongati complex. B) SE-part of the KM alignment with A-type granitoids of the Gitega-Mikebuka-Bukirasari alignment (reproduced from Deblond and Tack, 1999).

The Orom-Cross graphite mineralizations in Uganda (Blencowe Resources, 2022), which has the potential to become a world-class project, due to its size (it contains an estimated 250 million tons of graphite in 3.7 billion tons of ore) and quality. However, as opposed to other deposits of the Mozambique Belt, Ugandan graphite has very low levels of vanadium.

6. Vanadium deposits and occurrences in western Africa

6.1. Angola

Angola is well endowed with iron ore resources, with the most important being the Kassala and Kitungo deposits located in the Kwanza (Cuanza)-Norte Province, 150 km ESE of Luanda (Jourdan, 1990) (Fig. 3; Table 1). They contain an estimated 300 million tons of primary ore grading 30 to 35% Fe, mainly in the form of (titano)magnetite-bearing lenticular bodies in norite country rock, which contain vanadium in variable amounts.

Another vanadium occurrence has been reported in the Lueca historical mine (Millman, 1960; Pauly, 1962) in the northern Damba region. This occurrence shows many geological similarities with other vanadium deposits of Southwest Africa as those in Namibia. However, in the Lueca area the Proterozoic rocks are dominantly siliceous, and the vanadium-bearing minerals are associated with quartz and chalcedony. Mottramite is far more common at Lueca than descloizite. Well-formed euhedral crystals of *mottramite-descloizite* and rare *vanadinite* occur in vugs of the host rock. Relics of vanadinite crystals partially replaced by descloizite and mottramite are common, as well as green quartz, which inherited its color from fine prisms and acicular aggregates of vanadates (Millman, 1960). The most likely source of vanadium at Lueca are the red shales of the Pioka Series, which have been removed by erosion. The association of *descloizite-mottramite*, *volborthite, tarbuttite*, and *planchéite*-type copper silicates suggests deposition in a moderately acidic environment with extensive silicification of the limestone host.

6.2. Burkina Faso

During the French colonial period, intrusion-related iron ore was exploited from the Fe–V–Ti bearing magnetite veins of the Tin Edia deposit (Oudalan province) (Soussou, 1974; Markwitz et al., 2015) (Fig. 3; Table 1). The reserves were estimated at 60 million tons with an average grade of 1% V_2O_5 and 8–14% TiO_2. The magnetite-bearing veins crosscut layered intrusions of Paleoproterozoic ultramafic rocks (such as gabbro-norite and dunite). The major deposit is located on the limb of the NE-trending Oursi syncline (Neybergh et al., 1980). The ore consists of chalcopyrite, pyrite, V-bearing magnetite, hematite, goethite,

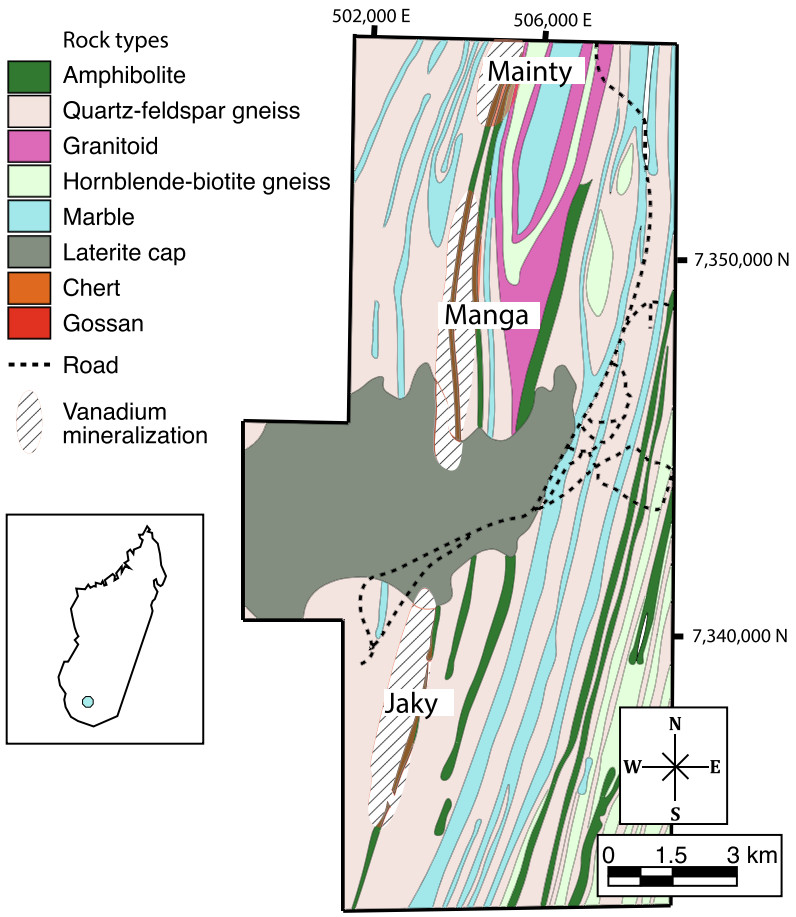

Fig. 13. Madagascar. Geological map of the Green Giant Vanadium project (reproduced from Di Cecco et al., 2018).

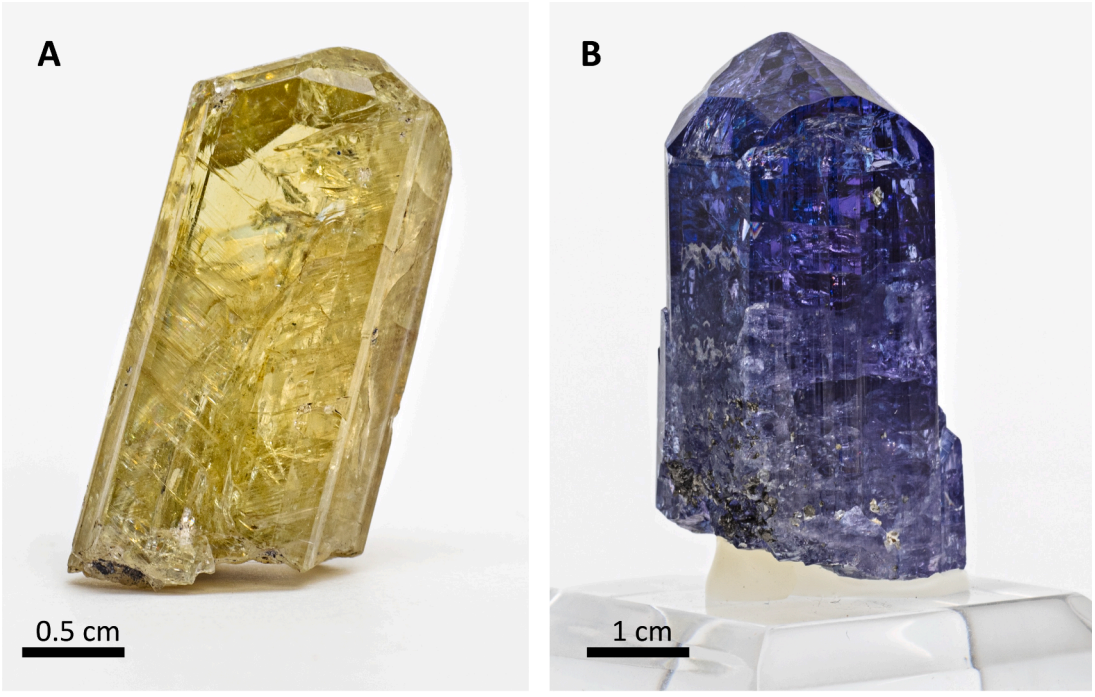

Fig. 14. Tanzania. A) Zoisite: Terminated green-yellow crystal showing prism striations and internal fractures (NHM Mineralogy collection, specimen # BM.2010,41). B) Tanzanite specimen (NHM Mineralogy collection, specimen # BM.2013,53).

pentlandite, and ilmenite. The V-concentration never rises above 1.4 wt % V_2O_5. The V_2O_5 concentration and the relatively low Cr_2O_3 content (less than0.11 wt%) of the Oursi ore are similar to those found in the upper part of the Bushveld Complex. Iron-manganese ore concentrations, bearing a minor amount of V and Cr, also exist near Tambao (Oudalan Province). The Nahouri Project (southeast of Tiebele) represents a V-Ti-magnetite target (Vital Metals; 2018).

6.3. Cameroon

Little is known about vanadium in Cameroon. Preliminary investigations indicated a small concentration of vanadium in two ferruginous laterite nodules (1.26% and 1.12% V_2O_5, respectively) from the Nkomakak area in South Cameroon. The vanadium contents at Fongo-Tongo (West Cameroon) range between 12 and 320 ppm in the laterites (derived from the weathering of basalts), 250 ppm in basalts, and 60–438 ppm in bauxites (Hiéronymus, 1985). The vanadium contents at Ngaoundal (Adamaoua Region) range from 0.25 to 0.33% V_2O_5 in basalt and from 0.37 to 1.18% V_2O_5 in the laterite profiles (Ndema Mbongué, 2020). Relevant vanadium occurrences in Cameroon are hosted in Ti-bearing mafic rocks (doleritic gabbro, peridotite, and amphibolite) and in their alteration products (not only at Fongo-Tongo but also in Adamaoua and Bamboutos bauxites). The vanadium content in bauxites varies from 0.47 to 1.12% V_2O_5 (Ndema Mbongué, 2020) (Fig. 3; Table 1).

In a sampling campaign conducted in the Loum area (southwestern part of the central Pan-African Fold Belt), vanadium concentrations slightly below 1,000 ppm were detected in loose sediments of the river Mbete (Ndema Mbongué, 2020). Vanadium in this area has been arguably sourced through a local volcanism.

6.4. The Central African Republic

In several areas of the Central African Republic, the Cretaceous M'Patou Series, comprising sandstones and conglomerates with intercalations of red clays, is host for phosphatic sediments consisting of a mixture of microcrystalline carbonates and F-apatite, which can constitute as much as 50% of the rock. In the Bakouma District these phosphate deposits are exploited for U and V (IAEA, 2020).

6.5. The Democratic Republic of Congo

The Proterozoic sediments in the Democratic Republic of Congo (DRC) include the cupriferous–uraniferous Roan-Kundelungu Series (Katanga System) of Shaba and equivalents such as the Marian, west of Kinshasa (Fig. 3; Table 1) (e.g., Cox et al., 2003; Cailteux et al., 2005). Vanadium is present at the Mutoshi mine in Katanga, but its mineralogical residency has not been determined yet.

More economically significant V-rich mineralizations occur in the Bamba Kilenda ore field, located in the Bas-Congo Province, in the southwestern part of the country (Tack et al., 2001). (Fig. 3; Table 1). The Bamba Kilenda mineralized bodies mostly occur at the boundary between the *Schisto-Calcaire* and *Schisto-Gréseux* Subgroups (Cahen et al., 1984). In the western part of Bamba Kilenda, the economic concentrations mostly consist of Cu-bearing minerals hosted in limestone. In contrast, in the eastern part of the ore field, the metallic minerals consist of Cu-Pb-Zn-bearing phases, with important amounts of vanadates in the supergene zone. The most common mineral phase is *mottramite*, generally associated with *duftite* and *conichalcite*. Most of the vanadium in the Bamba Kilenda deposit is present in solid solution series with As, to form Cu-, Pb- and Ca-rich minerals (Lesaffer, 2014).

In the oxidation zone of the Kusu deposit (Kongo Central), the rare vanadate mineral *kusuite* [$(Ce^{3+},Pb^{2+},Pb^{4+})VO_4$], currently referred to as *wakefieldite*-(Ce), has been described by Deliens and Piret (1977) (Fig. 3; Table 1). Associated minerals include mottramite, cuprite, dioptase, malachite, plancheite, and vanadinite.

6.6. Congo Brazzaville

High V concentrations have been found in the higher levels of the M'Passa Pb-Zn deposit (Niari syncline) (Buffet et al., 1987), which has a similar geological setting as the Lueca deposit in Angola.

6.7. Gabon

Uranium deposits in Gabon occur in Lower Proterozoic sandstones containing marine carbonaceous sediments. The most important economic deposits were Oklo and Mounana. The Oklo deposit is located in a 2.1 Ga old sedimentary succession of the Franceville basin in the southeasternmost part of Gabon (Fig. 3; Table 1) (Weber, 1968; Gauthier-Lafaye, 1986; Gauthier-Lafaye and Weber, 1989, 2003; Bros et al., 1992; Horie et al., 2005). The black shales, with their high total organic carbon content (up to 15% TOC), were the source rocks for hydrocarbons, making the Franceville basin one of the most promising targets for petroleum resources. Anomalous V enrichments are locally present in the above lithologies, but the main V source remains poorly constrained. The Mounana U-(V) ore deposit (similar to most deposits of the Colorado Plateau) contains *francevillite* [$(Ba,Pb)(UO_2)_2(VO_4)_2{\cdot}5H_2O$], *chervetite* ($Pb_2V_2O_7$) and other black oxides (Bariand et al., 1963).

6.8. Ghana

No vanadium ores are known in Ghana. However, some V-traces have been found in association with manganese ores. The carbonate-type Mn deposit of Nsuta in the Ashanti Belt (Southern Ghana) is hosted in Paleoproterozoic Birimian metasedimentary rocks (IAEA, 2020). It contains mainly rhodochrosite, alabandite, and the vanadium-bearing spinel *jacobsite* has been detected in the oxides and hydroxides derived from weathering events (Mücke et al., 1999).

6.9. Guinea

The Marela Project (Optiva Resources, 2023) is located on the northwestern border of the Archaean Craton in Guinea, and contains a large ultramafic intrusion composed of an inner dunite core surrounded by rims of wehrlites and pyroxenites (Douglas-Hamilton, 2023). The southern pyroxenite unit on the Project is particularly well mineralized in titanium (ilmenite) and vanadium (magnetite) with strong enrichment in the laterite profile. The hard rock pyroxenites contains 141 million tons at approximately 10% TiO_2 and 0.1% V_2O_5.

6.10. Liberia

Mineral resources, especially iron ore, have been of great importance in the past for the Liberian economy (Dorbor, 2010; Gunn et al., 2018). Economic deposits of Fe, Mn, Zn, Cu, Ni and Al (bauxite) are known and partially exploited in Liberia. Smaller deposits containing Ti-V, Cu-Mo, Cu-Ag, Sb, W, Sn, Nb-Ta, and Li have also been reported by Milési et al. (1992).

6.11. Togo

Tertiary phosphorites have been mined since 1959 in the coastal basin of Togo near Hahotoé-Kpogamé, in the southern part of the country. Like other phosphorites elsewhere in the world, Togo's phosphorites are highly enriched with numerous trace metals such as Cd, Cr, Cu, Ni, V, Zn, Pb, U, Th, Mo, Ag, F and Y (Tanouayi et al., 2016). However, their V potential in Togo is still unknown.

7. Vanadium deposits and occurrences in northern Africa

7.1. Algeria

No typical V deposits occur in Algeria, although this metal can be obtained as potential by-product from other ore types, as for example Fe ores. The biggest operations in the country are the Ouenza and Boukhadra mines in the province of Tébessa (eastern Algeria), which contain total reserves of approximately 60 million tons of Fe ore (Arcelor Mittal). The mines are exploiting a Fe-carbonate deposit hosted in Aptian neritic limestones proximal to Triassic evaporitic diapirs (Bouzenoune and Lécolle, 1997). The Djebel Had ironstone, a 8 m thick stratiform sedimentary iron formation of Tertiary age, is part of the south Tébessa province mining district (Fig. 3; Table 1). Geological evidence discussed by Diab et al. (2020) suggest that this mineralized formation may extend further into southwestern Tunisia (Diab et al., 2020). The ore consists of ooidal goethite and hematite (*"minette"*), with subordinate magnetite and piemontite. The Fe-oxy-hydroxide content of the ironstone averages 71%. High V content (512–560 ppm) in the ferruginous orebody is likely due to the presence of V-bearing goethite (Schwertmann and Pfab, 1997). The country's largest known Fe ore deposit is Gara Djebilet, located near Tindouf in the southwest of the country. Gara Djebilet also belongs to the oolitic "*minette*" type and contains goethite and chamosite. It is estimated to hold reserves of 1.54 billion tons of Fe ore with some V credits (Guerrak, 1988). The deposit belongs to the North African Palaeozoic oolitic ironstone belt, extending more than 3,000 km from Zemmour (Mauritania) to Libya, with ironstones of Ordovician, Silurian, and Devonian ages (Guerrak, 1988).

Uranium-(vanadium) mineralizations at the Tahaggart locality (Hoggar Massif) have been discovered in a minor unconformity-style deposit, which occurs at the contact between the Eburnean basement and the overlying Cambro-Ordovician sediments. The ore concentrations consist of disseminated secondary autunite, torbernite, and *carnotite* as cement and vein fillings in sandstone (Kinnaird and Nex, 2016; Badahmaoui et al., 2020).

Algeria also hosts ca. 2 billion tons of phosphate deposits, mostly located in the NE-most part of the country close to the Tunisian border. National phosphate production currently stands at 1.5 million tons/year, most of which takes place in two open-cast mines located near Djebel Onk in the Bir El Atar area (Tébessa province). Several metals including V have been detected in these Early Tertiary phosphate ores (Fig. 3; Table 1) (Bezzi et al., 2012).

After Lacroix (1908), the vanadates vanadinite, descloizite, and endlichite have also been found in karstified Bathonian dolomites of the Saida area (Oran). These vanadates, which are similar to those described in Tunisia and Morocco, are currently of no economic significance.

7.2. Egypt

Small V credits are associated with U occurrences in the western-central Sinai district in Egypt (IAEA, 2020). At Bir Nasib, carnotite has been found together with Fe-Cu-Mn in a deposit located in Middle Carboniferous siltstones. The ore assemblage occurs at Wadi Nasieb, where the mineralizations are hosted by carbonaceous marls and within karstic structures in a Carboniferous dolomitic horizon (IAEA, 2020). The Paleozoic clastic-carbonate units (Araba, Cambro-Ordovician and Um Bogma, Carboniferous) formations in southwestern Sinai are rich in mottramite, mimetite, duftite, beudantite, descloizite and vanadinite (Afify et al., 2022). The V minerals, together with supergene Cu concentrations, are disseminated in the arkose, subarkose, sublitharenite, graywacke, shale, siltstone and dolostone members of both formations. The vanadiferous mudstones and sandstones were probably formed by meteoric dissolution and intensive weathering of feldspar and sulfide grains during the uplifting of the Araba Formation. Although the Cu concentrations have a moderate economic value, the V ore resources have not been evaluated so far (Afify et al., 2022).

Significant V amounts have been also detected in black shales intercalated within phosphorite deposits in the Red Sea area (Baioumy, 2021). According to Baioumy and Ismael (2010), the V content in phosphorites ranges from 1,056 to 2,800 ppm and exhibits a positive correlation with the total organic carbon (TOC) in black shales. This suggests that V is enriched as an organometallic compound (Baioumy, 2021).

The Coniacian-Santonian high-phosphorus oolitic iron ore in the Aswan area is one of the major Fe-ore deposits in Egypt (Baioumy et al., 2017). The Aswan "*minette*" type Fe ores consist of ooids with hematite and chamosite. Among trace elements contained in these ores, V has the highest concentrations, with an average of 484 ppm. However, these V levels are considered so far of no economic value.

The northern termination of the Proterozoic Mozambique Belt in the SE Desert of Egypt (Mersa Alam), which hosts several graphite bodies (Bishady, 2017), is believed to contain vanadium as in the southern parts of the Belt (Parnell, 2022).

7.3. Libya

Vanadium concentrations in Libya occur in the Devonian oolitic ironstones (Dabdab, Tarut, and Ashkidah Formations), located in the Wadi As Shati desert area within the Murzuq Basin (Shaltami et al., 2017). The Fe-bearing minerals detected in the ironstones are goethite, siderite, hematite, magnetite, chamosite, and pyrite. Other elements concentrated in the Wadi As Shati ore are Ni, Co, Cr, Mo, Pb, As, Zr, Nb, Th, U, and REEs. Vanadium values in the reduced facies range between 800 and 900 ppm and in the oxidized facies between 500 and 600 ppm. However, this vanadium enrichment remains of no economic value.

A limited exploration survey for U and V was carried out in 1969 in Libya. The main direct result was the discovery of small U occurrences in the Carboniferous and Triassic continental sandstones along the western flank of the Murzuk Basin in the southwestern part of the country (Fig. 3; Table 1). The main U-bearing mineral is carnotite, which is locally associated with *tyuyamunite* [$Ca(UO_2)_2(VO_4)_2{\cdot}5\text{-}8H_2O$]. The discovered occurrences have features in line with *roll-front* U ores (IAEA, 2020).

A small but unusual occurrence of vanadiferous goethite is located near the evaporites of the southeastern Hun Graben. Slightly radioactive goethite nodules occur in the dolomites of the Tertiary Rawaghah Formation (Lashhab and West, 1992), which bear V contents up to 3,380 ppm, an enrichment that might be due to precipitation from V and Ni porphyrins commonly associated with oil. Vanadium precipitation could have taken place through the action of hydrogen sulfide reducing V^{4+} to V^{3+} (Wanty, 1992). Source of metallic ions could be considered the volcanic rocks occurring at no great distance within the Hun Graben (Jabal As Swada). Until now, this V occurrence is just a mineralogical curiosity and has no economic significance.

7.4. Mauritania

Several Fe deposits occur within the Archean and Birimian Regueïbat Shield in northern Mauritania. Those at Kedia d'Idjil comprise large hematite and magnetite bodies in ridges known as *Guelbs* (e.g. Guelb Rhein and Oum Arwagen). The 14 km-long M'Haoudat ridge contains four lens-shaped deposits consisting of hematite with traces of V.

The Tiris uranium mineralizations, located in the Sahara Desert in northeast Mauritania, were discovered in 2008 (Fig. 3; Table 1). Tiris is the region's first major mineralized calcrete discovery with an average grade of 330 ppm V_2O_5, and a resource estimate of 18.4 million pounds of V (Aura Energy Ltd., 2022). The orebody lies 3 to 5 m from the surface. Vanadium is contained in *carnotite*, which is also the main U host. Further U-(V) mineralizations associated with calcrete deposits have been recognized around Bir Moghrein and Ain Ben Tili (Forte Energy and Aura Energy, 2022; Kinnaird and Nex, 2016). These deposits total 138.3 million tons at 331 ppm U_3O_8 with vanadium credits (Taylor et al., 2012).

7.5. Morocco

Most of the Moroccan V-bearing prospects and showings are related to two main deposit types: (1) igneous vanadiferous (titano)magnetite deposits and their supergene counterparts, and (2) sediment-hosted deposits. The last type includes either sandstone-hosted and MVT V-U-rich deposits (Figs. 3, 15; Table 1).

Vanadiferous titanomagnetite-bearing ores are the principal source of V in the country. They consist of magmatic accumulations of Fe-Nb-P-REE-Ti-V ± U-Th oxides containing up to 1.5 wt% V_2O_5. The orebodies are spatially and genetically related to the late Paleoproterozoic Gleibat Lafhouda magnesio-carbonatite and to the Upper Cretaceous Twihinate calcio-carbonatite and their weathered products. These newly discovered carbonatite occurrences were reported from the Oulad Dlim Massif in the Moroccan Sahara (Fig. 15; Table 1) (Bouabdellah et al., 2012; Boukirou et al., 2022). Total mineral resources have been estimated at 584.5 million tons grading 0.4% Nb_2O_5, 0.7% REE, 193 ppm U_3O_8, and 35% Fe_2O_3 for the Twihinate intrusion, and 67 million tons at 0.3% Nb_2O_5, and 400 ppm U_3O_8 for the Gleibat Lafhouda carbonatite (www.onhym.com). Although V could be recovered as a potential by-product, no quantitative resource information is available for this critical raw commodity yet. Vanadium-uranium-bearing mineralizations occur either as cm-thick Fe-Nb-P-REE-Ti-V ± U-Th oxide layers of disseminated ore or as gossanous-to-saprolitic material capping the unaltered carbonatite precursor. The mineral assemblage consists predominantly of coarse- to very coarse-grained V-rich magnetite with subordinate apatite, pyrochlore, ferrocolumbite, and sulfides in a matrix of magmatic carbonates (i.e., dolomite and calcite). Vanadium is constantly present in (titano)magnetite across the entire Twihinate prospect (Fig. 15; Table 1). Compared with magnetite compositions from other deposit types, the elemental contents of the Twihinate magnetite are typical of magmatic Fe-Ti-oxide deposits (Bouabdellah et al., 2022). An increased V-U amount along with variable REEs contents can be detected in the saprolitic weathering zone compared to the amounts measured in the unaltered precursor. The average REEs, Nb, V, and U amounts in fresh carbonatites range from 1,040 to 4,271 ppm, 2 to 409 ppm, 126 to 670 ppm, and 0.3 to 12 ppm, respectively. Conversely, the weathered units are enriched in total REEs, Nb, V, and U with

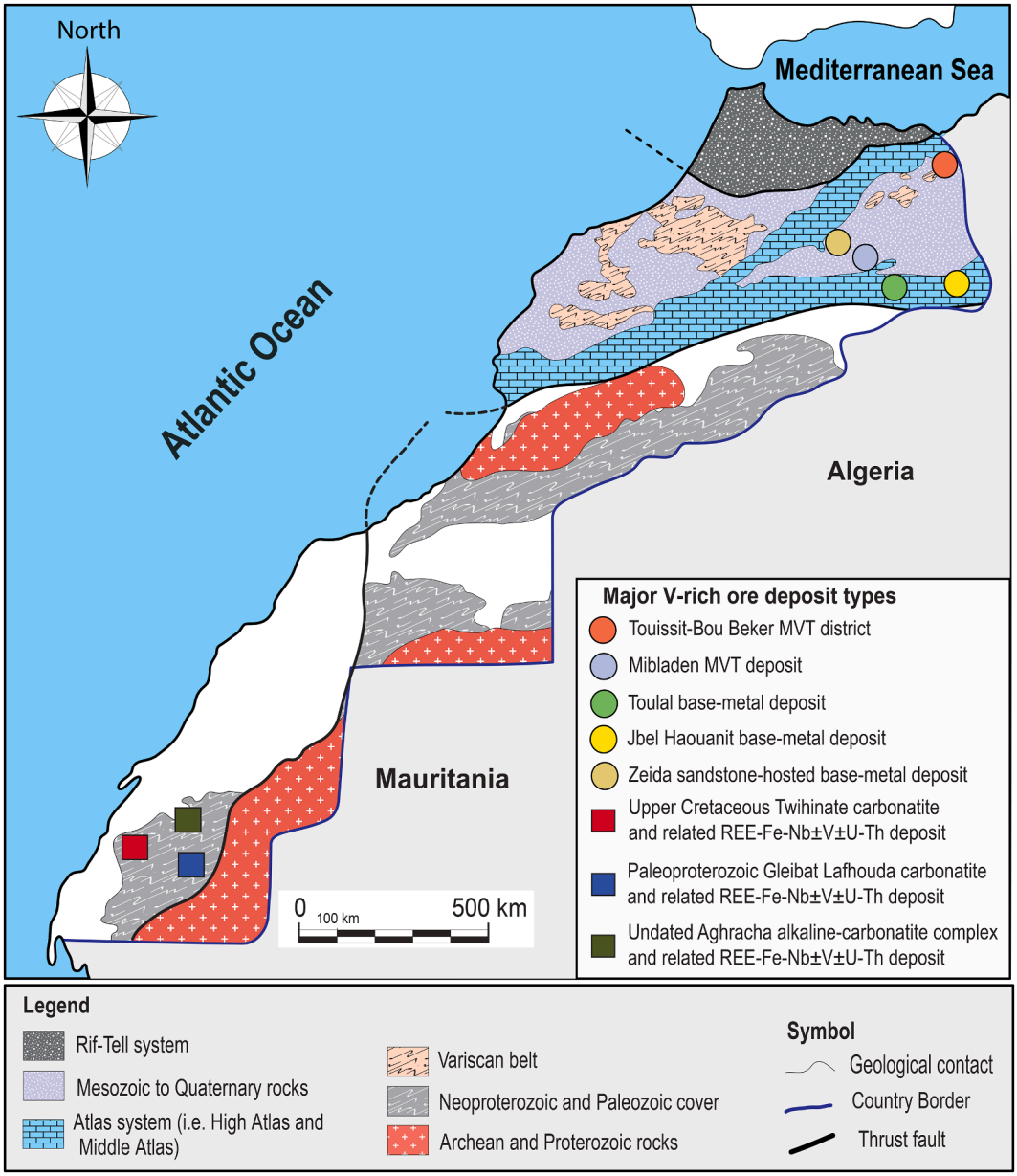

Fig. 15. Geological map and vanadium occurrences and deposits of Morocco (modified from Bouabdellah and Slack, 2016).

concentrations up to 3%, 2,790 ppm, 2,533 ppm, and 407 ppm, respectively: an increase exceeding 200%.

In addition to the Gleibat Lafhouda and Twihinate carbonatites, numerous deeply weathered carbonatite occurrences and related Fe-Nb-REEs-Ti-V ± U-Th mineralizations have been found in Morocco. Among these, the Aghracha, Awhifrite, and Awark prospects are of particular interest. (Fig. 15; Table 1). In the Aghracha prospect, the V-U enrichment is expressed as *carnotite* in calcretes overlying the igneous protolith (Fig. 16). Combined mineral resources are estimated at 35 million tons of ore at 3.8% REEs and 800 ppm U_3O_8 (ONHYM.com). The V concentrations range from 50 up to 1,495 ppm. Changes in mineralogy and metal concentrations with depth are related mainly to late magmatic-hydrothermal and supergene weathering processes.

Sediment-hosted V-U-rich deposits and prospects are widely distributed throughout the Upper Moulouya district and to a lesser extent in the Touissit-Bou Beker area of eastern Morocco (Fig. 15; Table 1). Typical examples include the Pb-rich Zeida (16 million tons at 3% Pb) and Mibladen (6.5 million tons at 5% Pb) deposits, along with the world-class MVT district of Touissit-Bou Beker. The Zeida deposit is a stratiform, sandstone-hosted Pb-Ba ± U-(V) deposit that comprises large-tonnage and low-grade disseminated ore (2–3 % Pb). The host rocks are Permian-Triassic arkosic sandstone, conglomerate, and siltstone with intercalated evaporite beds (Bouabdellah and Slack, 2016). The hypogene mineral association consists of galena and barite with subordinate chalcopyrite and pyrite. The late supergene association comprises cerussite, anglesite, malachite, azurite, and V-U-Mo-bearing minerals. Among the latter, vanadinite and wulfenite are the dominant phases occurring as spotty impregnations in the host sandstone.

The Mibladen Pb-Ba ± V deposit is known as the source of most of the world's finest specimens of vanadinite for mineral collectors and is considered the most promising economic target for V-rich mineralizations in the country (Fig. 17A; Table 1). High-grade orebodies are exclusively confined to the Domerian (Early Jurassic) dolomitized carbonates. Vanadium mineralizations derive from the supergene oxidation

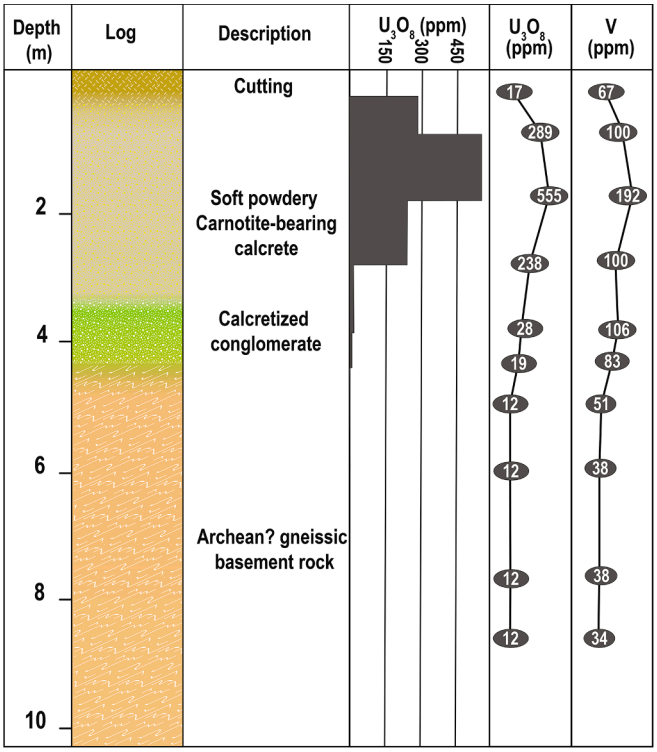

Fig. 16. Morocco. Detailed core log of the exploration drill hole LH4 in the Aghracha prospect (x = 524572; Y = 2565558; Z = 224). Vanadium is enriched in the supergene zone.

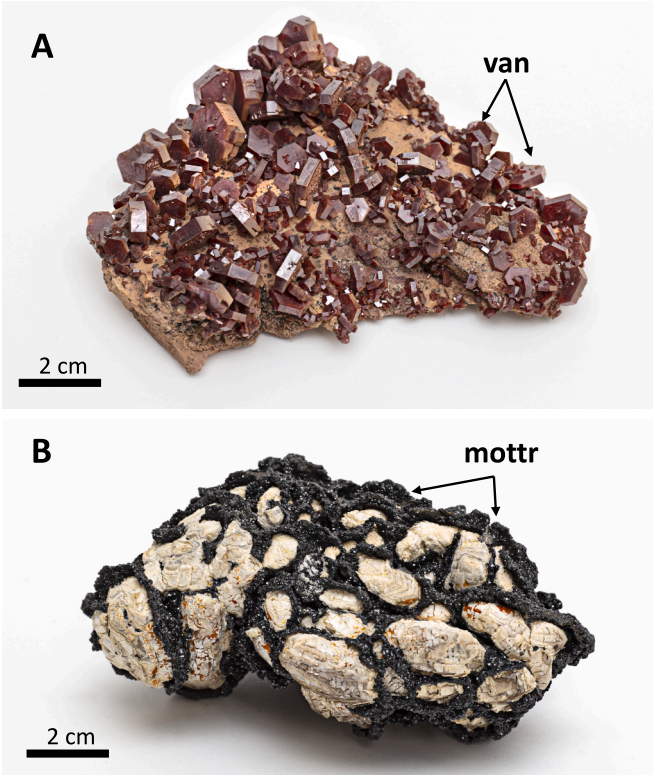

Fig. 17. Morocco. A) Agglomerate of red hexagonal-shaped vanadinite crystals from the Mibladen deposit (NHM Mineralogy collection, specimen # BM.1987,332). B) Black crystalline crust of mottramite partly coating curved barrel-shaped pale-brown arsenian vanadinite (endlichite) crystals from Touissit (NHM Mineralogy collection, specimen # BM.1993,380).

of pre-existing sulfides and consist of Zn-Cu-Pb vanadate ores with mottramite, descloizite and vanadinite. Vanadinite occurs in the oxidation zone of primary Pb-sulfides either as sprays of reddish to orange tabular plates lining the walls of the cavities, or concentrated along bedding planes and in veins. A supergene model involving a series of reactions between downward percolating meteoric waters, metal sulfides, and reactive host rocks concurrently with Late Miocene to Holocene tectonic uplift and/or water table depression is proposed as the main driving mechanism for the precipitation of the V-U-Mo rich mineralizations (Bouabdellah et al., 2021). Similar to the Mibladen deposit, the Touissit-Bou Beker MVT district (greater than100 million tons at 4 wt% Pb, 3.5 wt% Zn, less than1 wt% Cu, 120 g/t Ag) shows occurrences of vanadates (Fig. 17B), which are considered to have formed during a late stage of supergene alteration (Bouabdellah et al., 2021). Two small deposits, located at the Jbel Klakh and the Jbel Haouanit, close to the city of Bou Arfa, also show a supergene assemblage of Zn-Pb-Cu minerals. A significant proportion of vanadates (mainly mottramite) occur in the Jurassic dolostones at Jbel Haouanit (Verhaert et al., 2017) close to the Cu mineralizations. The high V content observed at Jbel Haouanit may be related to the initial occurrence of this element in hypogene minerals and the percolation of V-bearing fluids through the entire deposit (Verhaert et al., 2017). In the Toulal Zn-Pb supergene deposit in the east of the country, Choulet et al. (2014) detected descloizite concentrations associated with the gossanous assemblage, not evaluated at the resource level.

7.6. Niger

In Niger U was discovered in 1957 at Azelik by the French Bureau de Recherches Géologiques et Minières (BRGM) (IAEA, 2020). Further discoveries were made in the late 50 s and 60 s, including Abokurum

(1959), Madaouela (1963), Arlette, Ariège, Artois and Tassa/Taza (1965), Imouraren (1966), and Akouta (1967). The first production started at Arlit in 1971 (Kinnaird and Nex, 2016). Vanadium could be present in either of the above prospects (Fig. 3; Table 1). The Imouraren U mine, which is the largest U deposit in Africa (IAEA, 2020), is located in the Jurassic-Cretaceous Tchirezrine sandstones 80 km south of Arlit. The U-(V) mineralizations are hosted in heterogranular fluvial sandstone (Mamadou et al., 2022) and vanadium is mostly associated with chlorites in the form of *montroseite* [$(V^{3+},Fe^{3+})O(OH)$]. The presence of V, Zr, Mo and Zn in the Imouraren deposit is related to volcanic sources (Pagel et al., 2005). Imouraren is estimated to contain 179,000 tons of U, but the V amounts have not been fully determined.

7.7. Nigeria

Coniacian to Santonian oolitic Fe ores similar to the Egyptian ones, occur in Nigeria (Sokoto, Lokoja) (Mücke, 2000). However, no V anomaly has been recorded in this country yet. Bamalli et al. (2011) have mentioned the occurrence of V at Abuja (where this element also occurs as a pollutant in soils), but no further research has followed up on this topic.

7.8. Sudan

In Sudan, U was discovered in 1977 in the area of the Nuba Mountains and at Hufrat El Nahas in Darfur. Two types of occurrences have been further detected in the Jebel Kurun and Uro areas in the center of the eastern Nuba Mountains, containing U and V in vein-like phosphates (Dill et al., 1991; Adam et al., 2014). The V concentrations exceed those of U, sometimes with a 3:1 ratio. Vanadium values up to 10,000 ppm were mentioned by Sedig (2018) in these deposits. Dill et al. (1991) considered this mineralization as being of potential economic interest for P, U, and V. However, more recently, H. Dill (personal communication, 2022) re-evaluated these mineralizations as not being feasible for economic use.

After Dill et al. (1991), phosphate precipitation in Sudan is related to Quaternary supergene processes under arid to semi-arid conditions. Vanadium was probably derived from weathered ultramafic rocks and associated metamorphosed black shales.

Coniacian-Santonian oolitic Fe ores with similar characteristics as the Egyptian "*minette*" equivalents also occur in Sudan (Wadi Haifa) (Mücke, 2000), but no V anomaly has been reported in them yet.

Exploration for possible V concentrations might be carried out in Sudan in the metamorphic graphite-hosting lithologies of the Northern Mozambique Belt, as in Madagascar and Mozambique (Parnell, 2022).

7.9. Tunisia

The oolitic ironstone deposit of Jebel Ank (central Tunisia) is a stratiform orebody of about 2.5–8 m in thickness, located in the upper part of the Souar Formation (Late Eocene) (Fig. 3; Table 1). This deposit contains about 20 million tons of ore with an average grade of 50% Fe (Garnit and Bouhlel, 2016). An enrichment in V, Cr, Ni, Zn, and REEs-Y has been detected in the Fe-orebody. The ironstone's V concentration ranges between 600 and 900 ppm, with the highest amounts being detected in goethite (greater than1,000 ppm V). No economic significance is currently associated with this deposit.

Vanadates of the same type as those of Moroccan deposits (Bouabdellah et al., 2021) have been detected and partly exploited in the Atlas Mountains of Tunisia (Fig. 3; Table 1). The best examples are the Djebba (Beja) Zn-Pb mine in the Jebel Goraa syncline and several smaller mineralized occurrences around it, which contain significant amounts of V. The exploited Djebba ores were mainly nonsulfides (smithsonite and cerussite) and Pb-vanadates associated with the oxidation ores (Solignac, 1935; Sainfeld, 1952; Mahjoub, 1973; Garnit et al., 2022). Other ore types with similar characteristics are known at Jebel El Agab in Central Tunisia. Vanadium mineralizations are developed in karst cavities filled with clayey materials (smectite) and oxidized ores (goethite, smithsonite, and hemimorphite) (Garnit et al., 2022). The paragenesis of supergene ores reveals two stages of deposition: 1) early supergene weathering with the formation of Fe-bearing carbonates, subsequently oxidized to goethite; smithsonite, hemimorphite, and cerussite; and 2) late supergene weathering with deposition of Pb-Zn > Cu-As-P vanadium minerals like vanadinite, descloizite, minor mimetite, and vanadinite-pyromorphite (Garnit et al., 2022).

Tunisian phosphate deposits are of sedimentary origin; the P ores are mainly composed of francolite, in a matrix of calcite, dolomite, quartz, gypsum, and clay minerals. Uranium and vanadium occur in the Tunisian phosphorites, but are not very abundant.

8. Discussion

The African continent hosts significant and economically attractive V resources, which include all types of natural vanadium ore deposits, from the traditionally exploited Namibian-style vanadates and the Bushveld V-bearing magnetite types, to more unconventional V mineralizations, such as the V-graphite deposits of Mozambique and Madagascar, or the vanadium occurrences sporadically hosted in U, phosphate, Fe and bauxite deposits.

8.1. Vanadiferous (titano)magnetite deposits

The economically most important vanadium resources in Africa are associated with magnetite layers in mafic–ultramafic magmatic intrusions, especially of the Bushveld Complex (South Africa; Witley et al., 2019) and of the Great Dyke and its satellite intrusions (Zimbabwe). Most of the vanadium in titaniferous magnetite deposits is concentrated as a solid solution in magnetite-ulvöspinel, where V^{3+} has replaced Fe^{3+} (Fischer, 1975). The vanadium-rich spinel mineral *coulsonite* (FeV_2O_4) was reported as small blebs and exsolution blades in magnetite in a few South African deposits (Balsley, 1943; Fischer, 1975). Even though the mechanisms causing the concentration of millions of tons of vanadium in massive Fe-Ti oxide deposits remain poorly understood, there is a general agreement that partial melting of mantle rocks and magmatic fractionation are the critical early-stage processes (Kelley et al., 2017). Large-scale crystallization of plagioclase and other anhydrous phases (olivine, pyroxene) in the basal parts of magma chambers fractionates Fe and water in the residual melt, with the eventual formation of an immiscible oxide melt fraction (Reynolds, 1985; Eales and Cawthorn, 1996; Shellnut and Jahn, 2010; Ivanic et al., 2018). Such oxide ore melts are denser than silicate melts and therefore settle at the bottom of the magma chamber (Eales and Cawthorn, 1996; Zhou et al., 2005). Many layered intrusions show evidence of multiple magma injections (Eales and Cawthorn, 1996), suggesting that magma mingling may have played a role in developing the titaniferous magnetite deposits. Deposit types similar to the Bushveld have been recorded in association with the Kabanga-Musongati intrusions (Burundi) and with the Tete metagabbros and the Atchiza Suite in Mozambique. Smaller occurrences of V-magnetite ores occur also in the Tin Edia deposit in Burkina-Faso. The age of the V-bearing mafic–ultramafic igneous rocks ranges from 2,540 Ma (Great Dyke of Zimbabwe) to 1,403 ± 14 Ma (Kabanga-Musongati, Burundi); the Bushveld V-bearing magnetite layers have an age around 2,000 Ma.

Vanadium occurrences of variable economic significance are also hosted in carbonatites, as those detected in the magnetite at Phalaborwa in South Africa (2,047 Ma in age), in the Paleoproterozoic Gleibat Lafhouda, and the Upper Cretaceous Twihinate carbonatites in Morocco. The magnetite–copper–phosphate–rare earth element pipe-like orebody occurring at Loolekop, within the larger Phalaborwa Carbonatite Complex, has many features to suggest that it might represent an end member of the Olympic Dam-type deposit class (Groves and Vielreicher, 2001). Vanadium is almost constant in titanomagnetite across the entire

Twihinate prospect in Morocco (0.2 to 0.7 wt%). However, the V content in African carbonatites is currently still considered a by-product of other metallic resources, even if locally reaching grades above 1% V_2O_5 (Milani et al., 2017).

8.2. Graphite-associated vanadium deposits in metamorphic terranes

The vanadium mineralizations associated with graphite bodies in the Mozambique Metamorphic Belt are of particular interest. The Bekily Block, where the Neoproterozoic Green Giant project (Madagascar) is located, and the Xixano Complex (Mozambique) are the most representative areas where several examples of this mineralizations type are recorded. In this category of deposits, V is thought to be primarily associated with organic-rich sediments, which have been deposited between 800 and 600 Ma not only in the African continent but worldwide (Parnell, 2022). Vanadium became available to the surface during Neoproterozoic, when anomalous amounts of this element were introduced in large igneous provinces. In fact, global magmatic activity caused the enrichment in vanadium of the Neoproterozoic crust (Li et al., 2008), followed by a global glacial erosion, which transported significant amounts of vanadium to the oceans (Parnell, 2022). Under anoxic conditions, V was incorporated in carbon-rich sediments as silicates and/or associated with organic matter (Breit and Wanty, 1991). When carbonaceous rocks were metamorphosed, as in the African Mozambique Belt, their clay minerals were converted to micas, a process that helped the sequestration of V. In fact, the main residence mineral of V is the vanadian mica roscoelite (Di Cecco et al., 2018; Parnell, 2022). The minerals identified in the Green Giant deposit in Madagascar are similar to those described by Koneva (2002) from the Sludyanka area in the Lake Baikal region, Russia (Di Cecco and Tait, 2018). After Parnell (2022), the graphite concentrations also detected in Ethiopia, Sudan, and Egypt, as in the northern equivalent of the Mozambique Belt, could be a vector to discover also in those countries V ores with similar characteristics as in south Madagascar (Asia Pacific Gold Mining Investment Ltd., 2013). The weathering of this kind of deposit enriches V in secondary minerals typical of the supergene realm (i.e., clays, oxides etc.).

Continued metamorphism caused the formation of the semi-precious stone vanadian grossular tsavorite, which occurs in graphitic gneisses in Madagascar, Tanzania, and Kenya (Adamo et al., 2012; Feneyrol et al., 2017; Giuliani et al., 2018). Tsavorite is emerald-green colored by reduced V^{3+} and Cr^{3+}, and has the following ideal stoichiometry $Ca_3(Al,V,Cr)_2(SiO_4)_3$ (Feneyrol et al., 2012). After Suwa et al. (1996), the mode of occurrence of V-grossular in Kenya is quite similar to that in the Sør Rondane Mountains, East Antarctica. The blue V variety of zoisite (tanzanite) is also a precious stone, much more sporadically found than tsavorite (Harris et al., 2014). Both *tsavorite* and *tanzanite* are not ore minerals for vanadium meant as commodity.

8.3. Sandstone- and calcrete-hosted (U)-vanadium deposits

The presence of vanadium in U-(V) minerals is ubiquitous in sandstone-hosted systems, discovered and locally exploited in the Upper Paleozoic-Mesozoic Karoo continental sediments (IAEA, 2020). Typical examples occur in Botswana, South Africa, and Zimbabwe. In several U occurrences, such as the giant Kayelekera deposit in Malawi or the Mounana deposit in Gabon, V can be considered a valuable by-product. Many U deposits in Niger, currently closed, which contain V credits, also belong to this category of ore deposits. The presence of V and Zr, Mo, and Zn at Imouraren, the major deposit in Niger, is related to volcanic sources (Pagel et al., 2005).

Significant U-(V) concentrations (where carnotite prevails) occur in relatively recent (Tertiary-Quaternary) calcrete formations located in former fluviatile beds and paleochannels throughout the African continent. Typical examples are the deposits of the Erongo region in Namibia: e.g., Langer Heinrich and Klein Trekkopje, with U and V sourced by the weathering and dissolution of the granites and metamorphites nearby (Lilende, 2012; Kinnaird and Nex, 2016). Oxidizing conditions were fully achieved at Langer Heinrich and the subsurface water spent longer in ponds, resulting in the long-lasting interaction with air and seasonal rains. As a result, V^{4+} could be effectively oxidized to V^{5+}, which is pivotal for the precipitation of carnotite (Lilende, 2012). Carnotite-rich ores have been detected in calcretes in Mauritania, Morocco, Somalia, Tanzania, and Botswana.

8.4. Vanadate deposits

The Pb-Zn-Cu vanadates are unique among the V occurrences, representing an ore type that occurs in several African countries in the oxidation zone of base-metal deposits (Millman, 1960; Boni et al., 2007; Bouabdellah and Slack, 2016). The vanadates are generally associated with nonsulfide ores, but are genetically distinct from them. The specific vanadates association (e.g., vanadinite, descloizite, mottramite) ranges from a mineralogical curiosity to an economic resource (Namibia, Morocco, Botswana) and can represent a real asset, especially in those countries where old tailings and slags have been accumulated in historic mining areas (Namibia, Zambia). The Otavi Mountainland vanadates are considered to have formed during a late phase in the depositional history of the post-Damaran supergene ores (Verwoerd, 1957). In fact, throughout the African realm, their age is restricted to Tertiary and Quaternary, and their formation is associated with a series of alternating humid-arid weathering phases in a continental environment (Boni et al., 2007; Choulet et al., 2014; Bouabdellah et al., 2021; Garnit et al., 2022). The age of most deposits in the Otavi Mountainland appears to be confined to the Tertiary, with a distinct period of descloizite formation dated from 24 to 33 Ma (Boni et al., 2007). The V-rich ores are genetically related to post-Gondwanan erosional episodes, controlled by a tectono-morphological and climatic evolution following rifting phases in the Atlantic realm. The base metals occurring in the vanadates originate from the same sulfides present deep down in the primary deposits, while the origin of vanadium is considered variable: from magmatic, sedimentary, or metamorphic rocks or from a mixture of all of them, derived from the older basements nearby. Similar genesis is also suggested for vanadate deposits in northern Botswana. Also, in central Zambia (Kabwe), it is unlikely that the sulfides were the source of vanadium for the vanadates occurring in the oxide zone. The descloizite at Kabwe (Zambia) was dated at 20–37 Ma (N.J. Evans, unpublished U/Th-He data in Boni et al., 2007). As in Namibia, the age of the Zambian vanadates could reflect a regional climate effect. The Lueca V deposit in Angola has several similarities with the Namibian vanadate ores because it is probably also of residual origin, being formed at the expense of a preexisting Cu-Pb-Zn orebody. However, the presence of abundant quartz, intimately associated with vanadates, phosphates, and Cu silicates, and the silicification of the host dolomitic limestone are unusual. They may be due to a resurgence of low-temperature hydrothermal solutions associated with renewed movement along faults (Millman, 1960).

The vanadium concentrations in the weathering zone of the giant sulfide deposit of Bamba Kilenda (DRC) (Lesaffer, 2014) have several similarities with those of the upper levels in the Tsumeb deposit in Namibia (Boni et al., 2007). However, the Tsumeb orebody is restricted to limestone-dolomite host rocks, and that of Bamba Kilenda occurs in arkose. For this reason, Bamba Kilenda share more analogies with the Lueca deposit in Angola (Millman, 1960).

The vanadate deposits of Morocco and Tunisia are located in the oxidation zone of the sulfide deposits of the Atlas chain. A supergene model involving an interplay between downward percolating acidic meteoric waters, Late Miocene uplift, and climate changes is proposed as the main ore-forming process that triggered the vanadate ore deposition (Bouabdellah et al., 2021). In Tunisia, the main characteristic in the composition of vanadates is the significant presence of As and P. During Late Neogene-Pleistocene, several episodes of uplift and erosion enabled

here the exhumation and karstification of the Early Eocene organic-rich rocks, the alteration of hypogene Pb-Zn-Fe sulfides, and the final formation of supergene ores. Paleoclimatic studies allowed constraining the age of the vanadates in Tunisia between Late Miocene and Early Pliocene (Garnit et al., 2022).

8.5. Other vanadium deposits

In the African continent, V is also present in U-bearing apatite in phosphorite horizons interbedded with marine muds, shale, carbonate, and sandstone (Abed et al., 2014). Vanadium > uranium enrichments occur in Northern African sedimentary phosphorites, which are part of the Late Cretaceous-Eocene Giant Phosphorite Belt, extending from the Caribbean to the Middle East through North Africa (Buccione et al., 2021). In this kind of phosphorites V is generally hosted in organic matter.

Variable but significant V amounts have been observed in Fe ore deposits (different from the V-magnetite types), in laterites, and bauxites; in most cases V is contained in goethite. Vanadium anomalies, as other related elements, have been recorded in the Fe-oxy-hydroxides of Ethiopian and Ghanan Fe ore deposits, and in the ironstone occurrences in Algeria and Lybia. As in the case of bauxite ores (Liberia, Cameroon), V anomalies in these lithotypes could only be considered a potential by-product if their extraction is relatively easy and not exceedingly costly.

9. Conclusions

On the whole, vanadiferous titanomagnetite (VTM) deposits, generally associated with mafic and ultramafic magmatic episodes of different ages, are still the principal vanadium source of the African continent. The most significant V concentrations are in South Africa (Bushveld Complex), but also in Zimbabwe, associated with the Great Dike intrusion and its satellites. In Central and Eastern Africa similar Fe-Ti-V ores have been found and locally exploited in Burundi (Mukanda-Buhoro mafic intrusion), in Mozambique (Tete Metagabbro, Atchiza Suite etc.) and in other countries as well. In western Africa there are only few significant vanadium occurrences, like the Kassala-Kitungo Fe-Ti-V deposits in Angola, the Fe-Ti-V Tin Edia concentrations in Burkina Faso and the newly explored Marela project in Guinea. In Northern Africa the most significant V occurrences are in Morocco, in association with carbonatite bodies and their weathering products.

The main V mineral occurring in African calcretes is carnotite. Calcrete deposits are limited to Tertiary-Quaternary and are the result of the precipitation of U-V minerals during arid climate phases. The geological occurrence of these deposits, however, is multifaceted. They can occur: i. as real calcretes in old fluviatile beds cutting the old basements (Erongo, Namibia), ii. as weathering horizons derived from sandstone-hosted U-(V) bodies (Botswana, South Africa), iii. in carnotite-enriched weathering profiles on carbonatites or metamorphic rocks (Mauritania, Morocco).

The V ores associated to graphite-schists are mainly restricted to the Eastern areas of the African continent. They occur in several countries of the Mozambique Metamorphic Belt: Madagascar, Kenia, Tanzania, Mozambique, Ethiopia, and Uganda. Their economic potential is variable, ranging from minor occurrences to deposits.

The vanadate deposits are also widespread through the whole continent, with significant concentrations in Namibia, Botswana and Zambia and in Northern Africa. They are generally associated with a primary source of base metal ores, “contaminated” by an external (igneous, metamorphic) contribution of V. This kind of occurrences, however, are not currently considered of high economic importance, due to their low tonnages and sporadic distribution throughout the host rock.

Vanadium assets in the African continent may include newly discovered occurrences, re-exploitable concentrations in old mining licenses, and re-processable waste material from several areas. The already known mining districts, where V in (titano)magnetite ore types prevails, are considered having the best economic potential. Nevertheless, it is important to stress the growing significance of U-(V) concentrations in relatively recent (Tertiary-Quaternary) calcrete formations in former fluviatile beds or in several weathered zones. This type of deposits is quite widespread throughout the continent, where available sources and paleoclimatic conditions have been favorable to the fixation of V and U in surficial environments.

Variable V amounts have been also recorded in iron ore deposits, phosphorites, and laterites.

In conclusion, as also highlighted by Kinnaird and Nex (2016), world demand, market price, and the political stability of the countries in which the deposits are hosted will determine the economic value of the V deposits. Many projects that were explored in the past are currently viable because of the steadily increasing prices of several elements, including V. South Africa, which holds the highest-grade primary vanadium resources globally, leading to growth in demand in the energy sector, could mostly benefit from exploiting its resources. However, also many other African countries, where V could be profitably extracted as a by-product of other economic ores, could also be at the forefront of V production in the near future.

Declaration of Competing Interest

The authors declare that they have no known competing financial interests or personal relationships that could have appeared to influence the work reported in this paper.

Data availability

No data was used for the research described in the article.

Acknowledgements

We would like to thank Prof. F. Pirajno and the Editorial Board of Ore Geology Reviews for having invited our research team to present this review on the Vanadium deposits and prospects in the African continent. A special thank is to B. Orberger, who initiated one of us (M. Boni) to this interesting subject and to F. Aponte, who provided the data on the vanadium deposits in Zimbabwe. Part of this study was a contribution to the 7th SGA-IUGS-UNESCO-SEG- Short Course on African Metallogeny: “Energy Metals for a Sustainable Society”, held in Windhoek (Namibia), from 29th November to 3rd December 2021.

A first revision by H. Dill of an earlier version of this manuscript has been greatly appreciated, as well as the useful comments of two anonymous reviewers.

We are also indebted to M. Rumsey, curator of the Mineralogy Collection of the Natural History Museum, London, for allowing us to access vanadium mineral specimens. No funding was allotted to this research work.

References

Abbate, E., Bruni, P., Sagri, M., 2015. Geology of Ethiopia: A review and geomorphological Perspectives. In: Billi, P. (Ed.), Landscapes and Landforms of Ethiopia, World Geomorphological Landscapes. Springer Science+Business Media Dordrecht, pp. 33–64.

Abed, A.M., Saffarini, G.A., Sadaqah, R.M., 2014. Spatial distribution of uranium and vanadium in the upper phosphorite member in Eshidiyya basin, southern Jordan. Arab J. Geosci. 7, 253–271.

Adam, A.A., Eltayeb, M.A.H., Ibrahim, O.B., 2014. Uranium recovery from Uro area phosphate ore, Nuba Mountains, Sudan. Arab. J. Chem. 7, 758–769.

Adamo, I., Diella, V., Pezzotta, F., 2012. Tsavorite and other grossulars from Itrafo, Madagascar. Gems Gemol. (3), 178–187.

Afify, A.M., Osman, R.A., Wanas, H.A., Khater, T.M., 2022. Mineralogical and geochemical studies of copper mineralization in the Paleozoic sedimentary section in southwestern Sinai, Egypt. Ore Geol. Rev. 147, 104994.

AGP Mining Consultants Inc., 2011. Green Giant Project, Fotadrevo, Province of Toliara, Madagascar Technical Report Update NI 43-101.

Akinlua, A., Olise, F.S., Akomolafe, A.O., McCrindle, R.I., 2016. Rare earth element geochemistry of petroleum source rocks from northwestern Niger Delta. Mar. Pet. Geol. 77, 409–417.
Amm, F.L., 1940. The geology of the country around Bulawayo. Southern Rhodesia Geological Survey Bulletin 35, 307.
Asia Pacific Gold Mining Investment Ltd. 2013. Asia Pacific Gold Mining Investment Ltd announces graphite potential in western Ethiopia. https://www.investegate.co.uk/asia-pacific-gold-mining-inves–apgm /prn/announces-graphite-potential in westernethiopia/20130930095355PB1D8/.
Aura Energy Ltd., 2022. Vanadium at Tiris: In-demand resource adds magic to Aura's Mauritanian uranium project. https://stockhead.com.au/resources/vanadium-at-tiris-in-demand-resource-adds-magic-to-auras-mauritanian-uranium-project-2/.
Austrade, 2020. Australian Critical Minerals Prospectus 2020 (Australian Government Report, p. 172).
Badahmaoui, T., Bugrieva, E.P., Lavrukhin, A.A., 2020. Characteristics of uranium mineralization in the Tin-Seririne sedimentary basin (Algeria). J. Phys. Conf. Ser. 1689, 012050 https://doi.org/10.1088/1742-6596/1689/1/012050.
Baioumy, H.M., 2021. Geology of Rare Metals in Egypt - A review. Publish. Int. J. Mater. Technol. Innov. 1, 58–76.
Baioumy, H.M., Ismael, S.I., 2010. Factors controlling the compositional variations among the marine and non-marine black shales from Egypt. Int. J. Coal Geol. 83, 35–45.
Baioumy, H.M., Omran, M., Fabritius, T., 2017. Mineralogy, geochemistry and the origin of high-phosphorus oolitic iron ores of Aswan, Egypt. Ore Geol. Rev. 80, 185–199.
Balsley, J.R., 1943. Vanadium-bearing magnetite-ilmenite deposits near Lake Sanford Essex County, New York. USGS, Bulletin 940-D, p. 123.
Bamalli, U.S., Moumouni, A., Chaanda, M.S., 2011. A review of Nigerian metallic minerals for technological development. Nat. Resour. 2, 87–91.
Baobab, 2010. Interim Results for the 6 Months Ended 31 December 2010. Baobab Resources plc., p. 16.
Baobab-Steel.com, 2022. Baobab Steel and Vanadium Project. Baobab Steel Ltd, Maputo. https://baobab-steel.com/tete-steel-and-vanadium (accessed February 27, 2023).
Bariand, P., Chantret, F., Pouget, R., Rimsky, A., 1963. Une nouvelle éspèce minérale: la chervetite, pyrovanadate de plomb $Pb_2V_2O_7$. Bulletin de la Société française de Minéralogie et de Cristallographie 86 (2), 117–120.
Barr, M.W.C., Brown, M.A., 1987. Precambrian gabbro–anorthosite complexes, Tete Province, Mozambique. Geol. J. 22 (S2), 139–159.
Barrie, T.C., 2009. Genesis of the Green Giant Vanadium Deposit (quoted in "Green Giant Project Fotadrevo, Province of Toliara, Madagascar, Technical Report Update Ni 43-101").
Becker, B., Kärner, K., 2009. Geological setting of the Langer Heinrich uranium deposit, Namibia. Proceedings International Symposium IAEA in cooperation with the OECD Nuclear Energy Agency, the Nuclear Energy Institute and the World Nuclear Association Vienna, Austria, 22–26 June 2009, p. 12.
Bezzi, N., Aifa, T., Hamoudi, S., Merabet, D., 2012. Trace elements of Kef Es Sennoun natural Phosphate (Djebel Onk, Algeria) and how they affect the various mineralurgic modes of treatment. In: 20th International Congress of Chemical and Process Engineering CHISA 2012, 25- 29 August, Prague, Czech Republic. Procedia Engineering, Elsevier, 42, 2097-2111. 10.1016/j.proeng.2012.07.588 . insu-00727211.
Bishady, A.M., 2017. Mineralogy of graphite from the graphite-bearing schists of Wadi Lawi, South Eastern Desert. Egypt. Journal of Geological Resource and Engineering 4, 178–187.
Boni, M., Terracciano, R., Evans, N.J., Laukamp, C., Schneider, J., Bechstädt, T., 2007. Genesis of Vanadium Ores in the Otavi Mountainland, Namibia. Econ. Geol. 102, 441–469.
Bouabdellah, M., Boukirou, W., Potra, A., Melchiorre, E., Bouzahzah, H., Yans, J., Zaid, K., Idbaroud, M., Poot, J., Dekoninck, A., Levresse, G., 2021. Origin of the Moroccan Touissit-Bou Beker and Jbel Bou Dahar supergene non-sulfide biomineralization and its relevance to microbiological activity, late Miocene Uplift and climate changes. Minerals 11, 401.
Bouabdellah, M., Boukirou, W., Jébrak, M., Bigot, F., Yans, Y., Mouttaqi, A., El Gadarri, M., Errami, A., Levresse, G., 2022. Discovery of antiskarn-hosted strategic metal mineralization in the Upper Cretaceous Twihinate carbonatite intrusion (West African Craton Margin, Moroccan Sahara). Ore Geol. Rev. 149, 105105 https://doi.org/10.1016/j.oregeorev.2022.105105.
Blencowe Resources, 2022. Pre-Feasibility Study for Orom-Cross Graphite Project, July 2022. https://blencoweresourcesplc.com/.
Bouabdellah, M., Chakhmouradian, A., Mouttaqi, A., Cuney, M., Ait Kassi, A., 2012. Potentiel en métaux stratégiques (REE, Nb, Zr, Ta, U, Th) des carbonatites à travers des exemples de gisements du Maroc et d'ailleurs. In: Rabeau, et al. (eds), Programme et résumés. Ressources minérales et nouvelle économie: Innovation et découvertes. Colloque international dans le cadre du 80ème Congrès de l'ACFAS: Quatrièmes journées De Launay. Ministère des Ressources Naturelles et de la Faune, Québec, p. 17. GM 66219, 8-9 mai 2012.
Bouabdellah, M., Sangster, D.F., 2016. Geology, geochemistry, and current genetic models for major Mississippi Valley-type Pb–Zn deposits of Morocco. In: Bouabdellah, M., Slack, J.F. (Eds.), Mineral Resource Reviews. Springer-Verlag, Berlin-Heidelberg, pp. 463–495.
Bouabdellah, M., Slack, J.F., 2016. Geologic and metallogenic framework of North Africa. In: Bouabdellah, M., Slack, J.F. (Eds.), Mineral Deposits of North Africa. Mineral Resource Reviews. Springer-Verlag, Berlin-Heidelberg, pp. 3–81.
Bouaziz, S., Barrier, E., Soussi, M., Turki, M.M., Zouari, H., 2002. Tectonic evolution of the northern African margin in Tunisia from paleostress data and sedimentary record. Tectonophysics 3571, 227–253.
Boukirou, W., Bouabdellah, M., Chakhmouradian, A.R., Mouttaqi, A., Reguir, E.P., Hauff, F., Cuney, M., Jébrak, M., Yans, J., Hoernle, K., 2022. Petrogenesis of the late Paleoproterozoic Gleibat Lafhouda dolomite carbonatite (West African Craton Margin, Moroccan Sahara) and its relevance to the onset of fragmentation of the Columbia supercontinent. Chem. Geol. 594, 120764.
Bouzenoune, A., Lécolle, P., 1997. Petrographic and geochemical arguments for hydrothermal formation of the Ouenza siderite deposit (NE Algeria). Miner. Deposita 32, 189–196.
Bowden, R.A., Shaw, R.P., 2007. The Kayelekera uranium deposit, Northern Malawi: past exploration activities, economic geology and decay series disequilibrium. Appl. Earth Sci. (Trans. Inst. Mining Metallurgy) B 116 (2), 55–67.
Bowell, R.J., Davies, A.A., 2017. Assessment of supergene uranium-vanadium anomalies, Meob Bay deposit, Namibia. Geochemistry Exploration Environment. Analysis 17 (2). https://doi.org/10.1144/geochem2015-406.
Bowell, R.J., Booysens, M., Pedley, A., Church, J., Moran, A., 2008. Characterization of carnotite uranium deposit in calcrete channels, Trekkopje, Namibia. In: Proceedings of Africa Uncovered: Mineral Resources for the future. SEG-GSSA 2008 Conference, Johannesburg, 7–10 July 2008, 114–121.
Boyd, R., Nordgulen, O., Thomas, B., Bingen, B., Bjerkgård, T., Grenne, T., Henderson, I., Melezhik, V.A., Sandstad, J.S., Solli, A., Tveten, E., Viola, G., Jacobs, J., Bauer, W., 2010. The geology and geochemistry of the East African orogen in northeastern Mozambique. S. Afr. J. Geol. 113 (1), 87–129.
Breit, G.N., 2016. Resource potential for commodities in addition to uranium in Sandstone-Hosted Deposits. Rev. Econ. Geol. 18 (13), 323–337.
Breit, G.N., Wanty, R.B., 1991. Vanadium accumulation in carbonaceous rocks. A review of geochemical controls during deposition and diagenesis. Chem. Geol. 91 (2), 83–97.
Briot, P., 1984. Surficial uranium deposits in Somalia. International Atomic Energy Agency, Vienna (Austria), pp. 217–220.
Bros, R., Stille, P., Gauthier-Lafaye, F., Weber, F., Clauer, N., 1992. Sm-Nd isotopic dating of Proterozoic clay material. Example from Francevillian sedimentary Series (Gabon). Earth and Planetary Science and Letters 113, 207–218.
Brough, C., Bowell, R.J., Larkin, J., 2019. The geology of Vanadium deposits. In: An Introduction to Vanadium, Chap. 4; R. Bowell Editor, Nova Science Publishers, Inc., 87-117.
Buffet, G., Amosse, J., Mouzita, D., Giraud, P., 1987. Geochemistry of the M'Passa Pb-Zn deposit (Niari syncline, People's Republic of the Congo). Arguments in favor of a hydrothermal origin. Miner. Deposita 22, 64–77.
Burundi Ministry of Energy and Mines, 1991. Burundi mineral resources—An investment brochure: Bujumbura, Burundi. Burundi Ministry of Energy and Mines, p. 41.
Cahen, L., Snelling, N.J., Delhal, J., Vail, J.R., Bonhomme, M., Ledent, D., 1984. In: The geochronology and evolution of Africa. Oxford University Press, pp. 162–178.
Cailteux, J.L.H., Kampunzu, A.B., Lerouge, C., Kaputo, A.K., Milesi, J.P., 2005. Genesis of sediment-hosted stratiform copper–cobalt deposits, central African Copperbelt. J. Afr. Earth Sc. 42, 134–158.
Cairncross, B., Dixon, R., 1995. Minerals of South Africa. Geological Society of South Africa, PO Box 44283, Linden 2104, South Africa, p. xviii + 290.
Cairney, T., Kerr, C.D., 1998. The geology of the Kabwe area: explanation of degree sheet 1428, NW quarter. Geological Survey of Zambia, Report 47, 40.
Callaghan, C., 2011. Mozambique Mineral Scan Report. Trademark Southern Africa TMSA 193.
Carlisle, D., 1983. Concentration of uranium and vanadium in calcretes and gypscretes. Geological Society of London, Special Publications 11, 185–195.
Carney, J.N., Aldiss, D.T., Lock, N.P., 1994. The geology of Botswana. Geological Survey Department, Bulletin 37, Ministry of Natural Resources and Water Affairs, Republic of Botswana, p. 113.
Cawthorn, R.G., 2005. Contrasting sulphide contents of the Bushveld and Sudbury Igneous Complexes. Miner. Deposita 40, 1–12.
Cawthorn, R.G., and Molyneux, T.G., 1986, Vanadiferous magnetite deposits of the Bushveld Complex, in: Anhaeusser, C.R., and Maske, S., eds., Mineral deposits of southern Africa: Johannesburg, Geological Society of South Africa, v. 2, 1251–1266.
Cawthorn, R.G., Merkle, R.K.W., Viljoen, M.J., 2002. Platinum-group element deposits in the Bushveld Complex, South Africa. In: Cabri, L.J. (ed) The geology, geochemistry, mineralogy and beneficiation of platinum-group elements. Canadian Institute of Mining, Metallurgy and Petroleum 54, 389–430.
Choulet, F., Charles, N., Barbanson, L., Branquet, Y., Sizaret, S., Ennaciri, A., Badra, L., Chena, Y., 2014. Non-sulfide zinc deposits of the Moroccan High Atlas: multi-scale characterization and origin. Ore Geol. Rev. 56, 115–140.
Ciacci, L., Reck, B.K., Nassar, N.T., Graedel, T.E., Lost by Design. Environment Science Technology 49 (16), 9443–9451.
Collier, R.W., 1984. Particulate and dissolved vanadium in the North Pacific Ocean. Nature 309 (5967), 441–444.
Collins, A.S., 2006. Madagascar and the amalgamation of Central Gondwana. Gondw. Res. 9 (1–2), 3–16.
Cox, D.P., Lindsey, D.A., Singer, D.A., Moring, B.C., Diggles, M.F., 2003. Sediment-hosted copper deposits of the world: deposit models and database. USGS Open-File Report 03–107.
De Bruin, J., 2017. Molo Feasibility Study NI 43-101. NextSource Materials Inc., p. 942.
Deblond, A., 1994. Géologie et pétrologie des massifs basiques et ultrabasiques de la ceinture Kabanga-Musongati au Burundi. Annales du Musée Royal de l'Afrique Centrale Tervuren. Sciences géologiques 99, 123.
Deblond, A., Tack, L., 1999. Main characteristics and review of mineral resources of the Kabanga-Musongati alignment in Burundi. J. Afr. Earth Sc. 29, 313–328.
Deliens, M., Piret, P., 1977. La kusuïte (Ce^{3+}, Pb^{2+}, Pb^{4+})VO_4, nouveau mineral. Bulletin de la Société Française de Minéralogie et de Cristallographie 100, 39–41.

Desautels, P., McCracken, T., Holloway, A., 2011. Green Giant project, Fotadrevo, province of Madagascar. NI 43–101 Technical Report, p. 247.
Desautels, P., McCracken, T., Holloway, A., 2012. Technical Report Update NI 43-101, Fotadrevo, Province of Toliara, Madagascar, p.175.
Di Cecco, V.E., Tait, K.T., Spooner, E.T.C., Scherba, C., 2018. The vanadium-bearing oxide minerals of the Green Giant vanadium graphite deposit, southwest Madagascar. Can. Mineral. 56, 247–257.
Diab, H., Chouabbi, A., Fru, E.C., Nacer, J.-E., Krekeler, M., 2020. Mechanism of formation, mineralogy and geochemistry of the ooidal ironstone of Djebel Had, northeast Algeria. J. African Earth Sci. 162, 103736. https://doi.org/10.1016/j.jafrearsci.2019.103736.
Dickinson, R., 2014. Triton's Nicanda Hill show rolls on. Australia's Paydirt 1 (221), 51.
Dill, H.G., 2007. A review of mineral resources in Malawi: with special reference to aluminium variation in mineral deposits. J. Afr. Earth Sc. 47, 153–173.
Dill, H.G., 2010. The "chessboard" classification scheme of mineral deposits: Mineralogy and geology from aluminum to zirconium. Earth Sci. Rev. 100, 1–420.
Dill, H.G., Busch, K., Blum, N., 1991. Chemistry and origin of veinlike phosphate mineralization, Nuba Mts. (Sudan). Ore Geol. Rev. 6, 9–24.
Dorbor, J.K., 2010. The regional geology and mineral potential of the Republic of Liberia: a Summary. Liberian Geological Survey, Ministry of Lands, Mines and Energy.
Douglas-Hamilton, C., 2023. The Marela Ultramafic Project: Developing a potentially world-class polymetallic nickel-cobalt-scandium and titanium-vanadium project in Guinea, West Africa. Mineral Deposits Studies Group, Leicester 2023, Abstract Volume, p. 32.
Eales, H.V., Cawthorn, R.G., 1996. The Bushveld Complex. In: Cawthorn, R.G. (Ed.), Layered intrusions. Elsevier, Amsterdam, pp. 181–230.
Ettler, V., Štěpánek, D., Mihaljevič, M., Drahota, P., Jedlicka, R., Kříbek, B., Vaněk, A., Penížek, V., Sracek, O., Nyambe, I., 2020. Slag dusts from Kabwe (Zambia): Contaminant mineralogy and oral bioaccessibility. Chemosphere 260, 127642.
European Commission, 2023. Study on the EU's list of Critical Raw Materials – Final Report. https://ec.europa.eu/docsroom/documents/54114/attachments/1/translations/en/renditions/native.
Feneyrol, J., Giuliani, G., Demaiffe, D., Ohnenstetter, D., Fallick, A.E., Dubessy, J., Martelat, J.E., Rakotondrazafy, A.F.M., Omito, E., Ichang'I, D., Nyamai, C., Wamunyu, A.W., 2017. Age and origin of the tsavorite and tanzanite mineralizing fluids in the Neoproterozoic Mozambique Metamorphic Belt. The Canadian Mineralogist 55, 763–786.
Feneyrol, J., Ohnenstetter, D., Giuliani, G., Fallick, A., Rollion-Bard, C., Robert, J., Malisa, E., 2012. Evidence of evaporates in the genesis of the vanadian grossular 'tsavorite' deposit in Namalulu, Tanzania. Can. Mineral. 50, 745–769.
Fentaw, H.M., Mohammed, S., Sebhat, N., Gautneb, H., 2000. The Moyale graphite deposit (Southern Ethiopia). Norges Geol. Unders. Bull. 436, 169–173.
Fischer, R.P., 1975. Geology and resources of base-metal vanadate deposits. U.S. Geol. Surv. Prof. Pap. 926–A14.
Frost-Killian, S., Sharad Master, S., Viljoen, R.P., Wilson, M.G.C., 2016. The Great Mineral Fields of Africa Introduction. Episodes 39 (2), 85–103.
Gamaletsos, P.N., Godelitsas, A., Kasama, T., Fiordaliso, E.M., Göttlicher, J., Steininger, R., 2017. Vanadium in Al-ore (bauxite) from mines of Central Greece. Abstracts from V.M. Goldschmidt Conference 2017, Paris, France.
Gao, F., Olayiwola, A.U., Liu, B., Wang, S., Du, H., Li, J., Wang, X., Chen, D., Zhang, Y., 2022. Review of vanadium production Part I: primary resources. Miner. Process. Extr. Metall. Rev. 43 (4), 466–488. https://doi.org/10.1080/08827508.2021.1883013.
Garnit, H., Bouhlel, S., 2016. Petrography, mineralogy and geochemistry of the Late Eocene oolitic ironstones of the Jebel Ank, Southern Tunisian Atlas. Ore Geol. Rev. 84, 134–153.
Garnit, H., Bouhlel, S., Kraemer, D., Ben Halima, K., Beaudoin, G., 2022. Characterization and genesis of supergene karstic vanadium ores in the Djebba Pb-Zn district (Triassic Diapirs zone, North Eastern Tunisia). J. Afr. Earth Sc. 196, 104688.
Gauthier-Lafaye, F., 1986. Les gisements d'uranium du Gabon et les réacteurs d'Oklo. Modèle métallogénique de gites à fortes teneurs du Protérozoique inférieur. Memoires Sciences Géologiques 78, 206.
Gauthier-Lafaye, F., Weber, F., 1989. The Francevillian (Lower Proterozoic) uranium ore deposits of Gabon. Econ. Geol. 84, 2267–2285.
Gauthier-Lafaye, F., Weber, F., 2003. Natural nuclear fission reactors: time constraints for occurrence and their relation to uranium and manganese deposits and to the evolution of the atmosphere. Precambr. Res. 120, 81–101.
Gautneb, H., Korneliussen, A., Baccha, H., 2001. Analysis of ilmenite, vanadium-bearing titanomagnetite and apatite from the Melka Arba deposit. Ethiopia Norges geologiske undersøkelse (NGU) Report 2001.095.
Ghebre, W.M., 2010. Geology and mineralization of Bikilal phosphate deposit, Western Ethiopia, implication and outline of gabbro intrusion to East Africa zone. The 1st International Applied Geological Congress, Department of Geology, Islamic Azad University - Mashad Branch, Iran, 26-28 April 2010, 2072-2077.
Geological Survey of Tanzania, 2015. Minerogenetic Map of Tanzania + Explanatory notes. GST, Dodoma.
Gilligan, R., Nikoloski, A.N., 2020. The extraction of vanadium from titanomagnetites and other sources. Miner. Eng. 146, 106106.
Giuliani, G., Dubessy, J., Ohnenstetter, D., Banks, D., Branquet, Y., Feneyrol, J., Fallick, A.E., Martelat, J.E., 2018. The role of evaporites in the formation of gems during metamorphism of carbonate platforms: a review. Miner. Deposita 53, 1–20.
Golden Deeps, 2022. High-Grade Vanadium (+ Cu, Pb, Zn, Ag) Development Studies & Copper-Silver Discovery In Namibia. Africa Down Under Presentation, September 2022. https://www.goldendeeps.com/wp-content/uploads/2022/09/Vanadium_Development_Studies_CuAg_Drilling_in_Namibia.pdf.
Gomez, F., Allmendinger, R., Barazangi, M., Beauchamp, W., 2000. Role of the Atlas Mountains (northwest Africa) within the African-Eurasian plate-boundary zone. Geology 28, 769–864.
Goscombe, B., Gray, D., Hand, M., 2004. Variation in metamorphic style along the northern margin of the Damara Orogen, Namibia. J. Petrol. 45, 1261–1295.
Graedel, T.E., Allwood, J., Birat, J.-P., Buchert, M., Hagelüken, C., Reck, B.K., Sibley, S. F., Sonnemann, G., 2011. What do we know about metal recycling rates? J. Ind. Ecol. 15 (3), 355–366.
Grantham, G.H., Maboko, M., Eglington, B.M., 2003. A review of the evolution of the Mozambique Belt and implications for the amalgamation and dispersal of Rodinia and Gondwana. Geol. Soc. Lond. Spec. Publ. 206, 401–425.
Grantham, G.H., Macey, P.H., Ingram, B.A., Roberts, M.P., Armstrong, R.A., Hokada, T., Shiraishi, K., Bisnath, A., Manhica, V., 2008. Terrane correlation between Antarctica, Mozambique and Sri Lanka; comparisons of geochronology, lithology, structure and metamorphism and possible implications for the geology of southern Africa and Antarctica. Geological Society of London, Special Publications 308, 91–119.
Gray, D.R., Foster, D.A., Goscombe, B., Passchier, C.W., Trouw, R.A.J., 2006. $^{40}Ar/^{39}Ar$ thermochronology of the Pan-African Damara orogen, Namibia, with implications for tectonothermal and geodynamic evolution. Precambrian Res. 150, 49–72.
Groves, D.I., Vielreicher, N., 2001. The Phalaborwa (Palabora) carbonatite-hosted magnetite-copper sulfide deposit, South Africa: An end-member of the iron-oxide copper-gold-rare earth element deposit group? Miner. Deposita 36 (2), 189–194. https://doi.org/10.1007/s001260050298.
Guerrak, S., 1988. Geology of the early Devonian oolitic iron ore of the Gara Djebilet field, Saharan Platform. Algeria. Ore Geology Reviews 3 (4), 333–358.
Guiraud, R., Bosworth, W., Thierry, J., Delplanque, A., 2005. Phanerozoic geological evolution of northern and central Africa: an overview. J. Afr. Earth Sci. 43, 83–143.
Gunn, A.G., Dorbor, J.K., Mankelow, J.M., Lusty, P.A.J., Deady, E.A., Shaw, R.A., Goodenough, K.M., 2018. A review of the mineral potential of Liberia. Ore Geol. Rev. 101, 413–431.
Hambleton-Jones, B.B., 1976. The geology and geochemistry of some epigenetic uranium deposits near the Swakop River (South West Africa). University of Pretoria, PhD Thesis, 306p.
Harris, C., Hlongwane, W., Gule, N., Scheepers, R., 2014. Origin of tanzanite and associated gemstone mineralization at Merelani, Tanzania. South Africa J. Geol. 117, 15–30.
Hartleb, J.W.O., 1988. The Langer Heinrich uranium deposit: Southwest Africa/Namibia. Ore Geol. Rev. 3 (1–3), 277–287.
Hiéronymus, B., 1985. Study of the weathering of eruptive rocks in the West Cameroon. Earth Science Thesis, University of Paris VI, 85 p.
Hope, D., 2022. Battery Tech Report: Lithium-Ion vs Vanadium Redox Flow Batteries (VRFB). Capital 10x.com, The Future of Battery Tech: Vanadium Redox Flow Batteries (accessed on February 24, 2023).
Horie, K., Hidaka, H., Gauthier-Lafaye, F., 2005. U-Pb geochronology and geochemistry of zircon from the Franceville series at Bidoudouma. Gabon. Geochimica et Cosmochimica Acta 69 (10), A11.
Hund, K., La Porta, D., Fabregas, T.P., Laing, T., Drexhage, J., 2020. Minerals for climate action: the mineral intensity of the clean energy transition. World Bank Group, Washington, DC, p. 112. https://pubdocs.worldbank.org/en/961711588875536384/Minerals-for-Climate-Action-The-Mineral-Intensity-of-the-Clean-Energy-Transition.pdf.
Hussein Al-Zuhairi, M.A., 2014. Vanadium extraction from residual of fired crude oil in power plants. Iraqi J. Mech. Mater. Eng. 14 (4), 423–431.
IAEA, 2020. World Uranium Geology, Exploration, Resources and Production. International Atomic Energy Agency 2020, Vienna, p. 972.
Ibraimo, D.L., Larsen, R.B., 2015. Geological setting, emplacement mechanism and igneous evolution of the Atchiza mafic-ultramafic layered suite in north-west Mozambique. J. Afr. Earth Sc. 111, 421–433.
International Gold Exploration AB, 2007. Annual Report 2006: Stockholm, Sweden, International Gold Exploration AB, Press release n° 21, p. 50.
Ivanic, T.J., Nebel, O., Brett, J., Murdie, R.E., 2018. The Windimurra Igneous Complex: an Archean Bushveld? In: Characterization of Ore-Forming Systems From Geological, Geochemical and Geophysical Studies, K. Gessner, T.G. Blenkinsop, and P. Sorjonen-Ward, (eds) Geological Society, London, Special Publications 453(1), 313. https://doi.org/10.1144/SP453.1.
Johnson, M.R., Anhaeusser, C.R., Thomas, R.J. (eds), 2006. The Geology of South Africa. Pretoria: Geological Society of South Africa/Council for Geoscience, p. 691.
Jourdan, P., 1990. The Minerals Industry of Angola. Report No. 116 Institute of Mining Research University of Zimbabwe, p. 16.
Kabete, J.M., Groves, D.I., McNaughton, N.J., Mruma, A.H., 2012. A new tectonic and temporal framework for the Tanzanian Shield: Implications for gold metallogeny and undiscovered endowment. Ore Geol. Rev. 48, 88–124.
Kadima, E., Delvaux, D., Sebagenzi, S.N., Tack, L., Kabeyaz, S.M., 2011. Structure and geological history of the Congo Basin: an integrated interpretation of gravity, magnetic and reflection seismic data. Basin Res. 23, 499–527. https://doi.org/10.1111/j.1365-2117.2011.00500.x.
Kamona, A.F., Friedrich, G.H., 2007. Geology, mineralogy and stable isotope geochemistry of the Kabwe carbonate-hosted Pb–Zn deposit, Central Zambia. Ore Geol. Rev. 30, 217–243.
Kampunzu, A.B., Cailteux, J.L.H., Kamona, A.F., Intiomale, M.M., Melcher, F., 2009. Sediment-hosted Zn–Pb–Cu deposits in the Central African Copperbelt. Ore Geol. Rev. 35, 263–297.
Kelley, K.D., Scott, C.T., Polyak, D.E., Kimball, B.E., 2017. Vanadium—U.S. Geological Survey Professional Paper 1802. In: Critical Mineral Resources of the United States—Economic and Environmental Geology and Prospects for Future Supply.

Schulz, K.J., DeYoung, J.H. Jr., Seal, R.R., II, Bradley, D.C., (eds), U.S. Geological Survey: Reston, VA, USA, p. U1–U36.
Key, R., Ayers, N., 2000. The 1998 Edition of the Geological Map of Botswana. Journal of African Earth Sciences 30, 427–451.
Kinnaird, J.A., Nex, P.A.M., 2016. Uranium in Africa. Episodes 39 (2), 335–359.
Komuro, K., Suzuki, S., Yamamoto, M., Ohtsuka, Y., Koyama, K., 1994. Geochemistry and mineral alteration around the Kanyemba-1 uranium deposit, Zimbabwe. Annual report of the Institute of Geoscience, the University of Tsukuba 20, 67-72.
Koneva, A.A., 2002. Cr–V oxides in metamorphic rocks, Lake Baikal, Russia. Neues Jb. Mineral. Monat. 12, 541–550.
Konka, B., Gebreselassie, S., Nesro Hussen, E., 2013. Petrography and geochemistry of ferricrete near Shire, northern Ethiopia. Momona Ethiopian J. Sci. 5 (1), 32–50.
Lacroix, A.M., 1908. Sur quelques vanadates des environs de Saïda (Oran). Bull. Minér. 31 (1), 44–46.
Lardeaux, J.-M., Martelat, J.-E., Nicollet, C., Pili, É., Rakotondrazafy, R., Cardon, H., 1999. Metamorphism and tectonics in southern Madagascar: An overview. Gondw. Res. 2 (3), 355–362.
Lashhab, M.L., West, I.M., 1992. Sedimentology and geochemistry of the Jir Formation in Jabal al Jir and the Western Sirt Basin. Third Symposium on The Geology of Libya, Tripoli, September 27-30th 1987, vol. 5; Salem, M.J. (ed), 1855-1869.
Lehmann, B., Frei, R., Xu, L.G., Mao, J.W., 2016. Early Cambrian black shale-hosted Mo-Ni and V mineralization on the rifted margin of the Yangtze Platform, China: reconnaissance chromium isotope data and a refined metallogenic model. Econ. Geol. 111, 89–103.
Lesaffer, A., 2014. Nature and formation processes of the supergene Pb-Zn-Cu-V mineralization of Bamba Kilenda, Bas-Congo Province, DR Congo. MsThesis University of Gent, p. 121.
Li, Z.X., Bogdanova, S.V., Collins, A.S., Davidson, A., De Waele, B., Ernst, R.E., Fitzsimons, I.C.W., Fuck, R.A., Gladkochub, D.P., Jacobs, J., Karlstrom, K.E., Lu, S., Natapov, L.M., Pease, V., Pisarevsky, S.A., Thrane, K., Vernikovsky, V., 2008. Assembly, configuration, and break-up history of Rodinia: a synthesis. Precambr. Res. 160, 179–210.
Li, C., Wei, C., Deng, Z., Li, M., Li, X., Fan, G., 2010. Recovery of vanadium from black shale. Trans. Nonferrous Met. Soc. China 20, 127–131.
Lilende, A., 2012. The source of uranium and vanadium at the Langer Heinrich and Klein Trekkopje uranium deposits – Genesis and controlling factors for uranium mineralization. Ms Thesis University of Namibia, Windhoek, Namibia, p. 267.
Loxton, R.F., 1981. A photogeological study of the Aha Hills, Northwest Botswana. Loxton, Hunting and Associates, Report for Billiton Botswana (Pty). Ltd, Gaborone, Botswana, p. 27.
Mahjoub, M.N., 1973. Étude de minéralisations vanadifères dans les poches karstiques du Jebel Gorraa (Djebba-Tunisie). Thèse de Doctorat de 3ème cycle. Paris 76.
Malisa, E., Muhongo, S., 1990. Tectonic setting of gemstone mineralization in the Proterozoic metamorphic terrane of the Mozambique Belt in Tanzania. Precambr. Res. 46, 167–176.
Mamadou, M.M., Cathelineau, M., Deloule, E., Reisberg, L., Cardon, O., Vallance, J., Brouand, M., 2022. The Tim Mersoï Basin uranium deposits (Northern Niger): Geochronology and genetic model. Ore Geol. Rev. 145, 10495.
Mapani, B., Ellmies, R., Kamona, F., Kříbek, B., Majer, V., Knésl, I., Pašava, J., Mufenda, M., Mbingeneeko, F., 2010. Potential human health risks associated with historic ore processing at Berg Aukas, Grootfontein, Namibia. J. Afr. Earth Sc. 58, 634–647.
Mapeo, R.B., 2007. Geological and Structural Analysis of the Kihabe Base Metal Prospect in NW Botswana. In: Internal Report for Mount Burgess (Botswana). (Pty) Ltd., Gaborone, Botswana, p. 41.
Marketscreener.com., 2018. Mustang Resources Ltd. changes name to New Energy Minerals (accessed 8 October, 2018).
Markwitz, V., Hein, K.A.A., Miller, J., 2015. Compilation of West African mineral deposits: Spatial distribution and mineral endowment. Precambr. Res. 274, 61–81.
Martelat, J.-E., Lardeaux, J.-M., Nicollet, C., Rakotondrazafy, R., 2000. Strain pattern and late Precambrian deformation history in southern Madagascar. Precambr. Res. 102 (1–2), 1–20.
Matrix Reference Materials, 2021. https://amis.co.za/product/v-0-97-vanadium-mapochs-south-africa.
McCourt, S., 2016. A brief geological history of southern Africa. In: Knight, J., Grab, S. (Eds.), Quaternary Environmental Change in Southern Africa: Physical and Human Dimensions. Cambridge University Press, pp. 18–29. https://doi.org/10.1017/CBO9781107295483.002.
McNulty, B.A., Jowitt, S.M., 2021. Barriers to and uncertainties in understanding and quantifying global critical mineral and element supply. Science 24 (7), 1–19. https://doi.org/10.1016/j.isci.2021.102809.
Medenbach, O., Schmetzer, K., 1978. Schreyerite ($V_2Ti_3O_9$), a new mineral. Am. Mineral. 63, 1182–1186.
Mercier, A., Moine, B., Delorme, J., Rakotondrazafy, M.A.E., 1997. A note of a new occurrence of vanadian grossular garnet from Madagascar. J. Gemmol. 25 (6), 391–393.
Meulenkamp, J.E., Sissingh, W., 2003. Tertiary palaeogeography and tectonostratigraphic evolution of the Northern and Southern Peri-Tethys platforms and the intermediate domains of the African-Eurasian convergent plate boundary zone. Palaeogeogr. Palaeoclimatol. Palaeoecol. 196 (1), 209–228. https://doi.org/10.1016/s0031-0182(03)00319-5.
Michard, A., 1976. Éléments de géologie marocaine. Notes et Mémoires du Service Géologique du Maroc 252, 408.
Milani, L., Bolhar, R., Cawthorn, R.G., Frei, D., 2017. In situ LA–ICP-MS and EPMA trace element characterization of Fe–Ti oxides from the phoscorite–carbonatite association at Phalaborwa, South Africa. Miner. Deposita 52, 747–768.
Milési, J., Ledru, P., Feybesse, J., Dommanget, A., Marcoux, E., 1992. Early Proterozoic ore deposits and tectonics of the Birimian orogenic belt, West Africa. Precambrian Res. 58 (1), 305–344.
Battery Minerals, 2019. Substantial maiden vanadium Resource further strengthens economic outlook for Montepuez graphite project. ASX Announcement 29 April 2019.
Miller, R.McG., 2008. Geology of Namibia. 3 Volumes. Windhoek, Namibia: Ministry of Mines and Energy, Geological Survey.
Millman, A.P., 1960. The descloizite-mottramite series of vanadates from minas de Lueca, Angola. Am. Mineral. 45, 763–773.
Mondillo, N., Boni, M., Balassone, G., Forrester, N., Putzolu, F., Santoro, L., 2020. Mineralogy and genesis of the Kihabe Zn-Pb-V prospect, Aha Hills, Northwest Botswana. Minerals 10 (8), 685.
Becker, E., Karner, K., Corbin, J.C., Mwenelupembe, J., 2014. The geology of the Kayelekera uranium mine, Malawi (IAEA-TECDOC-CD–1739). Proceedings of an International Symposium organized by the International Atomic Energy Agency in Cooperation with the OECD Nuclear Energy Agency,the Nuclear Energy Institute and the World Nuclear Association held in Vienna, Austria, 22–26 June 2009.
Mosiane, C., 2006. An overview of South Africa's Vanadium Industry during the period 1997–2006. Department of Mineral Resources Republic of South Africa; Directorate: Mineral Economics, p. 17.
MSA Group (Pty) Ltd, 2022. Vametco Inferred & Indicated Mineral Resource and Ore Reserve Update for Annual Reporting purposes, prepared for the. Bushveld Minerals Limited, p. 9.
Mücke, A., 2000. Environmental conditions in the Late Cretaceous African Tethys: conclusions from a microscopic-microchemical study of ooidal ironstones from Egypt, Sudan and Nigeria. J. Afr. Earth Sc. 30 (1), 25–46.
Mücke, A., Dzigbodi-Adjimah, K., Annor, A., 1999. Mineralogy, petrography, geochemistry and genesis of the Paleoproterozoic Birimian manganese-formation of Nsuta/Ghana. Miner. Deposita 34, 297–311. https://doi.org/10.1007/s001260050205.
Naldrett, A.J., 2010. Secular Variation of Magmatic Sulfide Deposits and Their Source Magmas. Econ. Geol. 105, 669–688.
Ndema Mbongué, J.L., 2020. Assessment of vanadium in stream sediments from River Mbete, Loum Area (Pan-African Fold Belt, Cameroon): implications for vanadium exploration. Int. J. Innov. Sci. Res. Technol. 5 (1), 133–146.
Next Source Materials, 2017. The Green Giant Vanadium Project. https://www.nextsourcematerials.com/vanadium/green-giant-vanadium-project/.
New Energy Minerals, 2018. Caula Vanadium-Graphite Project Scoping Study, 87.
Neybergh, H., Laduron, D., Martin, H., Verkaeren, J., 1980. The vanadiferous magnetite deposits of the Oursi region, Upper Volta. Econ. Geol. 75, 1042–1052.
Nicollet, C., 1990. Crustal evolution of the granulites of Madagascar. In: Vielzeuf, D., Vidal, P. (eds.) Granulites and Crustal Evolution. NATO ASI Series 311, Springer, Dordrecht, 291-310.
Nimpagaritse, G., 1986. Pétrographie, minéralogie et géochimie de l'indice vanadifère de Mukanda, massif gabbroïque de Buhoro, Burundi. Thèse (M.Sc.A.) École polytechnique, Montréal, Québec, p. 86.
Ntiharirizwa, S., Boulvais, P., Poujol, M., Branquet, Y., Morelli, C., Ntungwanayo, J., Midende, G., 2018. Geology and U-Th-Pb dating of the Gakara REE Deposit, Burundi. Minerals 8(9), 394; https://doi.org/10.3390/min8090394.
Optiva Resources Ltd., 2023. The Marela Project: Advancing a potentially world class Fe-Ti-V-Ni-Co-Sc polymetallic project in Guinea, West Africa. optivaresources.com. (accessed February 25, 2023).
Osman Sedig, Y.M., 2018. Uranium and Vanadium mining and ore processing at Sudan. Sudan University of Science and Technology PhD Degree in Physics College of Graduate Studies, p. 70.
Ossa Ossa, F., Hofmann, A., Ballouard, C., Voster, C., Schoenberg, R., Fiedrich, A., Mayaga-Mikolo, F., Bekker, A., 2020. Constraining provenance for the uraniferous Paleoproterozoic Francevillian Group sediments (Gabon) with detrital zircon geochronology and geochemistry. Precambrian Research, 105724.
Pagel M., Cavellec, S., Forbes, P., Gerbaud, O., Vergely, P., Wagani, I., Mathieu, R., 2005. Uranium deposits in the Arlit area (Niger). 8th Biennal SGA Meeting, August 2005, Bejing, China. In: Mineral Deposit Research: Meeting the Global Challenge, (Jingwen Mao and F.P. Bierlen, eds.), 303-305.
Paredis, B., Muchez, P., Dewaele, S., 2017. Platinum group element mineralization at Musongati (Burundi): concentration and Pd-Rh distribution in pentlandite. Geol. Belg. 20 (1–2), 15–32.
Parnell, J., 2022. Snowball Earth to Global Warming: coupled vanadium carbonaceous deposits in the Cryogenian-Cambrian. Ore Geol. Rev. 145, 104876.
Partridge, T.C., Maud, R.R., 1987. Geomorphic evolution of southern Africa since the Mesozoic. S. Afr. J. Geol. 90, 179–208.
Patterson, S.H., Kurtz, H.F., Olson, J.C., Neeley, C.L., 1986. World bauxite resources: U.S. Geological Survey Professional Paper 1076–B, p. 151 (quoted by Kelley et al., 2017). http://pubs.er.usgs.gov/publication/pp1076B.
Pauly, E., 1962. Geology and Mineralization of the Lueca-Region (Damba, Northern Angola). Boletim dos Serviços de Geologia e Minas, No. 5- Luanda.
Perks, C., Mudd, G., 2021. Soft rocks, hard rocks: the world's resources and reserves of Ti and Zr and associated critical minerals. Int. Geol. Rev. 64, 987–1008. https://doi.org/10.1080/00206814.2021.1904294.
Petranikova, M., Tkaczyk, A.H., Bartl, A., Amato, A., Lapkovskis, V., Tunsu, C., 2020. Vanadium sustainability in the context of innovative recycling and sourcing development. Waste Manag. 113, 521–544.
Piper, D.Z., 1994. Seawater as the source of minor elements in black shales, phosphorites and other sedimentary rocks. Chem. Geol. 114 (1–2), 95–114.

Pirajno, F., Joubert, B.D., 1993. An overview of carbonate-hosted mineral deposits in the Otavi Mountain Land, Namibia: Implications for ore genesis. Journal African Earth Sciences 16, 265–272.
Pohl, W.L., Nauta, W.J., Niedermayr, G., 1979. Geology of the Mwatate Quadrangle and the Vanadium Grossularite Deposits of the Area (with a Geological Map 1:50 000). Kenya Geological Survey Report No. 101, p. 55, Nairobi.
Putzolu, F., Abad, I., Balassone, G., Boni, M., Lupo, F., Mondillo, N., 2023. Zn-clays in the Kihabe and Nxuu prospects (Aha Hills, Botswana): a XRD and TEM study. Am. Mineral. 108, 362–382. https://doi.org/10.2138/am-2022-8439.
Qi, M.J., 1999. The current situation and prospect of the vanadium extraction from stone coal. Hydrometallurgy China 72 (4), 1–10.
Ray, G.E., 1974. The structural and metamorphic geology of northern Malawi. J. Geol. Soc. London 130, 427–440.
Reck, B.K., Graedel, T.E., 2012. Challenges in metal recycling. Science 337, 690–695.
Reynolds, I.M., 1985. Contrasted mineralogy and textural relationships in the uppermost titaniferous magnetite layers of the Bushveld Complex in the Bierkraal area north of Rustenburg. Econ. Geol. 80, 1027–1048.
Roig, J.Y., Tucker, R.D., Delor, C., Peters, S.G., Théveniaut, H., 2012. Carte Géologique de la République de Madagascar à 1/1,000,000. Ministère des Mines, PGRM, Antananarivo, République de Madagascar.
Roskill, 2021. Vanadium, Outlook to 2030, 19th Edition, Roskill. (accessed by Simandl and Paradis July 20, 2021). https://roskill.com/market-report/vanadium/.
Sainfeld, P., 1952, Les gîtes plombo-zincifères de Tunisie. Annales des mines et de la géologie n°9, Tunis, p. 285.
Scherba, C., Montreuil, J.-F., Barrie, C.T., 2018. Geology and Economics of the Giant Molo Graphite Deposit, Southern Madagascar. Society of Economic Geologists Special Publication 21, 347–363.
Schlüter, T., 2008. Geological Atlas of Africa: with notes on stratigraphy, tectonics, economic geology, geohazards, geosites and geoscientific education of each country. Springer Verlag, Science and Business Media, p. 272.
Schwellnus, C.M., 1945. Vanadium deposits in the Otavi Mountains, southwest Africa. Transactions of the Geological Society of South Africa 48, 49–73.
Schwertmann, U., Pfab, G., 1997. Structural vanadium and chromium in lateritic iron oxides: genetic implications. Geochim. Cosmochim. Acta 60, 4279–4283.
Shaltami, O.R., Fiannacca, P., Fares, F.F., EL Oshebi, F.M., Siasia, G.D., Errishi, H., 2017. Geochemistry of Iron Ore at Wadi As Shati, SW Libya: Implications on Origin, Depositional Environment, Paleooxygenation, Paleoclimate and Age. Proceedings of the SGA-14th Biennial Meeting of Society for Geology Applied to Mineral Deposits, Québec, Canada, 36-50.
Silin, I., Hahn, K., Gürsel, D., Kremer, D., Gronen, L., Stopić, S., Friedrich, B., Wotruba, H., 2020. Mineral processing and metallurgical treatment of lead vanadate ores. Minerals 10 (2), 197. https://doi.org/10.3390/min10020197.
Simandl, G.J., Paradis, S., 2022. Vanadium as a critical material: economic geology with emphasis on market and the main deposit types, Applied Earth Science, IMM Transactions section B · August 2022, p. 19. DOI: 10.1080/25726838.2022.2102883.
Smejkal, S., 1985. Gite vanadifère de Mukanda. État des récherches et bilan des reserves, Rapport final. République du Burundi. Projet de Recherche et Développement Minier BDI/81/007 (unpubl. report), Bujumbura, Burundi.
Smith, W.D., Maier, W.D., 2021. The geotectonic setting, age and mineral deposit inventory of global layered intrusions. Earth Sciences Review 220, 103736. https://doi.org/10.1016/j.earscirev.2021.103736.
Solignac, M., 1935. Les minerais de zinc et de vanadium du gîte plombo-zincifère de Djebba Tunisie. Congrès International de Mines, Métallurgie Géologie Appliquée VII session, Paris, 20-26 Oct., Section de Géologie Appliquée, t. 1, p. 121.
Soussou, J.E., 1974. A framework for evaluating long-term strategies for the development of the Sahel-Sudan region. Annex 9. Energy and Mineral Resources. Report for Center for Policy Alternatives, Massachusetts Institute of Technology, Massachusetts 02139, p. 160.
Sracek, O., Mihaljevič, M., Kříbek, B., Majer, V., Filip, J., Vaněk, A., Penížek, V., Ettler, V., Mapani, B., 2014. Geochemistry and mineralogy of vanadium in mine tailings at Berg Aukas, northeastern Namibia. J. Afr. Earth Sc. 96, 180–189.
Suwa, K., Suzuki, K., Takashi, A., 1996. Vanadium grossular from the Mozambique metamorphic rocks, south Kenya. J. SE Asian Earth Sci. 14 (3–4), 299–308.
Syrah Resources, 2019. Syrah Resources Annual Report 2019. 108 p.
Tack, L., Wingate, M.T.D., Liégeois, J.P., Fernandez-Alonso, M., Deblond, A., 2001. Early Neoproterozoic magmatism (1000–910 Ma) of the Zadinian and Mayumbian Groups (Bas-Congo): onset of Rodinia rifting at the western edge of the Congo craton. Precambr. Res. 110, 277–306.
Tadesse, S., Milési, J.-P., Deschamps, Y., 2003. Geology and mineral potential of Ethiopia: a note on geology and mineral map of Ethiopia. J. Afr. Earth Sc. 36, 273–313.
Tanouayi, G., Gnandi, K., Ouro-Sama, K., Aduayi-Akue, A.A., Ahoudi, H., Nyametso, Y., Hodabalo, Y., Solitoke, H.D., 2016. Distribution of fluoride in the Phosphorite mining area of Hahotoe-Kpogame (Togo). Journal of Health and Pollution 6 (10), 84–94.
Taylor, C.D., Schulz, K.J., Doebrich, J.L., Orris, G.J., Denning, P.D., Kirschbaum, M.J., 2009. Geology and nonfuel mineral deposits of Africa and the Middle East: U.S. Geological Survey Open-File Report 2005–1294-E, 246 p.
Taylor, C.D., Anderson, E.D., Bradley, D.C., Beaudoin, G., Cosca, M.A., Eppinger, R.G., Fernette, G.L., Finn, C.A., Friedel, M.J., Giles, S.A., Goldfarb, R.J., Horton, J.D., Lee, G.K., Marsh, E., Mauk, J.L., Motts, H.A., Ould El Joud, M.Y., Ould Soueidatt, S., Ould Taleb Mohamed, A., Rockwell, B.W., 2012. Mauritania: a Greenfields exploration opportunity in Northwestern Africa. SEG Newsletter 91, 1–10.
Taylor, J., 1955. The lead-zinc-vanadium deposits at Broken Hill, Northern Rhodesia (London: Her Majesty's Stationery Office 1955), p. 9.
Tegner, C., Cawthorn, R.G., Kruger, F.J., 2006. Cyclicity in the main and Upper Zones of the Bushveld Complex, South Africa: crystallization from a zoned magma sheet. J. Petrol. 47, 2257–2279.
Trittschack, R., 2008. Geological identification and mineralogical characterization of palaeo-surfaces and channel fills at the Langer Heinrich uranium deposit, Namibia. Martin-Luther University Halle Germany. Unpublished MSc. Thesis, p. 155.
Triton Minerals, 2020. Developing world-class projects for the graphite revolution. Presentation given at the Mines and Money APAC June 2020.
U.S. Geological Survey, 2023. Mineral commodity summaries 2023: U.S. Geological Survey, p. 202. https://doi.org/10.3133/mcs2023.
USDOI, 2018. Final List of Critical Minerals 2018 (US Department of the Interior), p. 2.
Van der Westhuizen, W.A., Tordiffe, E.A., de Bruiyn, H., Beukes, G.J., 1988. The composition of descloizite-mottramite in relation to the trace element distribution of Pb, Zn, Cu and V in the Otavi Mountain Land, South West Africa/Namibia. J. Geochem. Explor. 34, 21–29.
Van Gosen, B.S., Hall, S.M., 2017. The discovery and character of Pleistocene calcrete uranium deposits in the Southern High Plains of west Texas, United States: U.S. Geological Survey Scientific Investigations Report 2017–5134, p. 27.
Vanitec, 2022. Making Vanadium. https://vanitec.org/vanadium/making-vanadium.
Verhaert, M., Bernard, A., Dekoninck, A., Lafforgue, D., Saddiqi, O., Yans, J., 2017. Mineralogical and geochemical characterization of supergene Cu–Pb–Zn–V ores in the Oriental High Atlas, Morocco. Miner. Deposita 52, 1049–1068.
Verwoerd, W.J., 1957. The mineralogy and genesis of the lead-zinc-vanadium deposit of Abenab West in the Otavi Mountains, south west Africa: Annals University of Stellenbosch, v. 33. Section A, 1–11, 235–329.
Vital Metals, 2018. Vital identifies vanadium exploration target in Burkina Faso. ASX Media Announcement 4 October 2018. https://vitalmetals.com.au/wp-content/uploads/2020/05/43yz6pm3jngcbb.pdf.
Wanty, R.B., 1992. Thermodynamics and kinetics of reactions involving vanadium in natural systems: Accumulation of vanadium in sedimentary rocks. Geochim. Cosmochim. Acta 56 (4), 1471–1483.
Wartha, R.R., Schreuder, C.P., 1992. Minerals resource series—vanadium: Windhoek, Ministry of Mines and Energy, Geological Survey of Namibia, p. 16.
Weber, F., 1968. Une série Précambrienne du Gabon: le Francevillien. Sédimentologie, géochimie et relation avec les gîtes minéraux associés. Mémoires Service Carte Géologiques Alsace Lorraine 28, 328.
Welch, B.K., 1958. The occurrence and paragenesis of the ores of titanium. PhD Thesis, Durham University, p. 211. Available at Durham E-Theses Online: http://etheses.dur.ac.uk/9186/.
Wilson, A.H., 1996. The Great Dyke of Zimbabwe. In: Cawthorn, R.G. (Ed.), Layered intrusions: Amsterdam. Elsevier, pp. 365–402.
Witley, J., Garner, R., van der Merwe, A.J., 2019. Competent Persons Report on the Brits Vanadium Project North West and Gauteng Provinces, South Africa Prepared by The MSA Group (Pty) Ltd for. Bushveld Minerals Limited 117.
Wu, T., Yang, R., Gao, J., Li, J., 2021a. Age of the lower Cambrian vanadium deposit, East Guizhou, South China: Evidences from age of tuff and carbon isotope analysis along the Bagong section. Open. Geosciences 13(1), id. 287, 14.
Wu, T., Yang, R., Gao, L., Li, J., Gao, J., 2021b. Origin and enrichment of vanadium in the Lower Cambrian Black Shales, South China. ACS Omega 6 (41), 26870–26879.
Yager, T.R., 2009. The Mineral industry of Burundi. USGS 2006 Minerals Yearbook, U.S. Geological Survey, p. 3.
Yeo, G., 2011. The Karoo sandstone-hosted uranium deposits at Mutanga, Zambia. Denison Mines Corp, p. 2.
Youlton, B., 2007. Controls on Uranium Mineralization at the Klein Trekkopje Prospect, Namibia. University of the Witwatersrand, p. 63. BSc Honours thesis.
Zhou, M.-F., Robinson, P.T., Lesher, C.M., Keays, R.R., Zhang, C.-J., Malpas, J., 2005. Geochemistry, petrogenesis and metallogenesis of the Panzhihua gabbroic layered intrusion and associated Fe–Ti–V oxide deposits, Sichuan Province, SW China. J. Petrol. 46 (11), 2253–2280. https://doi.org/10.1093/petrology/egi054.
Zientek, M.L., 2012. Magmatic ore deposits in layered intrusions—Descriptive model for reef-type PGE and contact-type Cu-Ni-PGE deposits. U.S. Geological Survey Open-File Report 2012–1010, p. 48.
Zou, K., Xiao, J., Liang, G., Huang, W., Xiong, W., 2021. Effective extraction of vanadium from bauxite-type vanadium ore using roasting and leaching. Metals 11 (9), 1342.